AFWL-TR-
70-110

COUPLED ELECTROMAGNETIC AND ELECTRON ACOUSTIC WAVE PROPAGATION IN AN INHOMOGENEOUS LOSSY PLASMA LAYER

Hugh L. Southall
Lt USAF

TECHNICAL REPORT NO. AFWL-TR-70-110

September 1970

AIR FORCE WEAPONS LABORATORY
Air Force Systems Command
Kirtland Air Force Base
New Mexico

171

DISCLAIMER NOTICE

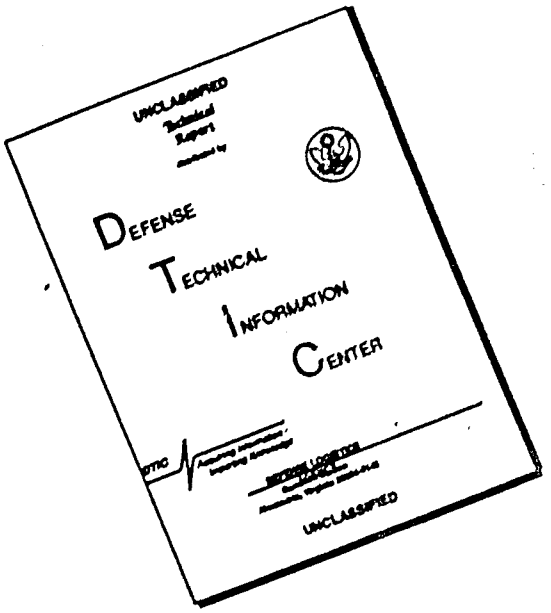

THIS DOCUMENT IS BEST QUALITY AVAILABLE. THE COPY FURNISHED TO DTIC CONTAINED A SIGNIFICANT NUMBER OF PAGES WHICH DO NOT REPRODUCE LEGIBLY.

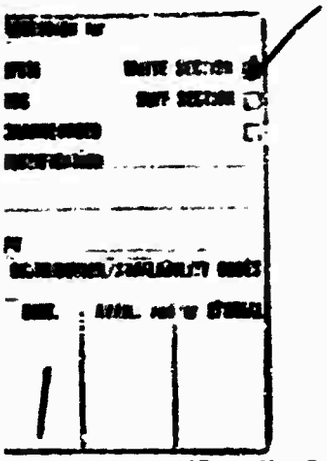

AIR FORCE WEAPONS LABORATORY
Air Force Systems Command
Kirtland Air Force Base
New Mexico

COUPLED ELECTROMAGNETIC AND ELECTRON ACOUSTIC WAVE PROPAGATION IN AN INHOMOGENEOUS LOSSY PLASMA LAYER

Hugh L. Southall
Lt USAF

TECHNICAL REPORT NO. AFWL-TR-70-110

FOREWORD

This research was performed under Program Element 62601F, Project 5791, Task 27.

Inclusive dates of research were November 1969 through August 1970. The report was submitted 14 August 1970 by the Air Force Weapons Laboratory Project Officer, Lt Hugh L. Southall (WLEA).

The material in this report was also published as a thesis in partial fulfillment of the requirements for an MS degree in Electrical Engineering at Texas Tech University.

This technical report has been reviewed and is approved.

Hugh L. Southall

HUGH L. SOUTHALL
Lieutenant, USAF
Project Officer

Walter M. Hart, Jr.

WALTER M. HART, JR.
Lt Colonel, USAF
Chief, Arming and Fuzing Branch

Carl F. Davis

CARL F. DAVIS
Colonel, USAF
Chief, Electronics Division

ABSTRACT

(Distribution Limitation Statement No. 1)

A hydrodynamic treatment is used to derive the coupled wave equations for wave propagation in a compressible plasma. Electron acoustic waves in the plasma are assumed to be excited by a vertically polarized electromagnetic wave obliquely incident upon a plane dielectric-plasma interface. Finite difference numerical solutions for the electromagnetic field and the scalar pressure field are obtained in a reentry-type plasma layer surrounding high-performance hypersonic reentry vehicles. An inhomogeneous plasma layer (or sheath) is modelled with a linearly increasing electron density profile. The coupling of acoustic waves to electromagnetic waves in this inhomogeneous region is investigated. Numerical results are obtained for the conversion of electromagnetic energy to plasma wave energy and vice versa.

CONTENTS

LIST OF TABLES

LIST OF FIGURES

LIST OF FIGURES (cont'd)

LIST OF FIGURES (cont'd)

LIST OF SYMBOLS

Symbol	Meaning	Units
A	$j\omega + \nu$	sec^{-1}
d	Distance to peak electron density in the plasma layer	meters
α	Attenuation factor of pressure wave in the plasma	nepers/meter
e	Electronic charge (-1.602×10^{-19})	coulombs
ϵ_p	Relative dielectric constant of the plasma ($1 - \omega_p^2/\omega^2$)	dimensionless
ϵ	Complex dielectric constant of the plasma ($\epsilon_o \epsilon_p$)	farads/meter
ϵ_o	Free space dielectric constant (8.854×10^{-12})	farads/meter
ϵ_d	Dielectric constant of the dielectric material ($\epsilon_o K_d$)	farads/meter
η_d	Characteristic impedance of the dielectric	ohms
f_p	Electron plasma frequency	hertz
$\vec{F}_o$	Static acceleration per electron (equilibrium value)	meters/sec^2
$\vec{F}$	First order acceleration per electron	meters/sec^2
γ	Ratio of specific heat at constant pressure to specific heat at constant volume	dimensionless
γ_{dx}	Propagation constant in the dielectric (x direction)	$meter^{-1}$
γ_{hx}	Complex electromagnetic propagation constant in the plasma (x direction)	$meter^{-1}$
γ_{px}	Complex pressure wave propagation constant in the plasma (x direction)	$meter^{-1}$

LIST OF SYMBOLS (cont'd)

Symbol	Meaning	Units
$\vec{E}$	Electric field intensity	volts/meter
$\vec{H}$	Magnetic field intensity	amperes/meter
H_o	Amplitude of incident electromagnetic wave	amperes/meter
$\vec{J}$	Convection current density	amperes/meter^2
h	Step size for numerical solution	meter
j	Imaginary notation ($\sqrt{-1}$)	dimensionless
K_B	Boltzmann's Constant (1.38×10^{-23})	joules/°Kelvin
K_d	Relative dielectric constant of the dielectric material (assumed to be 3.5)	dimensionless
K_y	Propagation constant in the y direction ($\omega\sqrt{\mu_o \varepsilon_o K_d} \sin \theta_i$)	meter^{-1}
K_{px}	Plasma wave propagation constant (x direction)	meter^{-1}
K_o	Free space propagation constant ($\omega\sqrt{\mu_o \varepsilon_o}$)	meter^{-1}
K_{ox}	Free space propagation constant (x direction), $\sqrt{K_o^2 - K_y^2}$	meter^{-1}
m	Electron mass (9.108×10^{-31})	kilograms
n_o	Electron number density, equilibrium value	cm^{-3}
n	Electron number density, first-order perturbation	cm^{-3}
$\overline{P}$	Time averaged power	watts
p_o	Equilibrium pressure	newtons/meter^2
p	First-order perturbation pressure	newtons/meter^2
ρ_o	Equilibrium mass density (mn_o) or charge density (en_o) as stated	Kg/m^3 or coul/m^3

LIST OF SYMBOLS (cont'd)

Symbol	Meaning	Units
ρ	First-order perturbation mass density (mn) or charge density (en) as stated	Kg/m^3 or $coul/m^3$
R	Reflection coefficient	dimensionless
$\vec{r}$	Position vector	meters
S	Surface area	$meter^2$
T	Temperature	degrees Kelvin
ν	Electron-neutral particle collision frequency	sec^{-1}
μ_o	Free space permeability (1.25×10^{-6})	henrys/meter
u_o	RMS thermal velocity in the plasma	meters/second
U	$1 - j\,\nu/\omega$	dimensionless
$\vec{V}_o$	Plasma drifting velocity	meters/second
$\vec{V}$	Ordered electron velocity in the plasma	meters/second
ω	Frequency of the incident electromagnetic wave	radians/second
ω_p	Electron plasma frequency	radians/second
λ_p	Electron acoustic wavelength	meters
λ_d	Debye length	meters
θ_1	Angle of incidence of electromagnetic wave	degrees
θ_2	Angle of transmission of the electromagnetic wave into the plasma	degrees
θ_3	Angle of transmission of the electromagnetic wave into free space from the plasma layer	degrees
θ_p	Angle of propagation of the pressure wave in the plasma	degrees

CHAPTER I

INTRODUCTION

Electron acoustic modes have been used in experimentally determining the electron density in the plasma sheath surrounding a reentry vehicle (Ref. 1). However, these methods employed resonance effects which are unobservable in plasmas with large electron-neutral particle collision frequencies. A short-pulse diagnostic technique using electroacoustic resonances and time domain analysis of the reflected pulse is described by Lustig, Baird and Ewald (Ref. 2). For slender conical reentry vehicles which reenter the earth's atmosphere at hypersonic velocities, the plasmas of interest are collision-dominated. When the vehicle reaches lower altitudes, the collision frequency can be larger than the operating frequency of the electron acoustic probe. The plasma electron density is inhomogeneous and increases from some value at the skin of the vehicle to a peak value at a distance typically 1 mm from the skin. Rather than using resonance effects, it is proposed to use propagating electron acoustic waves to probe this region. The waves can be generated at the boundary between the vehicle and the plasma by an electromagnetic wave incident obliquely upon the boundary from a dielectric material. In the inhomogeneous plasma region the acoustic waves are reflected, due to the electron density gradient, and return to the boundary. The reflected acoustic wave which returns to the boundary will be converted into a transverse electromagnetic wave which can be detected (if it has sufficient amplitude). The acoustic wave travels much

slower than an electromagnetic wave and the returning pulse of acoustic energy will lag the returning electromagnetic pulse in time. It is proposed to determine the electron density profile from its effect on the acoustic waves by observing the reflected acoustic waves.

It is shown later (Fig. 22) that in a homogeneous plasma which is collision dominated the acoustic waves are attenuated very rapidly and are not likely to be observable for propagation distances larger than 0.05 mm at the most. In an inhomogeneous plasma, the acoustic waves are coupled to the electromagnetic wave and the acoustic waves may not be so severely attenuated. This investigation is concerned with a steady-state, plane wave analysis of this coupling effect and its implications on electron acoustic wave propagation in an inhomogeneous plasma.

Electron acoustic waves depend upon the dynamic properties of the plasma. For plasmas with sufficiently large electron densities, it is appropriate (Ref. 3) to describe the acoustic waves in the plasma by a scalar pressure field. The scalar pressure field can describe a propagating pressure wave and is physically determined by the dynamic properties of the plasma and the source exciting the wave.

Acoustic wave propagation in a plasma is possible only at a finite plasma temperature. A cold plasma (incompressible plasma) is one with zero temperature, and no motion of the particles in the plasma is assumed. A warm plasma (compressible plasma) exhibits a finite temperature with corresponding random thermal motions of the particles in the plasma. A hot plasma is one with extremely high temperatures

(e.g., fusion temperatures). Electron acoustic wave propagation will be considered for the warm plasma only. The propagation of an acoustic wave from one region of the plasma to another region is a consequence of the random thermal motions of the electrons. This makes the localization of a disturbance impossible, and the electrons carry the disturbance from one region to another (Ref. 3). The average effect is not isotropic even though the motions of the electrons are random. The electrons moving in the direction of the wave will experience a larger change of momentum and there will be a net tendency to carry the disturbance in the direction of the wave (Ref. 3). It is important to distinguish between the random motions of the individual electrons and the collective oscillatory motion of the electron plasma considered as a medium. The medium, in this sense, is described as a single-fluid electron gas. The dynamic effects give rise to the collective motion of the plasma and form the physical basis for acoustic wave propagation. The collective motion of the plasma medium is described in a macroscopic manner by a hydrodynamic formulation of the equations describing wave propagation in a plasma.

Two approaches used in solving plasma problems are: a microscopic gas-kinetic treatment using the Boltzmann transport equation together with Maxwell's equations of electrodynamics; and a macroscopic, hydrodynamic treatment using the equations of conservation of mass and momentum together with Maxwell's equations (Ref. 4). The kinetic treatment is very difficult to use in mathematically modelling the modes of plasma oscillations without the imposition of serious physical restrictions In order to simplify the mathematics in the

kinetic treatment, it is necessary to make assumptions which would make it more reasonable to use the simpler hydrodynamic treatment (Ref. 4). The fundamental equations of hydrodynamics can be obtained from the Boltzmann transport equation. To a certain extent, then, the hydrodynamic treatment is an approach to the correct kinetic treatment (Ref. 4). It must be stated, therefore, that the hydrodynamic treatment used in this study is only an approximation to an exact solution of the present plasma problem. It should be noted, however, that the hydrodynamic approach fails intrinsically only for cases requiring more than a phenomenological approach to damping effects caused by collisions of the plasma particles and for problems in which the velocity distribution function is specifically involved (Ref. 4). Such cases might include calculations of scattering cross sections or of the thermal conductivity of a plasma. In the present problem, we are concerned with macroscopic, organized behavior of a plasma medium in which the collision frequency is energy-independent and is described in a phenomenological manner. The effect of the collision frequency is included as a drag force on the ordered motion of the electrons in the conservation of momentum equation. The hydrodynamic treatment in this case should be an entirely justified approach. There are, however, certain effects, such as Landau damping, which are not included in the hydrodynamic treatment. These will be discussed in detail in Chapter II.

Electron acoustic waves can be excited by an electromagnetic wave incident obliquely upon a plane boundary between a uniform dielectric material and a plasma. Since the boundary conditions are

both electromagnetic and acoustic, the incident electromagnetic wave will excite an acoustic wave at the boundary. It is necessary, however, that the electromagnetic wave have a component of the electric field strength vector perpendicular to the boundary (Ref. 5). For the two-dimensional geometry considered, this means that the incident electromagnetic wave may be taken to be vertically polarized with the electric field strength vector in the plane of incidence in the most general case of interest. This is discussed further in Chapter III.

A survey of the literature was made to determine as completely as possible the previous work done in the area of wave propagation in compressible plasmas. A significant result was the fact that very few numerical results have been published which describe the propagation of an electron acoustic wave in an inhomogeneous, lossy and bounded plasma. The few numerical results published were obtained for wave propagation in the ionosphere (Ref. 6). The plasma under consideration in this report is much denser, has a higher collision frequency and contains much larger gradients in electron density. No numerical results seem to be available for this type of plasma.

The basic references used for the fundamental theory of plasma wave propagation were the works by Bohm and Gross (Ref. 3), Oster (Ref. 4), Stix (Ref. 7), and Friedlander (Ref. 8).

Three principal papers give experimental data verifying the existence of a propagating acoustic wave in a homogeneous plasma: Van Hoven (Ref. 9), Derfler and Simonen (Ref. 10), and Malmberg and Wharton (Ref. 11). These papers basically verify the dispersion relation for

the propagating waves and give experimental evidence of Landau damping of the waves.

Much work has been done on theories for wave propagation in compressible plasmas. Wait (Ref. 12) discusses the radiation from sources immersed in a compressible plasma. He shows that the compressibility effects of the plasma on the radiation of electromagnetic waves are increased as the ratio of the acoustic velocity to the speed of light is increased. Wait (Ref. 13) discusses the influence of boundaries on wave propagation in a compressible plasma. He also describes the absorptive (impedance) boundary condition for acoustic waves. Felsen (Ref. 14) derives first order coupled wave equations for the quasi-electromagnetic and quasi-dynamical fields which he describes in the paper. Burman (Ref. 15) derives alternative first order coupled wave equations for the full-wave variable field quantities (see Chapter III). In another paper (Ref. 5) Burman presents a detailed derivation of the first order coupled equations. He also discusses the coupling and power flow, and proposes some approximate solutions. Burman (Ref. 16) derives the second order coupled wave equations and specializes the equations for a planar geometry. The fields in a region of coupling are investigated. Several approximate techniques for treating the equations are discussed. The approximate techniques are not valid for the type of plasma considered here.

When considering wave propagation in a bounded plasma, the boundary conditions become a fundamental problem. Several authors have treated the subject of boundary conditions for a compressible plasma. Wait (Ref. 17) demonstrates that the boundary condition which requires

the vanishing of the normal component of the electron velocity leads to results which are consistent with cold plasma theory. Yeh (Ref. 18) and Wait (Ref. 19) discuss the boundary conditions at a dielectric-plasma interface. Sancer (Ref. 20) discusses the boundary conditions required for a unique solution to the equations of the hydrodynamic treatment. The conversion of electromagnetic waves into longitudinal plasma waves at a dielectric-plasma boundary is considered by Hessel, Marcuvitz and Shmoys (Ref. 21).

A number of authors have treated the effects of the compressibility of a plasma surrounding an antenna. Wait (Ref. 22) states that it is possible for a considerable portion of the power to be radiated as an electron acoustic type wave. The distribution of the power depends on the boundary conditions. Kuehl (Ref. 23) calculates the radiation resistance of a short antenna in a warm plasma. He uses both a kinetic treatment and a hydrodynamic treatment and compares the two methods.

A brief summary of the topics covered in this thesis includes Chapter II which gives a simplified derivation of the dispersion relation for a pressure wave propagating in a compressible plasma. The plasma model is described in detail and the basic equations are derived. Chapter III derives the second order coupled wave equations. Consideration is given to both vertical and horizontal polarizations of incident electromagnetic waves. In Chapter IV finite difference numerical solutions are presented for the coupled wave equations. A linearly increasing plasma profile (electron density and temperature) with a constant collision frequency is considered. A linearly

increasing electron density which increases to a peak value, then drops abruptly to zero is one model considered. The other model is a linear increase to a peak electron density with a transition at this point to a semi-infinite plasma which is homogeneous with an electron density equal to the peak plasma electron density. The homogeneous region is considered semi-infinite because of the extremely small depth to which acoustic waves would penetrate this region (assuming a collision-dominated plasma). Actually the homogeneous region would be of finite extent and at some distance beyond the transition point the electron density would decrease to zero, i.e., a plasma-free space boundary. Convergence of numerical solutions is considered and numerical solutions are compared with approximate analytical solutions. In Chapter V the conversion of an electromagnetic wave into a plasma wave (and vice versa) at a dielectric-plasma interface is studied as a function of the plasma properties and the parameters of the incident electromagnetic wave.

CHAPTER II

PLASMA MODEL DESCRIPTION

Plasma Model Geometry and Parameters

The planar geometry of either plasma model is illustrated in Fig. 1 which also pictures the Cartesian coordinate system used throughout. The boundaries are planes of infinite extent in the y and z coordinate directions. The plasma parameters are assumed to vary in the x direction only. The plasma can then be described as a layer (inhomogeneous in the x direction) in physical contact with a dielectric half-space. Plasma parameters of primary interest include: electron density, the electron-neutral particle collision frequency, electron temperature and the plasma layer thickness. Electron density and temperature vary with distance x. The collision frequency is assumed to be a constant throughout the layer. Plasmas of interest, in general terms, have very large peak (maximum) electron densities, very large collision frequencies (i.e., collision-dominated plasmas), and temperatures consistent with "warm" plasmas (approximately 4000°K).

Basic Assumptions

First consider the regions surrounding the plasma layer. The dielectric is uniform and lossless with a relative dielectric constant K_d. The region outside the plasma layer is free space. The permeability is that of free space in all three regions.

A plasma can be defined as a gas containing a certain density of free positive and negative charges. It is a well established

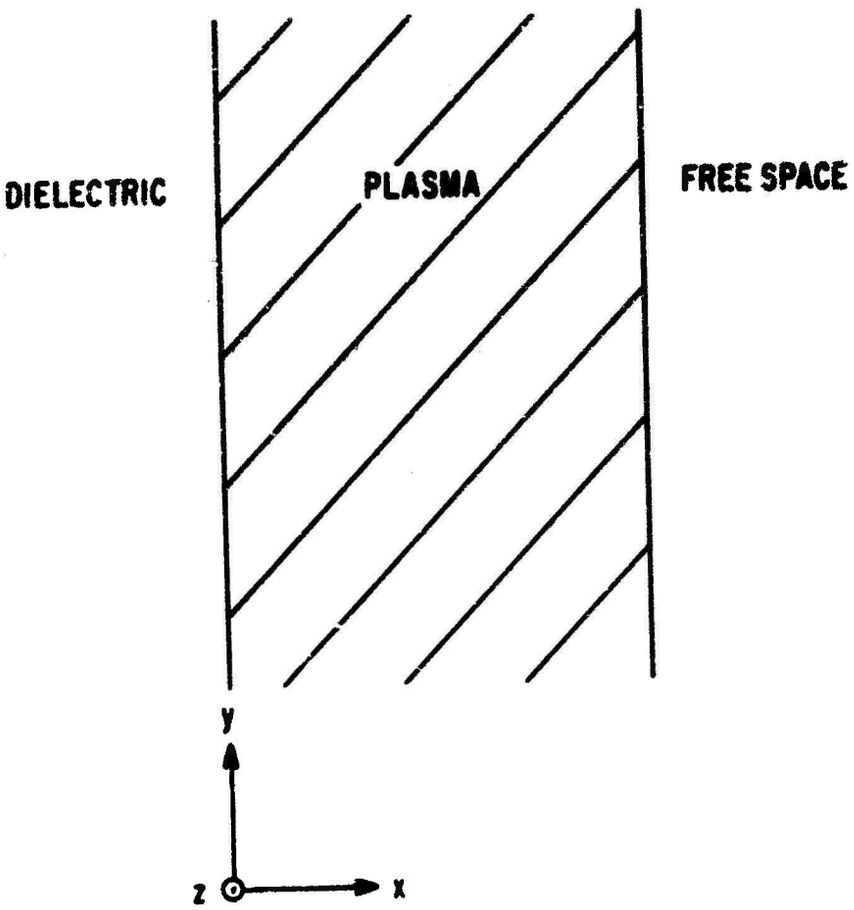

Figure 1. Geometry of the Plasma Model

fact that an electromagnetic wave will interact with charged particles. For the electromagnetic wave frequencies and plasma parameters considered, the interaction produces organized, steady-state oscillations in the plasma. Consider the frequency to be high enough so that the ions remain stationary and only the electrons interact with the electromagnetic wave. Also, model the plasma as a perfect electron gas with a uniform background charge of positive ions making it macroscopically neutral. It is a good approximation to consider the ions as a uniformly smeared background charge for wavelengths much greater than the interionic spacing (Ref. 3). Since this is also a requirement for any physical organized oscillation to exist, this will always be true. The assumption is made that the wavelengths considered must be much greater than the interionic spacing ($n_o^{-1/3}$, where n_o represents the equilibrium electron density).

The amplitudes of the fields in the plasma are assumed to be small enough so that the equations can be linearized (Ref. 11). This means that the electric field strength, magnetic field strength, ordered electron velocity, pressure field strength, and perturbed electron density are considered first order perturbation quantities.

Use an equilibrium (zero order) electron density of the plasma which is inhomogeneous only in the x direction. The plasma is considered to be compressible and therefore has a finite temperature, itself a function of x. The electron-neutral particle collision frequency is assumed to be energy-independent, independent of the ordered electron velocity, and constant across the plasma layer.

The plasma is collision-dominated, i.e., ν of the order of ω. This is a good assumption for reentry type plasmas.

The plasma is assumed to be isotropic with no external static magnetic or electric fields. The plasma is assumed to be stationary, i.e., the drifting velocity is zero. No external static body forces acting on the particles in the plasma are considered.

The two transport phenomena of viscosity and heat conduction are neglected in the plasma. The approximation then made is to neglect the terms in the equations of motion due to viscosity and heat conduction (Ref. 8). The absolute error in the approximate solutions is of the order of the product of the distance through which a wave propagates and of the ratio of the terms neglected in the equations of motion to those retained (Ref. 8). Since the distances considered for propagating waves in this case are very small, the approximation should be reasonable.

It is assumed that the plasma is sufficiently dense so that a description in terms of a force due to a gradient of the perturbed pressure field is valid. This approach is taken in solving plasma problems in the ionosphere (Ref. 24). The plasma presently considered is much denser than the ionospheric plasma, and this assumption thus a more valid one.

There are two important phenomena in acoustic wave propagation which do not appear in the hydrodynamic treatment. Physically, a plasma oscillation with a wavelength shorter than the inter-particle spacing is meaningless in terms of collective motion. This has been discussed earlier. The other phenomenon is a noncollisional damping

effect called Landau damping (Ref. 25). The organized plasma oscillations are damped by a transfer of energy from the wave to the energy in the random thermal motions of electrons which are moving at a speed close to the wave velocity. Landau damping becomes important when the acoustic wavelength approaches the Debye length of the plasma. When the acoustic wavelength is smaller than the Debye length, collective motion is essentially destroyed (Ref. 3). It will be assumed that in regions where a pressure field (acoustic wave) exists, the acoustic wavelength will be larger than the Debye length; however, since the plasma is inhomogeneous, an acoustic wavelength is difficult to determine. The assumption will be verified in Appendix D by calculating the wavelength from the dispersion relation for a lossy, homogeneous plasma having an electron density equal to the electron density at discrete points along the inhomogeneous plasma profile.

It is necessary now to specify the frequency range of interest. The constraint on the plasma wavelength due to Landau damping determines a maximum frequency of operation. For a collisionless, homogeneous plasma, Bohm and Gross (Ref. 3) have determined the maximum frequency to be approximately $\sqrt{2}\ f_p$, where f_p is the plasma frequency. Rather than specifying a maximum frequency, the approach in the previous paragraph will be used and frequencies larger than the frequency determining an acoustic wavelength equal to the Debye length will not be considered.

The electron plasma frequency is basically a cutoff frequency. Below the plasma frequency, the electrons can respond to an electromagnetic field but above it they cannot follow the field. Actually,

the cutoff is not that sharp. Van Hoven (Ref. 9) states that below the plasma frequency, acoustic waves are strongly damped by collisional effects. It is assumed that the hydrodynamic approach (including collisonal damping) can be used to investigate acoustic wave phenomena at frequencies well below the plasma frequency. There is no reason why the electron collective motion due to the interaction between the electromagnetic field and the charged particles should not still be described by the hydrodynamic equations, since the electrons can still collectively interact with the electromagnetic field for frequencies below the electron plasma frequency. A minimum operating frequency would be the ion plasma frequency, at which ion motion would have to be considered.

Rationalized MKS units are used for all numerical calculations.

Basic Equations

The basic equations are the two Maxwell's curl equations and two equations from hydrodynamic theory describing the dynamics of a continuum. These equations form the mathematical model for calculating the electromagnetic and acoustic fields in the plasma.

Maxwell's equations are given below, where it is assumed that the regions of space of interest are located far enough away from any magnetic or electric sources so that their effect is negligible.

$$\nabla \times \vec{E} = -\mu_o \frac{\partial \vec{H}}{\partial t} \tag{1}$$

$$\nabla \times \vec{H} = \epsilon_o \frac{\partial \vec{E}}{\partial t} + (n_o + n)\, e\vec{V} \tag{2}$$

A convection current density term has been included in the second equation. The equilibrium electron density is given by n_o and the electron density perturbation (fluctuation) is given by n. The charge accumulation or depletion is given by ne which is in general a function of both time and position. The charge of a single electron, e, is a negative number. The electron density fluctuation, n, can be either positive or negative. The acoustic vector field, $\vec{V}$, is the ordered velocity of the electrons.

The equation for conservation of momentum for an inviscid, non-heat-conducting medium is given by Friedlander (Ref. 8). This equation is sometimes called the hydrodynamic equation or dynamic equation.

$$\left(\rho_o + \rho\right)\left\{\frac{\partial \vec{V}}{\partial t} + \left(\vec{V}\cdot\nabla\right)\vec{V}\right\} + \nabla\left(p_o + p\right) = e\left(n_o + n\right)\vec{E} + e\left(\vec{V} \times \mu_o \vec{H}\right)\left(n_o + n\right) - \left(\rho_o + \rho\right)\nu\vec{V} \quad . \tag{3}$$

The equilibrium quantities are subscripted and the perturbation quantities are not. The mass density is given by ρ and is equal to the mass of an electron times the electron number density. The collision frequency is given by ν and its effect is included in the momentum equation as a drag force proportional to the ordered velocity of the electrons.

Equation (3) contains only one zero order term, ∇p_o. Friedlander (Ref. 8) has shown that for a plasma at rest with no static body forces acting upon it, $\nabla p_o = 0$ even if the plasma is inhomogeneous. This is a

consequence of hydrostatic equilibrium. Since $p_o = n_o K_B T$, this condition would imply

$$\nabla p_o = \nabla\left(n_o K_B T\right) = K_B T \nabla n_o + K_B n_o \nabla T = 0 \quad , \tag{4}$$

where K_B is Boltzmann's constant and T is the plasma temperature. This imposes a definite relationship between n_o and T. It is not, however, the relationship which has been assumed, i.e., that the temperature profile follows the electron density profile in form. This type of temperature variation is assumed because it is a good approximation to the temperature profile in a reentry type plasma where higher temperatures result in more ionization and give a higher value for n_o. It is concluded that $\nabla p_o \neq 0$. This case is discussed by Burman (Ref. 16). Equation (3) must now be modified to include a zero order term which will cancel the ∇p_o term, since $\nabla p_o \neq 0$. The modification is written:

$$\left(\rho_o + \rho\right)\left\{\frac{\partial \vec{V}}{\partial t} + \left(\vec{V}\cdot\nabla\right)\vec{V}\right\} + \nabla\left(p_o + p\right) - \left(\rho_o + \rho\right)\left(\vec{F}_o + \vec{F}\right)$$

$$= e\left(n_o + n\right)\vec{E} + e\left(\vec{V} \times \mu_o \vec{H}\right)\left(n_o + n\right)$$

$$- \left(\rho_o + \rho\right)\nu\vec{V} \quad , \tag{5}$$

where $\rho_o \vec{F}_o$ is the zero order term required to balance the zero order pressure gradient. A first order term, $\rho_o \vec{F} + \rho \vec{F}_o$, is also introduced. The force term $(\rho_o + \rho)(\vec{F}_o + \vec{F})$ is not due to any external static fields or forces since these are assumed negligible, but is due to an ambipolar diffusion electric field due to the static pressure gradient.

The zero order part of this force term balances the static pressure gradient while the effect of the first order part is considered to be negligible in the first order part of the momentum equation. The first order conservation of momentum equation then becomes:

$$m\left(n_o + n\right)\left\{\frac{\partial \vec{V}}{\partial t} + \left(\vec{V}\cdot\nabla\right)\vec{V}\right\} + \nabla p = e\left(n_o + n\right)\vec{E} + e\left(\vec{V} \times \mu_o \vec{H}\right)\left(n_o + n\right) - m\left(n_o + n\right)\nu\vec{V} \quad . \tag{6}$$

The exact equation of conservation of mass is given by the continuity equation

$$\frac{\partial}{\partial t}\left(\rho_o + \rho\right) + \nabla\cdot\left\{\left(\rho_o + \rho\right)\left(\vec{V}_o + \vec{V}\right)\right\} = 0 \quad . \tag{7}$$

The vector $\vec{V}_o$ represents any drifting velocity of the plasma and has been assumed to be zero. In addition, since the equilibrium mass density is not a function of time, Eq. (7) can be simplified as follows:

$$\frac{\partial \rho}{\partial t} + \nabla\cdot\left\{\left(\rho_o + \rho\right)\vec{V}\right\} = 0 \quad . \tag{8}$$

It is convenient at this point to linearize Eq. (8). This is done by neglecting the second order term $\rho\vec{V}$ inside the brackets. As stated in the basic assumption, the amplitudes of the disturbances are small enough so that the linearization approximation is valid. Then

$$\frac{\partial \rho}{\partial t} + \nabla\cdot\rho_o\vec{V} = 0 \quad . \tag{9}$$

Applying the vector identity $\nabla\cdot(\phi\vec{A}) = \phi\,\nabla\cdot\vec{A} + \vec{A}\cdot\nabla\phi$, one can write Eq. (9) as

$$n \frac{\partial n}{\partial t} + n n_o \nabla \cdot \vec{V} + n \vec{V} \cdot \nabla n_o = 0 \quad . \tag{10}$$

The term $\vec{V} \cdot \nabla \rho_o$ is neglected in the majority of works on acoustic wave propagation (Refs. 5, 14, 15, and 16). This is valid for a homogeneous plasma (since $\nabla \rho_o = 0$); however, this assumption may not be valid for a plasma with steep electron density gradients. For generality this term will be retained in this derivation of the wave equations.

Now combine Eq. (10) with the approximate adiabatic equation of state for a perfect electron gas:

$$\frac{p}{p_o} = \gamma \left(\frac{n}{n_o} \right) \tag{11}$$

where γ is the ratio of specific heat at constant pressure to specific heat at constant volume. The quantity γ is normally assumed to be 3 for an electron gas (Ref. 25). For a perfect electron gas, take

$$p_o = n_o K_B T \tag{12}$$

and

$$p = n K_B T \tag{13}$$

where K_B is Boltzmann's constant and T is the temperature.

Multiplying both sides of Eq. (10) by γ / n_o and using Eqs. (11), (12), and (13) yields

$$\frac{\partial p}{\partial t} + n n_o \left(\frac{\gamma K_B T}{m} \right) \nabla \cdot \vec{V} + n \left(\frac{\gamma K_B T}{m} \right) \vec{V} \cdot \nabla n_o = 0 \quad . \tag{14}$$

The term in parenthesis is the square of the acoustic velocity (rms thermal velocity) in the electron gas.

$$u_o = \sqrt{\frac{\gamma K_B T}{m}} \tag{15}$$

The final form of the equation is then

$$\frac{\partial p}{\partial t} + mn_o u_o^2 \nabla\cdot\vec{V} + mu_o^2 \vec{V}\cdot\nabla n_o = 0 \quad . \tag{16}$$

Now assume that all of the field quantities have a steady-state time dependence expressed by the factor $e^{j\omega t}$. This factor will be suppressed and the field quantity amplitudes will be considered as phasors having complex values which are functions of position only. Then if $\partial/\partial t$ is replaced by $j\omega$, Eqs. (1), (2), and (6) are linearized, and Eq. (16) is used:

$$\nabla \times \vec{E} = -j\omega\mu_o \vec{H} \quad , \tag{17}$$

$$\nabla \times \vec{H} = j\omega\varepsilon_o \vec{E} + n_o e\vec{V} \quad , \tag{18}$$

$$mn_o(j\omega + \nu)\vec{V} = n_o e\vec{E} - \nabla p \quad , \tag{19}$$

$$j\omega p + mn_o u_o^2 \nabla\cdot\vec{V} + mu_o^2 \vec{V}\cdot\nabla n_o = 0 \quad . \tag{20}$$

Compressibility and the Propagation of Pressure Waves

It will now be shown that an acoustic or pressure field can exhibit wave behavior only in a compressible plasma. For simplicity, assume a plasma that is homogeneous, lossless and of infinite extent. The plasma is excited by a steady-state oscillator at some point which is far from the observation region. Equilibrium quantities are subscripted by a zero. The first order perturbations are not. The basic equations were taken from Stix (Ref. 7) and specialized to a one-component electron plasma. The equations are linearized by neglecting products of all first order terms since small perturbations are assumed.

First consider an incompressible, or cold, plasma with zero temperature.

$$p_o = n_o K_B T = 0 \tag{21}$$

and

$$p = nK_B T = 0 \quad . \tag{22}$$

The convection current density is given by

$$\vec{J} = n_o e \vec{V} \quad . \tag{23}$$

The conservation of momentum equation is

$$m \frac{\partial \vec{V}}{\partial t} = e\vec{E} \quad , \tag{24}$$

since $p = 0$.

The conservation of charge equation is

$$\frac{\partial \rho}{\partial t} + \nabla \cdot \vec{J} = 0 \quad , \tag{25}$$

where the charge density is $\rho = en$.

From Gauss' law,

$$\nabla \cdot \vec{E} = \rho/\varepsilon_o = en/\varepsilon_o \quad . \tag{26}$$

Taking the partial derivative of Eq. (25) with respect to time gives

$$\frac{\partial^2 \rho}{\partial t^2} + \nabla \cdot \frac{\partial \vec{J}}{\partial t} = 0 \quad . \tag{27}$$

Taking the partial derivative of Eq. (23) with respect to time and using Eq. (24) gives

$$\frac{\partial \vec{J}}{\partial t} = \frac{e^2 n_o}{m} \vec{E} \quad . \tag{28}$$

Substituting Eq. (23) into Eq. (27) and using Eq. (26) gives

$$\frac{\partial^2 n}{\partial t^2} + \frac{e^2 n_o}{m\varepsilon_o} n = 0$$

or

$$\frac{\partial^2 n}{\partial t^2} + \omega_p^2 n = 0 \quad , \tag{29}$$

where

$$\omega_p = \sqrt{\frac{e^2 n_o}{m\varepsilon_o}} \tag{30}$$

is the electron plasma frequency.

Although the spatial dependence of a pressure field cannot be determined in this case (since $p = 0$), acoustic phenomena can be related to charge fluctuations, since the acoustic wave results from the collective motion of the particles. From Eq. (29) it is observed that the collective motion of the electron density perturbation (or charge fluctuation since $\rho = en$) is oscillatory in time but is spatially independent. This disturbance does not propagate.

For a compressible plasma, Eqs. (23), (25), and (26) still apply but a pressure term must be included in the conservation of momentum equation.

$$mn_o \frac{\partial \vec{V}}{\partial t} = en_o \vec{E} - \nabla p \quad . \tag{31}$$

For a finite temperature,

$$p_o = n_o K_B T$$

and

$$p = nK_B T \quad .$$

The approximate adiabatic equation of state for an ideal gas is given by

$$\frac{p}{p_o} = \gamma \left(\frac{n}{n_o}\right) \quad .$$

Using Eqs. (23), (25), (26), and (31) and the same procedure used previously gives

$$\frac{\partial^2 n}{\partial t^2} + \omega_p^2 n - \frac{1}{m} \nabla^2 n = 0 \quad ,$$

or

$$\frac{\partial^2 p}{\partial t^2} + \omega_p^2 p - u_o^2 \nabla^2 p = 0 \quad , \tag{32}$$

where u_o is the acoustic velocity (rms thermal velocity) in the electron gas and is given by Eq. (15).

For steady-state time dependence $e^{j\omega t}$, p has the form $p_1 e^{\left(j\omega t - j\vec{K}_p \cdot \vec{r}\right)}$ + $p_2 e^{\left(j\omega t + j\vec{K}_p \cdot \vec{r}\right)}$, where p_1 and p_2 are constants. This is the mathematical representation for a propagating plane wave. If this form of p is substituted into Eq. (32), the dispersion relation is found to be

$$\omega^2 = \omega_p^2 + u_o^2 K_p^2 \quad . \tag{33}$$

It is concluded that a pressure wave can propagate in a compressible plasma with a wavelength ($\lambda_p = 2\pi/K_p$) determined by Eq. (33) for a

given frequency. This is identical to the equation obtained by Bohm and Gross (Ref. 3).

For an inhomogeneous plasma, it is not possible to describe the acoustic wave in terms of a unique propagation constant. It is also found that an acoustic wave is coupled with an electromagnetic wave in an inhomogeneous plasma. The propagation of acoustic waves in an inhomogeneous plasma is described by the coupled wave equations derived in the next chapter.

CHAPTER III

DERIVATION OF THE COUPLED WAVE EQUATIONS

Full-Wave Variables

In a homogeneous plasma, the electromagnetic fields and the dynamic (plasma) fields can be separated into two distinct modes. Energy exchange between the two modes can occur only at an interface and each mode propagates independently of the other. There then exists a pure electromagnetic field and a pure dynamic (plasma) field. The electromagnetic field contains all of the magnetic field and the dynamic field contains all of the charge accumulation (Ref. 14).

In an inhomogeneous plasma (Ref. 6) the separation of the various fields into pure electromagnetic or pure dynamic fields is impossible due to the spatial variation of the plasma properties. Thus an electromagnetic field quantity would consist of an electromagnetic component plus a dynamic component and therefore could not be truly a transverse wave. Similarly, a dynamic field quantity would consist of a dynamic component plus an electromagnetic component and therefore could not be truly a longitudinal wave. This is a fundamental description of the coupling between the two field quantities. It is difficult, however, to investigate quantitatively the coupling effects by evaluating the electromagnetic component and the dynamic component in a given field quantity. These components are referred to as a quasi-electromagnetic mode and a quasi-plasma mode (Ref. 14). Since the given field quantities are described physically by the sum of these quasi-modes, it is desirable to obtain solutions in terms of the total field quantity,

i.e., the sum of the modes. These are referred to in the literature as full-wave variables (Ref. 6), and are simply the field quantities described by the basic equations given in Eqs. (17), (18), (19), and (20). The wave equations describing wave propagation in an inhomogeneous plasma are derived for the full-wave variables using the two-dimensional geometry of Fig. 1.

Vertical Polarization

The electromagnetic and pressure fields are shown in Fig. 2 for a vertically polarized incident electromagnetic wave. The electromagnetic field quantities $\vec{E}$ and $\vec{H}$ are vectors. The pressure p is a scalar quantity represented in Fig. 2 as a wave propagating at some angle θ_p. A steady-state situation is assumed with all field quantities having an $e^{j\omega t}$ time dependence. The radian frequency of the electromagnetic wave is ω. The $e^{j\omega t}$ factor will be suppressed in the derivation since it is common to all field quantities.

Since the plasma is homogeneous in the z direction and the incident wave is a plane wave, there is no loss of generality in assuming that the fields do not vary in the z direction and $\partial/\partial z = 0$ for any field quantity.

The electric field has components E_x and E_y. The magnetic field has only a z component, H_z. The velocity (ordered electron velocity) field has components V_x and V_y. The pressure field has only a magnitude p. These are all complex phasor quantities containing both amplitude and phase information. They are also functions of the spatial coordinates x and y. Instantaneous values are found by

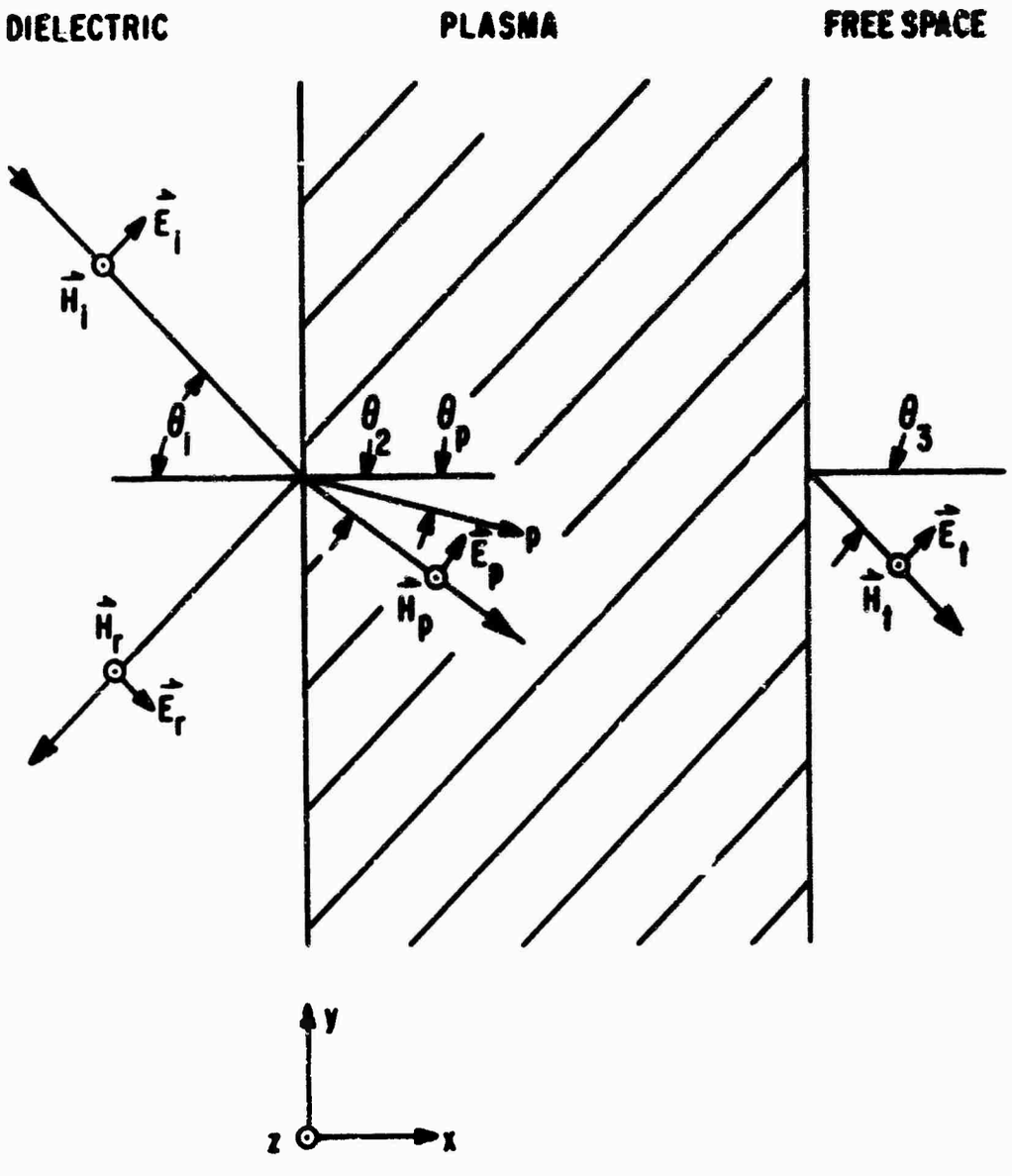

Figure 2. Vertical Polarization

multiplying by $e^{j\omega t}$ and taking the real part.

The linearized basic equations are given again for reference.

$$\nabla \times \vec{E} = -j\omega\mu_o \vec{H} \tag{34}$$

$$\nabla \times \vec{H} = j\omega\varepsilon_o \vec{E} + n_o e \vec{V} \tag{35}$$

$$mn_o(j\omega + \nu) \vec{V} = n_o e \vec{E} - \nabla p \tag{36}$$

$$j\omega p + mn_o u_o^2 \nabla\cdot\vec{V} + mu_o^2 \vec{V}\cdot\nabla n_o = 0 \tag{37}$$

Equations (34) to (37) will now be written in component form using the field components listed above. The approach used is to solve for all of the field components in terms of H_z and p. The wave equations will be derived for H_z and p and the solutions will allow all of the fields in the plasma to be determined.

From Eq. (34),

$$\frac{\partial E_y}{\partial x} - \frac{\partial E_x}{\partial y} = -j\omega\mu_o H_z \quad . \tag{38}$$

From Eq. (35),

$$\frac{\partial H_z}{\partial y} = j\omega\varepsilon_o E_x + n_o e V_x \quad , \tag{39}$$

and

$$-\frac{\partial H_z}{\partial x} = j\omega\varepsilon_o E_y + n_o e V_y \quad . \tag{40}$$

From Eq. (36),

$$mn_o(j\omega + \nu) V_x = en_o E_x - \frac{\partial p}{\partial x} \quad , \tag{41}$$

and

$$nm_o(j\omega + \nu)\ V_y = en_o\ E_y - \frac{\partial p}{\partial y} \quad . \tag{42}$$

From Eq. (37),

$$j\omega p + mn_o u_o^2 \left(\frac{\partial V_x}{\partial x} + \frac{\partial V_y}{\partial y}\right) + mu_o^2\ V_x \frac{\partial n_o}{\partial x} = 0 \quad . \tag{43}$$

For simplicity, define

$$A = j\omega + \nu \quad ,$$

and

$$U = 1 - j\ \nu/\omega \quad .$$

Since the collision frequency has been assumed constant, neither A nor U are functions of the spatial coordinates.

Solving Eq. (41) for V_x and substituting this into Eq. (39) gives

$$j\omega\epsilon_o \left(1 - \frac{\omega_p^2}{\omega^2 U}\right) E_x = \frac{\partial H_z}{\partial y} + \frac{e}{Am} \frac{\partial p}{\partial x} \quad , \tag{44}$$

where ω_p^2 has been defined in Eq. (30). Now define the two quantities

$$\epsilon = \epsilon_o \epsilon_p \tag{45}$$

and

$$\epsilon_p = 1 - \frac{\omega_p^2}{\omega^2 \eta} \quad , \tag{46}$$

where ϵ is the complex permittivity of the plasma.

Equation (44) can then be solved for E_x to give

$$E_x = \frac{1}{j\omega\epsilon} \frac{\partial H_z}{\partial y} + \frac{e}{j\omega\epsilon Am} \frac{\partial p}{\partial x} \tag{47}$$

Solving Eq. (42) for V_y and substituting this into Eq. (40) gives

$$E_y = -\frac{1}{j\omega\epsilon} \frac{\partial H_z}{\partial x} + \frac{e}{j\omega\epsilon Am} \frac{\partial p}{\partial y} \quad . \tag{48}$$

Solving Eq. (41) for E_x and substituting this into Eq. (39) gives

$$V_x = \frac{e}{j\omega\epsilon A m} \frac{\partial H_z}{\partial y} - \frac{\epsilon_o}{\epsilon A m n_o} \frac{\partial p}{\partial x} \quad . \tag{49}$$

Solving Eq. (42) for E_y and substituting this into Eq. (40) gives

$$V_y = - \frac{e}{j\omega\epsilon A m} \frac{\partial H_z}{\partial x} - \frac{\epsilon_o}{\epsilon A m n_o} \frac{\partial p}{\partial y} \quad . \tag{50}$$

Equations (47) to (50) agree with those obtained by Wait (Ref. 22). It is concluded that all field quantities in the plasma can be determined if solutions for H_z and p are found.

Since the plasma is homogeneous in the y direction, the y component of the propagation constant, denoted by K_y, is conserved for all x values. The y component of the propagation constant, K_y, of the plane electromagnetic wave in the dielectric is given by

$$K_y = \omega \sqrt{\mu_o \epsilon_o K_d} \sin \theta_1 \quad , \tag{51}$$

where K_d is the dielectric constant. Following references 5, 12, 13, 15, and 16, the assumed forms of the magnetic field and the pressure in the plasma are

$$H_z = H_z(x)\, e^{jK_y y} \tag{52}$$

and

$$p = p(x)\, e^{jK_y y} \quad . \tag{53}$$

All other field components are assumed to vary in the same manner.

The problem then becomes essentially one-dimensional, since from

Eqs. (52) and (53),

$$\frac{\partial H_z}{\partial y} = jK_y H_z \quad \text{and} \quad \frac{\partial p}{\partial y} = jK_y p$$

describe the y variations of H_z and p. Therefore, $\partial/\partial y$ can be replaced by jK_y and the derivatives with respect to x become total derivatives.

The component forms of the basic equations will now be written with the y dependence of the field components assumed above. Since the $e^{jK_y y}$ factor is common to all the field components, it will be suppressed.

$$\frac{dE_y(x)}{dx} - jK_y E_x(x) = -j\omega\mu_o H_z(x) \tag{54}$$

$$jK_y H_z(x) = j\omega\epsilon_o E_x(x) + n_o e V_x(x) \tag{55}$$

$$-\frac{dH_z(x)}{dx} = j\omega\epsilon_o E_y(x) + n_o e V_y(x) \tag{56}$$

$$mn_o A V_x(x) = en_o E_x(x) - \frac{dp(x)}{dx} \tag{57}$$

$$mn_o A V_y(x) = en_o E_y(x) - jK_y p(x) \tag{58}$$

$$j\omega p(x) + mn_o u_o^2 \left(\frac{dV_x(x)}{dx} + jK_y V_y(x)\right) + mu_o^2 V_x(x) \frac{dn_o}{dx} = 0 \tag{59}$$

The field components are now expressed as functions of x only. The functional dependence on x will be assumed and in the following derivation the notation $H_z(x)$ will be replaced by H_z and similarly for the other field components. Equations (47) to (50) will be used together with Eqs. (54) to (59) to derive the coupled wave equations.

Taking the derivative of Eq. (56) with respect to x gives

$$-\frac{d^2H_z}{dx^2} = j\omega\epsilon_o \frac{dE_y}{dx} + e\frac{d}{dx}\left(n_o V_y\right) \quad , \tag{60}$$

where the product $n_o V_y$ must be retained in the derivative operation since n_o and V_y are functions of x. Substituting dE_y/dx found from Eq. (54) and $n_o V_y$ found from Eq. (50) into Eq. (60) gives

$$-\frac{d^2H_z}{dx^2} = j\omega\epsilon_o\left[-j\omega\mu_o H_z + jK_y E_x\right]$$

$$+ e\frac{d}{dx}\left[-\frac{en_o}{j\omega\epsilon Am}\frac{dH_z}{dx} - \frac{jK_y\epsilon_o}{\epsilon Am}p\right] .$$

Substituting E_x found from Eq. (47) into the equation above gives

$$-\frac{d^2H_z}{dx^2} = K_o^2 H_z - \omega\epsilon_o K_y\left[\frac{K_y}{\omega\epsilon}H_z + \frac{e}{j\omega\epsilon Am}\frac{dp}{dx}\right]$$

$$+ e\frac{d}{dx}\left[-\frac{en_o}{j\omega\epsilon Am}\frac{dH_z}{dx} - \frac{jK_y\epsilon_o}{\epsilon Am}p\right] .$$

where $K_o^2 = \omega^2\mu_o\epsilon_o$. Expanding the derivative in the third term on the right-hand side of the previous equation, noting that n_o and ϵ are functions of x, and performing the necessary multiplications gives

$$-\frac{d^2H_z}{dx^2} = K_o^2 H_z - \frac{K_y^2}{\epsilon_p}H_z - \frac{K_y e}{j\epsilon_p Am}\frac{dp}{dx}$$

$$-\frac{d^2H_z}{dx^2} + \frac{1}{\epsilon_p}\frac{d^2H_z}{dx^2} + \left[\frac{d\left(1/\epsilon_p\right)}{dx}\right]\frac{dH_z}{dx}$$

$$+\frac{eK_y}{j\epsilon_p Am}\frac{dp}{dx} - j\frac{eK_y}{Am}\left[\frac{d\left(1/\epsilon_p\right)}{dx}\right]p \quad .$$

After some simplification:

$$\frac{d^2H_z}{dx^2} + \epsilon_p\left[\frac{d\left(1/\epsilon_p\right)}{dx}\right]\frac{dH_z}{dx} + \left[K_o^2\epsilon_p - K_y^2\right]H_z = \frac{eK_y}{\omega mU}\,\epsilon_p\left[\frac{d\left(1/\epsilon_p\right)}{dx}\right]p \quad .$$

Since

$$\frac{d\left(1/\epsilon_p\right)}{dx} = -\frac{1}{\epsilon_p^2}\frac{d\epsilon_p}{dx} \quad ,$$

the final form of the first of the two coupled differential equations in H_z and p is given by:

$$\frac{d^2H_z}{dx^2} - \left[\frac{1}{\epsilon_p}\frac{d\epsilon_p}{dx}\right]\frac{dH_z}{dx} + \left[K_o^2\epsilon_p - K_y^2\right]H_z = -\frac{eK_y}{\omega mU}\left[\frac{1}{\epsilon_p}\frac{d\epsilon_p}{dx}\right]p \quad . \quad (61)$$

The coupling, in this case, is introduced by the term involving p on the right-hand side of the above equation and the coefficient of p is called the coupling coefficient.

The second coupled differential equation will be obtained from Eq. (59), repeated here for reference.

$$j\omega p + mn_o u_o^2\left[\frac{dV_x}{dx} + jK_yV_y\right] + mu_o^2\,V_x\frac{dn_o}{dx} = 0 \quad .$$

Taking the derivative of V_x (Eq. (49)) with respect to x, multiplying V_y (Eq. (50)) by jK_y, substituting for V_x and replacing these terms in the above equation by the expressions just found give

$$j\omega p + mn_o u_o^2 \left[\frac{d}{dx} \left\{ \frac{eK_y}{\omega \epsilon Am} H_z - \frac{\epsilon_o}{\epsilon Amn_o} \frac{dp}{dx} \right\} \right.$$

$$\left. + jK_y \left\{ - \frac{e}{j\omega \epsilon Am} \frac{dH_z}{dx} - \frac{jK_y \epsilon_o}{\epsilon Amn_o} p \right\} \right]$$

$$+ mu_o^2 \left[\frac{eK_y}{\omega \epsilon Am} H_z - \frac{\epsilon_o}{\epsilon Amn_o} \frac{dp}{dx} \right] \frac{dn_o}{dx} = 0 \quad .$$

Performing the indicated operations and recalling that n_o and ϵ_p are functions of x gives

$$\frac{d^2p}{dx^2} - \left[\frac{1}{\epsilon_p} \frac{d\epsilon_p}{dx} \right] \frac{dp}{dx} + \left[\gamma_p^2 - K_y^2 \right] p$$

$$= \left\{ - \frac{eK_y n_o}{\omega \epsilon_o} \left[\frac{1}{\epsilon_p} \frac{d\epsilon_p}{dx} \right] + \frac{eK_y}{\omega \epsilon_o} \left[\frac{dn_o}{dx} \right] \right\} H_z \quad , \qquad (62)$$

where γ_p^2 is defined as

$$\gamma_p^2 = \frac{\omega^2}{u_o^2} \left[1 - \frac{\omega_p^2}{\omega^2} - j \frac{\nu}{\omega} \right] \quad . \qquad (63)$$

Equation (62) is the second coupled differential equation in H_z and p. The coupling, in this case, is introduced by the term involving H_z on the right-hand side of Eq. (62). The two Eqs. (61) and (62) are identical to those derived by Burman (Ref. 16) if the collision frequency is assumed constant and the third term on the left-hand side of Eq. (37) is neglected (which is not necessarily valid for the plasmas considered here). When this term is retained in the derivation, the

coefficient of dp/dx in Eq. (62) is modified slightly (the coefficient in Burman's equation is $-1/\varepsilon_p n_o \; d/dx \; (\varepsilon_p n_o)$, and the coupling coefficient contains an additional term which involves the derivative of the electron density with respect to x). The coupling coefficients in both Eqs. (61) and (62) depend on either $d\varepsilon_p/dx$ or dn_o/dx. If the plasma is homogeneous, both of these factors are zero and the equations are uncoupled.

Horizontal Polarization

An incident electromagnetic wave, horizontally polarized, is shown in Fig. 3. Again, there is no loss of generality in assuming that the field components do not vary in the z direction, with $\partial/\partial z = 0$. The electric field has only a z component, E_z, but now the magnetic field has components H_x and H_y. The ordered electron velocity will be assumed to have components V_x, V_y, and V_z. The pressure field represents a scalar quantity which can be a function of x and y.

Equations (34) to ( ) are now written in component form for the case of horizontal polarization:

$$\frac{\partial E_z}{\partial y} = -j\omega\mu_o H_x \tag{64}$$

$$-\frac{\partial E_z}{\partial x} = -j\omega\mu_o H_y \tag{65}$$

$$-\frac{\partial H_y}{\partial z} = 0 = n_o e V_x \tag{66}$$

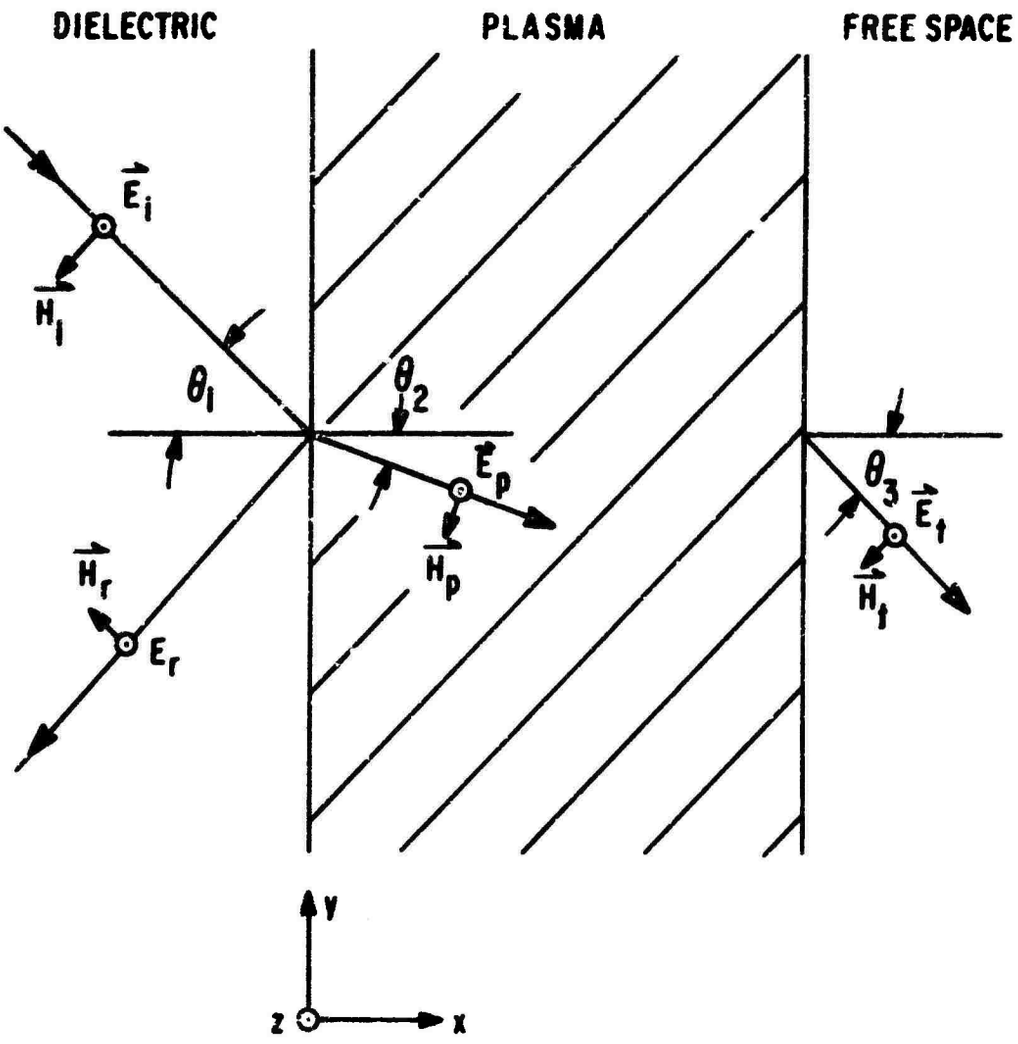

Figure 3. Horizontal Polarization

$$\frac{\partial H_x}{\partial z} = 0 = n_o e V_y \tag{67}$$

$$\frac{\partial H_y}{\partial x} - \frac{\partial H_x}{\partial y} = j\omega\epsilon_o E_z + n_o e V_z \tag{68}$$

$$j\omega p + m n_o u_o^2 \left[\frac{\partial V_x}{\partial x} + \frac{\partial V_y}{\partial y} + \frac{\partial V_z}{\partial z} \right] + m u_o^2 V_x \frac{dn_o}{dx} = 0 \tag{69}$$

Since H_y and H_x do not vary in the z direction, Eqs. (66) and (67) show that V_x and V_y are identically zero everywhere in the plasma. Equation (68) indicates that there can be a z component of the velocity; however, it has been assumed that all field components are constant in the z direction so $\partial V_z/\partial z = 0$. Also, since V_x and V_y are zero everywhere, $\partial V_x/\partial x = 0$ and $\partial V_y/\partial y = 0$. Equation (69) then becomes

$$j\omega p = 0$$

or

$$p = 0 \quad .$$

This implies that the pressure field is identically zero everywhere in the plasma; hence, the acoustic mode is not excited.

CHAPTER IV

NUMERICAL SOLUTION OF THE COUPLED WAVE EQUATIONS

Coupled Equations

The term "coupled equations" describes a set of simultaneous differential equations with the following properties (Ref. 26):

(1) There is one independent variable which in this derivation is the distance x.

(2) The number of equations is the same as the number of dependent variables.

(3) In each equation one dependent variable appears in derivatives of higher order than the others. The terms with this variable are called "principal" terms and the remaining terms "coupling" terms.

(4) The principal terms contain a different dependent variable in each equation, so that each dependent variable appears in the principal terms of one and only one equation.

Clemmow and Heading (Ref. 27) add one more property when the equations describe wave propagation:

(5) In a homogeneous medium the right-hand sides of the equations vanish since the coefficients of these coupling terms contain, as factors, derivatives of the properties of the medium. The left-hand sides then give the characteristic waves. Equations (61) and (62) have all of the properties described above.

There are several methods which can be used in solving coupled wave equations. Solutions can be found by successive approximations where the first approximation is to neglect the coupling terms and

solve the resulting equations. The values obtained for the dependent variables are substituted in the coupling terms and the resulting equations are solved to give a better approximation. Where a coupling term is large, the method of successive approximations cannot be used. When the coupling can be neglected, WKB solutions can be obtained; however, these solutions fail near regions of reflection or coupling (Ref. 26). The two equations can be uncoupled by combining the two into a single fourth order differential equation in one dependent variable. This equation must then be solved. The two second order equations can also be reduced to four first order equations which are also coupled. These can be solved by matrix methods. Burman (Ref. 15) gives four different methods of solution for the coupled wave equations; however, a slowly varying medium is assumed. Another possible solution is to integrate numerically the coupled wave equations. This is the method used later in this chapter. The main advantage of this method is that coupling terms are <u>not</u> neglected and the solutions are valid in media with rapidly varying properties.

The existence and uniqueness of solutions obtained for Eqs. (17) to (20) are considered here. Sancer (Ref. 20) has discussed the boundary conditions which yield unique solutions to the linearized warm plasma equations which are used in this derivation. Solutions to these equations exist, for simple geometries, if one requires that 2 + M scalar boundary conditions are satisfied at each boundary. The number of different types of particles, M, considered in the equations of motion is 1 for an electron gas. The boundary conditions used are the two electromagnetic boundary conditions (continuity of tangential $\vec{E}$

and $\vec{H}$), plus a single acoustic boundary condition which depends on the type of boundary considered. Therefore, solutions to the equations can be found. The two different acoustic boundary conditions are the vanishing of the normal component of the electron velocity and the continuity of the pressure across a boundary. Sancer shows that either of these conditions when used with the two electromagnetic boundary conditions leads to a unique solution.

Plasma Profiles

The plasmas of interest have steep electron density gradients near the wall ($x = 0$) rising to a peak value at a distance very near the wall. The electron density then decreases from the peak as the temperature becomes lower and ionization is less. Consideration is given to very thin plasma "sheaths" where the region of interest is 5 mm or less away from the wall. Electron density, temperature, and collision frequency profiles are illustrated for a typical sheath in Fig. 4. The temperature profile is similar in form to the electron density profile. This is due to the fact that the number of electrons depends on the degree of ionization which in turn depends on the temperature. For a reentry type plasma, the high temperatures are associated with aerodynamic heating which occurs when a vehicle reenters the atmosphere. The collision frequency profile is almost constant across the sheath. As a first approximation, the collision frequency will be taken to be constant. The collision frequency will be larger for larger peak electron densities.

An electron density profile that has a linear increase from the wall to the peak is used. This profile is simple enough for a fairly

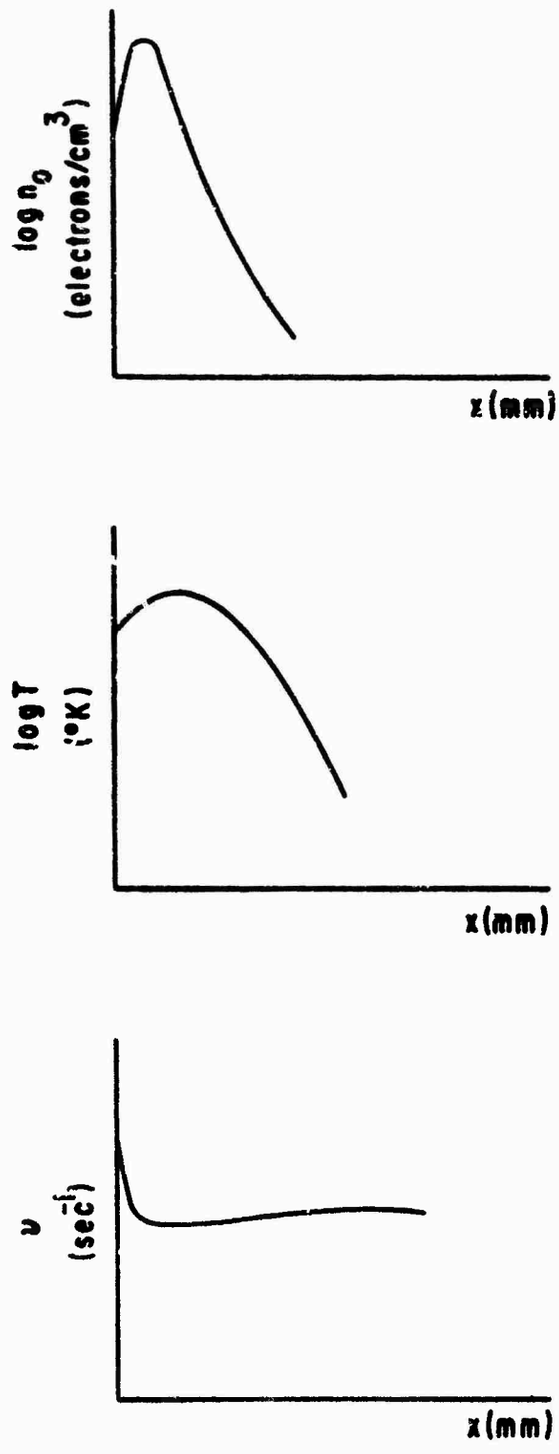

Figure 4. Typical Plasma Sheath Profiles

straightforward numerical analysis; however, by taking the linear increase near the wall large enough, a meaningful study of the effect of plasma inhomogeneity on pressure wave propagation in the plasma can be made. There are two basic profiles considered with the linearly increasing electron density. The first profile is shown in Fig. 5(a). In this case, the electron density is assumed to decrease abruptly to zero at the outer boundary. The outer boundary is then just a plane dividing the plasma and free space. The second profile is shown in Fig. 5(b). Here the electron density beyond the peak is taken to be a constant equal to the peak electron density. In this homogeneous region, the wave equations are uncoupled. The electromagnetic and acoustic waves propagate independently with propagation constants determined by Eqs. (129) and (130), respectively. It is shown later (Fig. 22) that the acoustic wave is attenuated rapidly in this region. Since the acoustic wave decays to a very small fraction of its amplitude at the peak within a very short distance from the peak, the model is shown as semi-infinite in the figure. The temperature profiles are taken to be linearly increasing also, and follow either Fig. 5(a) or 5(b) in form. The collision frequency is assumed to be a constant.

Boundary Conditions

First consider the boundary conditions at the wall ($x = 0$). For convenience (in the numerical solution and the approximate solution) the value of H_z at $x = 0$ is considered to be a known constant ($0.1 + j0.1$ in all cases) $H_z(0)$. Using $H_o = \frac{H_z(0)}{1 + R}$ and Poynting's theorem in the dielectric, and assuming that an area of 1 in^2 is considered, this value of $H_z(0)$ corresponds to an incident electromagnetic wave with a

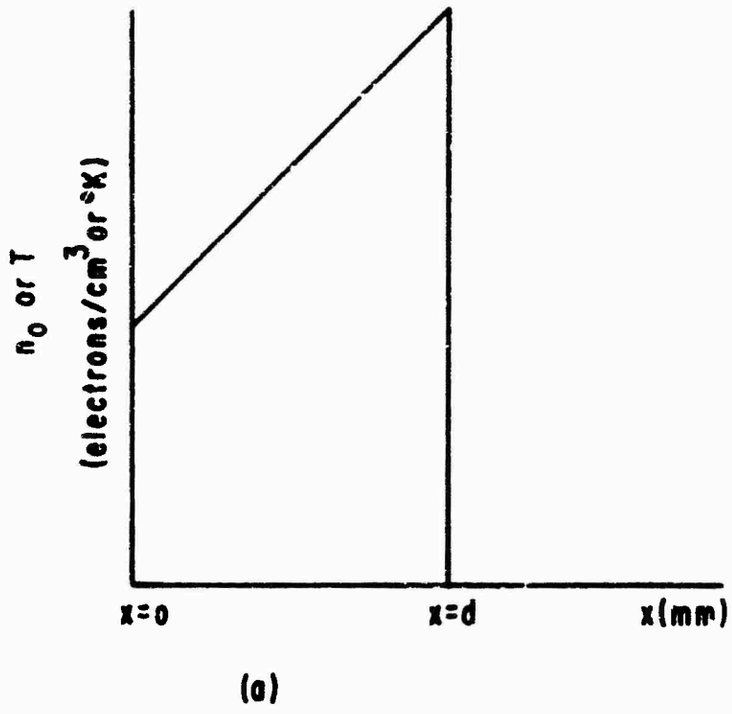

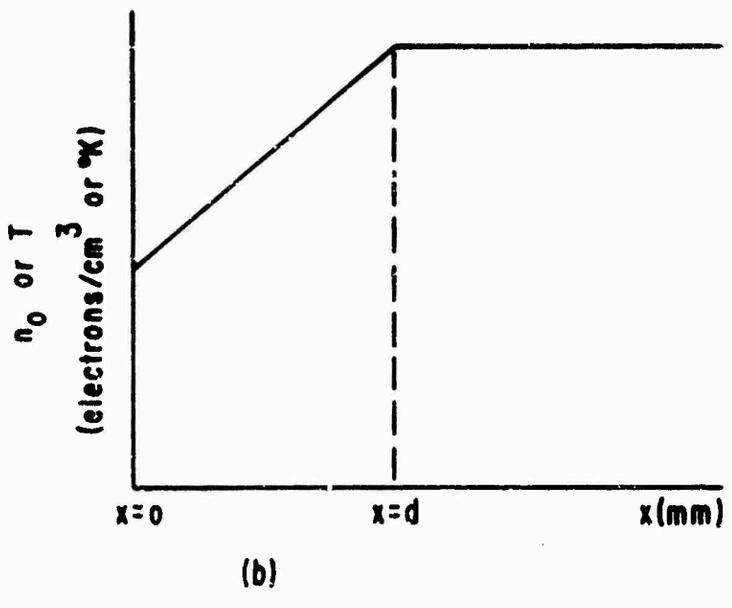

Figure 5. Plasma Profile Models

power of from 6 mw to 24 mw (for R = 1 or R = 0 above), which is an easily obtainable power level. The two electromagnetic boundary conditions can be used at this boundary to determine the amplitude of the incident electromagnetic wave and the value of the reflection coefficient. Using these two boundary conditions gives

$$R = \frac{\eta_d \cos \theta_1 \, H_z(0) - E_y(0)}{\eta_d \cos \theta_1 \, H_z(0) + E_y(0)} \quad , \tag{70}$$

where η_d is the characteristic impedance of the dielectric, and

$$H_o = \frac{H_z(0)}{1 + R} \quad , \tag{71}$$

where H_o is the amplitude of the incident electromagnetic field. The electric field at the boundary, $E_y(0)$, can be computed from the H_z and p solutions in the plasma using Eq. (48). The acoustic boundary condition used at this dielectric-plasma interface is the vanishing of the normal component of the electron velocity (V_x). From Eq. (49) this results in a specification of the derivative of the pressure at the boundary,

$$\left.\frac{dp}{dx}\right|_{x=0^+} = \frac{eK_y n_o(0^+)}{\omega \varepsilon_o} H_z(0^+) \tag{72}$$

where $n_o(0^+)$ is the electron density at the wall.

Now consider the boundary conditions at the distance corresponding to the peak in electron density. The two electromagnetic boundary conditions are the same for either of the two plasma profiles considered in Fig. 5. The acoustic boundary condition will be different for the two profiles. For the profile in Fig. 5(a) the rigidity boundary condition is used which imposes a zero normal component of the electron velocity at this boundary. This implies that all of the electrons

taking part in the collective motion are reflected at the boundary and none penetrate into free space. Using Eq. (49), the derivative of the pressure at this boundary is determined:

$$\left.\frac{dp}{dx}\right|_{x=d^-} = \frac{eK_y n_o(d^-)}{\omega\epsilon_o} H_z(d^-) \quad , \tag{73}$$

where $n_o(d^-)$ is the peak electron density and $H_z(d^-)$ is the amplitude of the magnetic field at this boundary. For the profile in Fig. 5(b) the dynamic boundary condition is used. This acoustic boundary condition states that the force on one side of the boundary must balance the force on the other side of the boundary. This implies that the pressure be continuous across the boundary except at an interface between a compressible medium and an incompressible medium. The kinetic boundary condition of continuity of the normal component of the electron velocity is also used.

The condition of continuity of E_y at the outer boundary ($x = d$) determines the derivative of H_z at the outer boundary. For the profile of Fig. 5(a), using Eq. (48) for E_y gives

$$-\frac{1}{j\omega\epsilon(d^-)}\left.\frac{dH_z}{dx}\right|_{x=d^-} + \frac{eK_y}{\omega\epsilon(d^-)Am}\,p(d^-) = -\frac{1}{j\omega\epsilon_o}\left.\frac{dH_z}{dx}\right|_{x=d^+} \quad . \tag{74}$$

Now assume that the electromagnetic field for $x > d$ has only an outward going component of the form $e^{-jK_{ox}x}$, where

$$K_{ox} = \sqrt{K_o^2 - K_y^2} \tag{75}$$

is the x component of the free space propagation constant for electromagnetic waves. Solving Eq. (74) for $(dH_z/dx)_{x=d^-}$, gives

$$\left.\frac{dH_z}{dx}\right|_{x=d^-} = j\frac{eK_y}{Am}\,p(d^-) - j\varepsilon_p(d^-)K_{ox}H_z(d^+) \quad .$$

It is shown in Appendix C that for the peak electron densities of interest, the second term on the left-hand side of Eq. (74) is completely negligible compared to the other terms in the equation. Therefore, to a very good approximation

$$\left.\frac{dH_z}{dx}\right|_{x=d^-} = -j\varepsilon_p(d^-)K_{ox}H_z(d^+) \quad . \tag{76}$$

A slightly different expression results for the derivative of H_z at the outer boundary for the profile of Fig. 5(b). If E_y is taken to be continuous at $x = d$ and Eq. (48) is used for E_y, the expression for the derivative of H_z at $x = d$ becomes

$$-\frac{1}{j\omega\varepsilon_p(d^-)}\left.\frac{dH_z}{dx}\right|_{x=d^-} + \frac{eK_y}{\omega\varepsilon_p(d^-)Am}\,p(d^-) = \frac{eK_y}{\omega\varepsilon_p(d^+)Am}\,p(d^+)$$

$$-\frac{1}{j\omega\varepsilon_p(d^+)}\left(-\gamma_{hx}H_z(d^+)\right) \quad . \tag{77}$$

Since p and H_z are continuous and $\varepsilon_p(d^-) = \varepsilon_p(d^+)$ at $x = d$,

$$\left.\frac{dH_z}{dx}\right|_{x=d^-} = -\gamma_{hx}H_z(d^+) \quad , \tag{78}$$

where γ_{hx} is the x component of the complex propagation constant of the electromagnetic wave in the homogeneous plasma region.

Solutions for all field quantities in all three regions can be obtained from six boundary conditions, three at each boundary. In the numerical solutions, four boundary conditions are used to solve the two second order coupled wave equations for the fields in the plasma layer for the profile of Fig. 5(a). The conditions are:

(1) $$H_z(0^+) = 0.1 + j0.1 \tag{79}$$

(2) $$\left.\frac{dp}{dx}\right|_{x=0^+} = \frac{eK_y E_c(0^+)}{\omega\epsilon_c} H_z(0^+) \tag{80}$$

(3) $$\left.\frac{dH_z}{dx}\right|_{x=d^-} = -j\epsilon_p K_{ox} H_z(d^-) \tag{81}$$

(4) $$\left.\frac{dp}{dx}\right|_{x=d^-} = \frac{eK_y E_c(d^-)}{\omega\epsilon_c} H_z(d^-) \tag{82}$$

The boundary at $x = d$ for the plasma profile of Fig. 5(b) is not associated with boundary conditions related to an interface dividing two different media, but to an interface where the form of the plasma profile changes (the medium remains the same). One extra unknown is introduced in this case--the pressure field in the homogeneous region which did not exist in the case of Fig. 5(a), since the region for $x > d$ was free space. Instead of the single acoustic boundary condition, two independent acoustic boundary conditions are used at this interface. The first one is the continuity of the pressure across the interface, or

$$p(d^-) = p(d^+) \tag{83}$$

The second one is the continuity of the normal component of the ordered electron velocity across the interface, or

$$V_x(d^-) = V_x(d^+) \tag{84}$$

which gives (using Eq. (49) and the continuity of H_z at $x = d$)

$$\left.\frac{dp}{dx}\right|_{x=d^-} = \left.\frac{dp}{dx}\right|_{x=d^+} \quad . \tag{85}$$

If only an outgoing pressure wave is assumed to exist in the homogeneous region (no reflection), this becomes

$$\left.\frac{dp}{dx}\right|_{x=d^-} = -\gamma_{px}\, p(d^+) \quad , \tag{86}$$

where γ_{px} is the x component of the complex propagation constant of the acoustic wave in the homogeneous plasma region. The ordinary electromagnetic boundary conditions (E_y and H_z continuous) are used at the x = d boundary for profile (b) also. The boundary conditions used in the numerical solution for profile (b) are:

(1) $$H_z(0^+) = 0.1 + j0.1 \tag{87}$$

(2) $$\left.\frac{dp}{dx}\right|_{x=0^+} = \frac{eK_\gamma n_o(0^+)}{\omega\varepsilon_o} H_z(0^+) \tag{88}$$

(3) $$\left.\frac{dH_z}{dx}\right|_{x=d^-} = -\gamma_{hx} H_z(d^-) \tag{89}$$

(4) $$\left.\frac{dp}{dx}\right|_{x=d^-} = -\gamma_{px}\, p(d^+) \tag{90}$$

(5) $$p(d^-) = p(d^+) \quad .$$

Finite Difference Numerical Solution

Solutions of the two coupled wave equations will be obtained by replacing the two ordinary differential equations with their finite difference approximations. The two equations are

$$\frac{d^2H_z}{dx^2} + A\frac{dH_z}{dx} + BH_z = Cp \tag{91}$$

and

$$\frac{d^2p}{dx^2} + D\frac{dp}{dx} + Ep = FH_z \quad , \tag{92}$$

where the principal terms are on the left-hand side of the equations and the coupling terms are on the right-hand side. The coefficients are defined as follows:

$$A = -\frac{1}{\epsilon_p}\frac{d\epsilon_p}{dx} \quad , \tag{93}$$

$$B = K_o^2\epsilon_p - K_y^2 \quad , \tag{94}$$

$$C = -\frac{eK_y}{\omega mU}\left[\frac{i}{\epsilon_p}\frac{d\epsilon_p}{dx}\right] \quad , \tag{95}$$

$$D = -\frac{1}{\epsilon_p}\frac{d\epsilon_p}{dx} \quad , \tag{96}$$

$$E = \frac{\omega^2}{u_o^2}\left[1 - \frac{\omega_p^2}{\omega^2} - j\frac{\nu}{\omega}\right] - K_y^2 \quad , \tag{97}$$

$$F = -\frac{eK_y n_o}{\omega\epsilon_o}\left[\frac{1}{\epsilon_p}\frac{d\epsilon_p}{dx}\right] + \frac{eK_y}{\omega\epsilon_o}\frac{dn_o}{dx} \quad . \tag{98}$$

The coefficients of the coupled equations are complex; therefore, the finite difference approximations will involve complex quantities. Computations involving the complex quantities are handled easily using the complex arithmetic capabilities of the FORTRAN IV language on the CDC 6600 computer. The main advantage of using the numerical solution is that the coupling terms are retained in the field solutions.

Since the equations are ordinary differential equations, in one independent variable, x, the first step is to divide the x-axis into a number of equally spaced points as shown in Fig. 6. The step size is indicated by h. In the finite difference numerical solution, the variable i corresponds to discrete points on the x-axis. Solutions for H_z and p will consist of values of H_z and p computed, at x values corresponding to i, from the finite difference approximations to the differential equations. The fields computed at the discrete points will be designated as H_{zi} and p_i.

Letting f represent either field quantity, the central difference approximation used for the second derivative is (Ref. 28)

$$\frac{d^2f}{dx^2} \cong \frac{f_{i+1} - 2f_i + f_{i-1}}{h^2} \quad , \tag{99}$$

where the error associated with this approximation is equal to

$$\frac{h^2}{12} \phi M_4$$

where $|\phi| \leq 1$ and M_4 is the largest value of the fourth derivative of the function in the region of interest. The finite difference approximation used for the first derivative is the central difference formula

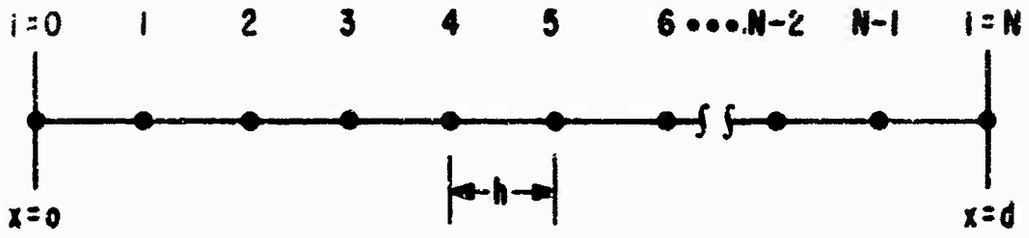

Figure 6. The x-Axis for a Finite Difference Solution

(Ref. 25)

$$\frac{df}{dx} \cong \frac{f_{i+1} - f_{i-1}}{2h} \quad , \tag{100}$$

where the error associated with this approximation is equal to

$$\frac{h^2}{6} \phi M_3$$

where $|\phi| \leq 1$ and M_3 is the largest value of the third derivative in the region of interest. When these approximations are used for the derivatives in Eqs. (91) and (92), the two equations become (in finite difference form):

$$\frac{H_{z(i+1)} - 2H_{zi} + H_{z(i-1)}}{h^2} + A\left[\frac{H_{z(i+1)} - H_{z(i-1)}}{2h}\right] + BH_{zi} = Cp_i \tag{101}$$

and

$$\frac{p_{i+1} - 2p_i + p_{i-1}}{h^2} + D\left[\frac{p_{i+1} - p_{i-1}}{2h}\right] + Ep_i = FH_{zi} \quad . \tag{102}$$

The solutions for H_{zi} and p_i now require the solution of 2(N+1) linear algebraic equations where N+1 is the number of points. The solution of 2(N+1) equations is required since H_{zi} and p_i must be determined from Eqs. (101) and (102) at a total of N+1 points. To improve the accuracy of the numerical solution, the step size h can be reduced (the errors are proportional to h^2); however, this would increase N, requiring the solution of a larger number of algebraic equations.

The replacement of the differential equations by the finite difference approximations, Eqs. (101) and (102), is standard. The numerical technique really depends upon the method chosen for the solution of the resulting algebraic equations. The method used here is to solve for H_{zi} and p_i from the finite difference equations. This gives

$$H_{zi} = \frac{-h^2 C p_i + H_{z(i+1)}\left[1 + \frac{hA}{2}\right] + H_{z(i-1)}\left[1 - \frac{hA}{2}\right]}{2 - h^2 B} \qquad (103)$$

and

$$p_i = \frac{-h^2 F H_{zi} + p_{i+1}\left[1 + \frac{hD}{2}\right] + p_{i-1}\left[1 - \frac{hD}{2}\right]}{2 - h^2 E} \,. \qquad (104)$$

An iterative method for solving the equations is used. A first approximation is used to calculate a second approximation which in turn is used to calculate a third, and so on. Since the same formula (Eqs. (103) and (104)) is used to calculate each approximation, the iterative process is said to be stationary. The formulas used describe a point-method since the next approximation at one point is explicitly expressed in terms of known values at other points. The iterative procedure is convergent when the differences between the exact solution and the iterative approximations tend to zero as the number of iterations increases. The iterative process described below is called a Jacobi iterative method (Ref. 29). Initial guesses are made for H_{zi} and p_i across the entire plasma layer ($x = 0$ to $x = d$). New values for H_{zi} and p_i are computed at each point using Eqs. (103) and (104) and the

initial guesses for H_{zi} and p_i. H_{zi} and p_i are again computed at each point using the H_{zi} and p_i values found in the first iteration. The procedure is repeated until the solution converges such that H_{zi} and p_i satisfy Eqs. (101) and (102) at all points across the layer. When this occurs, the H_{zi} and p_i computed from Eqs. (103) and (104) will be unchanged from one iteration to the next. This will never happen, of course, because of the errors in a finite difference solution; however, convergence will be assumed when the change in H_{zi} and p_i between successive iterations becomes small. The convergence of a typical H_{zi} solution is illustrated in Fig. 7 as a function of the number of iterations. The convergence of the p_i solution is much faster, as shown in Fig. 8. A typical value for h is d/50.

Since the plasma is bounded, the field solutions are constrained to obey certain conditions at the boundaries (see the previous section, Boundary Conditions). These are included in the numerical solutions by requiring that H_{zi} and p_i obey these conditions. One such condition is that $H_{zo}(i=0)$ be held constant. All other boundary conditions involve the derivative of the field quantities. The derivatives at the boundaries are finite difference approximations obtained from a Taylor series expansion of the function (Ref. 28) at the appropriate boundary. For the derivative at the wall (x = 0)

$$\left.\frac{df}{dx}\right|_{x=0^+} = \frac{-f_2 + 4f_1 - 3f_o}{2h}$$

where the number subscripts are the values of i. For the far boundary (x = d)

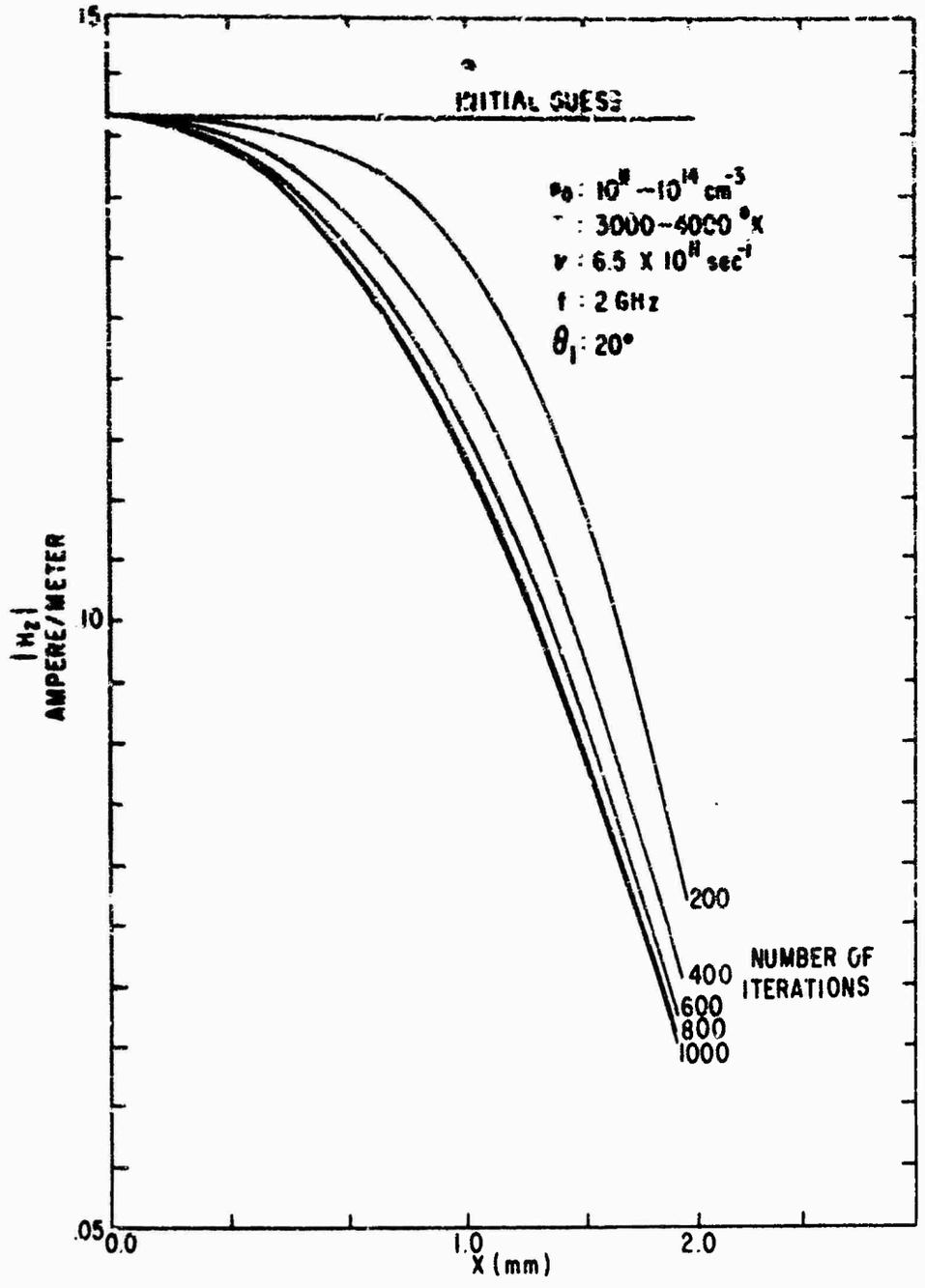

Figure 7. Sample Convergence of the H_{zi} Solution

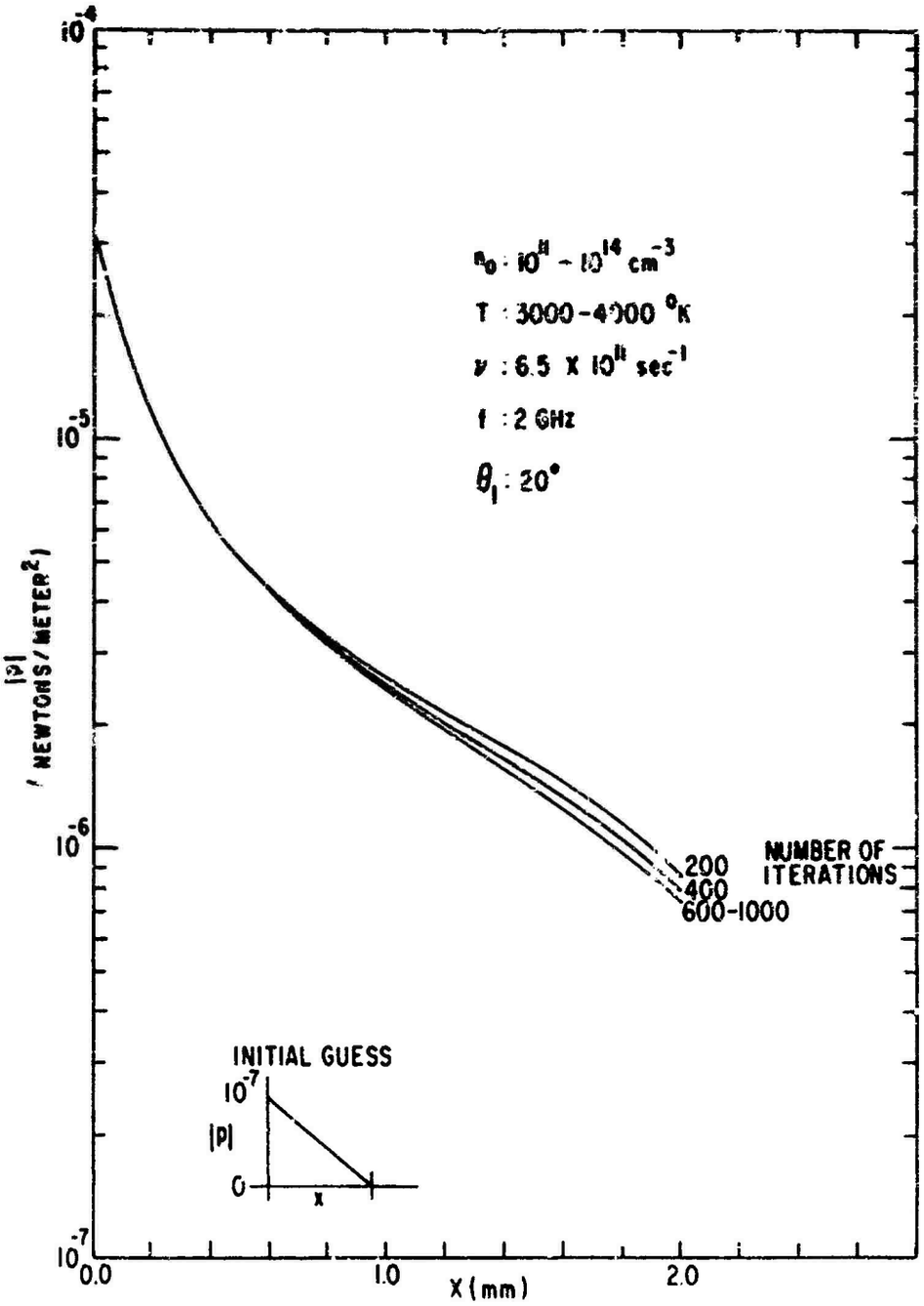

Figure 8. Sample Convergence of the p_i Solution

$$\left.\frac{df}{dx}\right|_{x=d^-} = \frac{3f_N - 4f_{N-1} + f_{N-2}}{2h} .$$

The derivative values will be used to solve for the field quantities at the boundaries. Letting

$$f'_{0^+,d^-} = \left.\frac{df}{dx}\right|_{x=0^+,d^-} ,$$

and solving for the boundary values gives

$$f_0 = \frac{-2hf'_{0^+} - f_2 + 4f_1}{3} \qquad (105)$$

and

$$f_N = \frac{2hf'_{d^-} - f_{N-2} + 4f_{N-1}}{3} . \qquad (106)$$

The boundary conditions applied in the numerical solution and used for either model (Fig. 5(a) or 5(b)) are expressed as follows:

$$\text{at } x = 0: \quad H_{z0} = Z_1$$

$$\frac{dp}{dx} = Z_2$$

$$\text{at } x = d: \quad \frac{dH_z}{dx} = Z_3$$

$$\frac{dp}{dx} = Z_4 ,$$

where Z_1 to Z_4 are complex numbers. The value of H_z at $x = 0$ is fixed. The values of the derivatives of the functions at the boundaries are used to calculate the function values at the boundaries (except, of

course, for the value of E_z at $x = 0$). Equations (105) and (106) are used to calculate the function values at the boundaries as follows:

$$p_0 = \frac{-2hZ_2 - p_2 + 4p_1}{3} \quad .$$

Using Eq. (106) at $x = d$ gives

$$p_N = \frac{2hZ_4 - p_{N-2} + 4p_{N-1}}{3}$$

and

$$H_{zN} = \frac{2hZ_3 - H_{z(N-2)} + 4H_{z(N-1)}}{3} \quad .$$

The boundary values are up-dated in this manner at the end of each iteration and are used for calculations in the succeeding iteration.

Coefficients of the Coupled Equations

The complex coefficients of the coupled wave equations (61) and (62) determine the forms of the solutions for H_z or p. The importance of the magnitudes of the coefficients is illustrated in the next section. By working with the coefficients for various plasma profiles and operating frequencies, one finds that certain coefficients are much more important than others. The coupling coefficient F is perhaps the most significant coefficient. When the exact form of the continuity equation (Eq. (10)) is used, coefficient F is given by

$$F = -\frac{eK_y n_0}{\omega\varepsilon_0}\left[\frac{1}{\varepsilon_p}\frac{d\varepsilon_p}{dx}\right] + \frac{eK_y}{\omega\varepsilon_0}\frac{dn_0}{dx} \quad . \qquad (107)$$

This coupling coefficient as given by Burman (Ref. 16) includes only

the first term. The absolute values of the coefficient F given by Eq. (10) and given by Burnam (Ref. 10) are plotted in Fig. 9. It is observed that the F including the additional term is larger, especially at the smaller electron densities. Since, in the inhomogeneous region, the pressure is essentially proportional to F, the magnitude of F could make a large difference in the pressure amplitude. The other coupling coefficient is plotted in Fig. 10. Both coupling coefficients reach a maximum value at the same distance into the plasma. The peak in the curve representing coefficient F is caused by a minimum in ε_p at a point where $\omega_p = \omega$; i.e., an x value where the electron density n_o results in a value of ω_p

$$\left[\omega_p = \sqrt{\frac{n_o e^2}{\varepsilon_o m}}\right]$$

equal to the operating frequency. Since n_o is assumed to be linearly increasing, the x dependence of F is given by n_o/ε_p; therefore, the coupling coefficient is directly proportional to the density and inversely proportional to the relative dielectric constant of the plasma given by

$$\varepsilon_p = 1 - \frac{\omega_p^2}{\omega^2+\nu^2} - j\frac{\nu}{\omega}\frac{\omega_p^2}{\omega^2+\nu^2}$$

for a lossy plasma and

$$\varepsilon_p = 1 - \frac{\omega_p^2}{\omega^2}$$

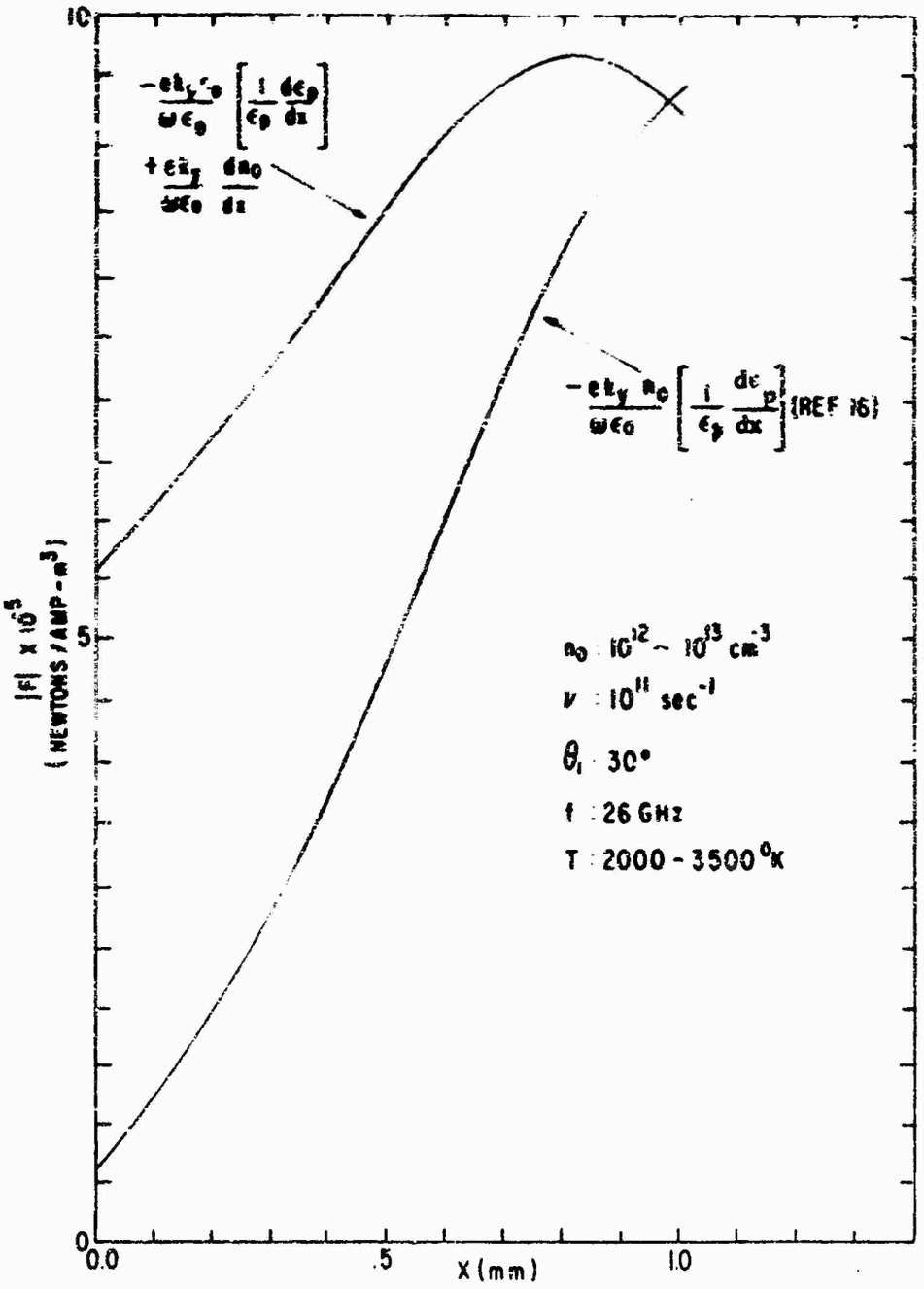

Figure 9. Coupling Coefficient F

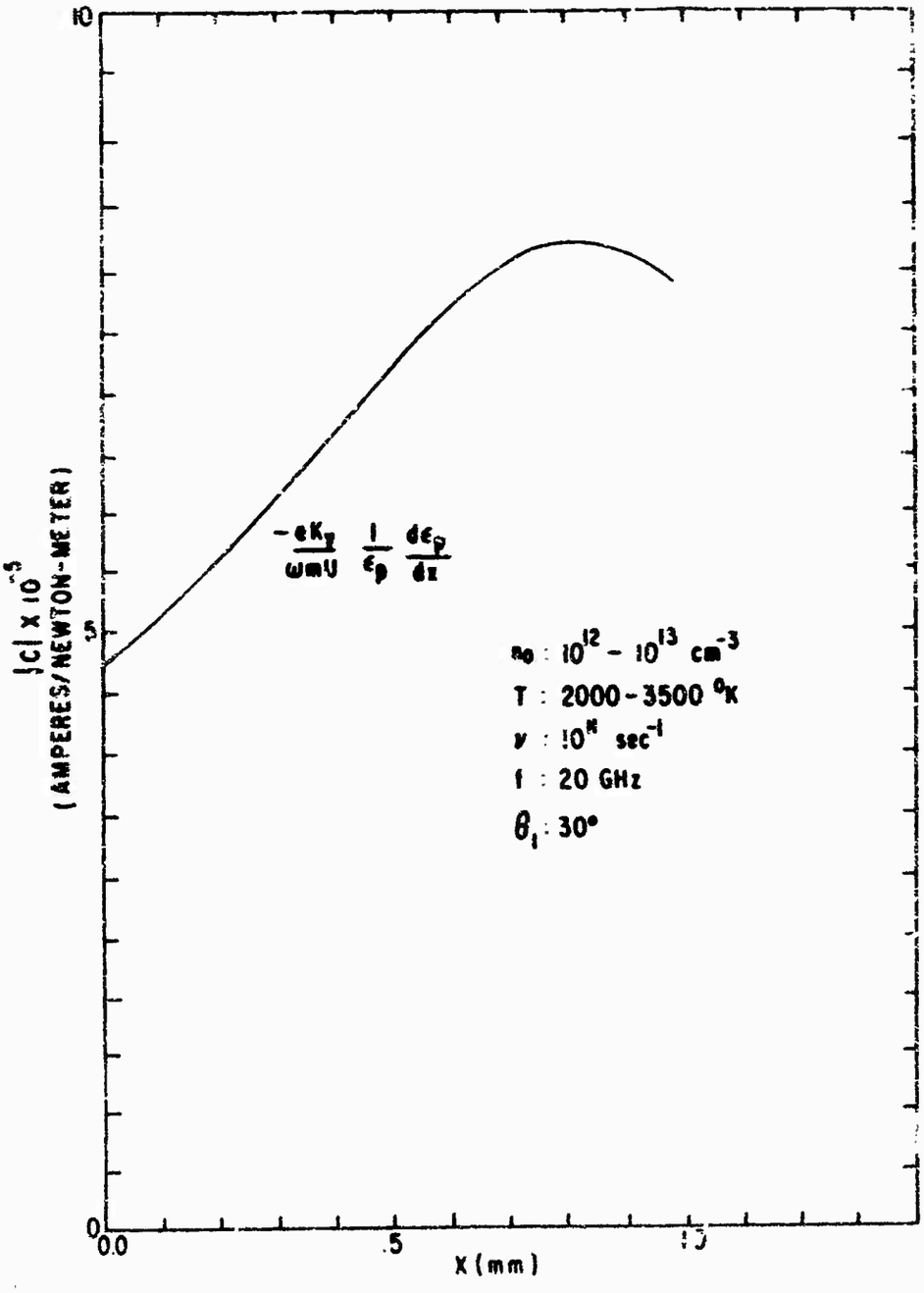

Figure 10. Coupling Coefficient C

for a lossless plasma. For a lossless plasma $\epsilon_p = 0$ for $\omega_p = \omega$ and F would be infinite; however, ϵ_p has a minimum for $\omega_p = \omega$ in a lossy plasma and F has a peak value at the distance x where $\omega_p = \omega$. The peak will be less sharp for larger collision frequencies.

The other coefficients are given in Appendix B for a typical plasma profile and operating frequency.

Approximate Solution

In determining an approximate solution, the relative magnitudes of the terms in the equations are considered. If some terms in the equations are much smaller than others, these can be neglected and the equations simplified. The procedure is described below:

(1) Replace a second derivative term by the dependent variable in the derivative divided by the square of the characteristic length (the plasma thickness, d).

(2) Replace a first derivative term by the dependent variable in the derivative divided by the characteristic length.

(3) Determine the relative magnitude of the resulting terms from the coefficient magnitudes.

For the two coupled differential equations the first two steps result in:

$$\left(\frac{1}{d^2} + \frac{A}{d} + B\right) H_z = Cp \tag{108}$$

$$\left(\frac{1}{d^2} + \frac{D}{d} + E\right) p = FH_z \tag{109}$$

For an electron density profile which increases linearly from 10^{11} electrons/cm^3 to 10^{12} electrons/cm^3 in 2 mm, it is shown in Appendix A that for certain frequencies the above equations become

$$\left(\frac{1}{d^2} + \frac{A}{d}\right) H_z = Cp \tag{110}$$

and

$$Ep = FH_z \tag{111}$$

with the other terms being much smaller. Substituting for p in Eq. (110) from Eq. (111) gives

$$\left(\frac{1}{d^2} + \frac{A}{d}\right) H_z = \frac{CF}{E} H_z \quad , \tag{112}$$

or

$$\left(\frac{1}{d^2} + \frac{A}{d} - \frac{CF}{E}\right) H_z = 0 \quad . \tag{113}$$

It is also shown in Appendix A that CF/E is negligible compared to the other terms in the parenthesis in Eq. (113). Equations (108) and (109) thus become

$$\left(\frac{1}{d^2} + \frac{A}{d}\right) H_z = 0$$

and

$$p = \left(\frac{F}{E}\right) H_z \quad .$$

Reintroducing the derivative notation, these equations become

$$\frac{d^2 H_z}{dx^2} + A \frac{dH_z}{dx} = 0 \tag{114}$$

and

$$p = \left(\frac{F}{\bar{\varepsilon}} \right) H_z \quad . \tag{115}$$

This procedure appears similar to a successive approximation technique; however, it should be noted that the coupling terms were neglected only when their magnitude was much smaller than the other terms in the equation. In the H_z equation the coupling term was negligible; however, in the p equation, the coupling term was a dominant factor.

Equation (114) can be solved for H_z. The pressure p can then be found from Eq. (115). First define

$$G = \frac{dH_z}{dx} \quad ;$$

then

$$\frac{dG}{dx} + AG = 0 \quad ,$$

where

$$A = - \frac{1}{\varepsilon_p} \frac{d\varepsilon_p}{dx} \quad .$$

Then

$$\frac{dG}{G} - \left(\frac{1}{\varepsilon_p} \frac{d\varepsilon_p}{dx} \right) dx = 0 \quad .$$

Integrating both sides of the above equation gives

$$\ln G = \ln \varepsilon_p + \ln C \quad ,$$

or

$$G = C_1 \varepsilon_p \quad ,$$

or

$$\frac{dH_z}{dx} = C_1 \varepsilon_p$$

where C_1 is the first constant of integration.

Integrating both sides of the above equation gives

$$H_z = C_1 \int_0^x \varepsilon_p \, dx + C_2$$

where C_2 is the second constant of integration.

Since $H_z(x=0) = H_z(0)$

$$H_z = C_1 \int_0^x \varepsilon_p \, dx + H_z(0) \, . \tag{116}$$

Using the rigidity boundary condition at x = d, it is shown by Eq. (76) that

$$\left.\frac{dH_z}{dx}\right|_{x=d^-} = -j\varepsilon_p(d^-) \, K_{ox} \, H_z(d^-)$$

Using this condition gives

$$C_1 = \frac{K_{ox} \, H_z(0)}{j - K_{ox} \int_0^d \varepsilon_p(x) \, dx} \tag{117}$$

where $\varepsilon_p(x)$ is the relative permittivity (complex) of the plasma evaluated at x, and K_{ox} is given by Eq. (75).

The approximate H_z solution is not always accurate for the plasmas of interest; however, the approximate p solution can be used for all profiles, since coefficient E is very large (see Appendix B). The

approximate solutions are compared with numerical solutions in Figs. 11 and 12. In most cases, the initial guesses for a numerical solution were the approximate solutions described above.

Solutions of the Coupled Wave Equations

The meaning of the H_z and p solutions will be discussed before the results are presented. The field solutions are valid solutions of the coupled wave equations; however, the curves describing the pressure field as a function of x show only a part of the solution. If the coupling term on the right-hand side of Eq. (61) is neglected, the pressure field solution has two parts. One part consists of the mathematical representation of two plane waves traveling in opposite directions (attenuated by the same amount as a function of x) and the other part consists of a pressure amplitude with a different x-dependence. It will be shown that the results presented in this chapter give only the second part of the pressure solution.

As discussed in the section on the approximate solution, the coupling (or influence) of the term on the right-hand side of Eq. (61) is negligible for many of the profiles and frequencies of interest. The complete analytical solution for p will be obtained by making some rather broad assumptions, hence the error in neglecting the coupling term in Eq. (61) will not present serious problems. The equations to be considered are:

$$\frac{d^2H_z}{dx^2} + A\frac{dH_z}{dx} + BH_z = 0 \qquad (118)$$

and

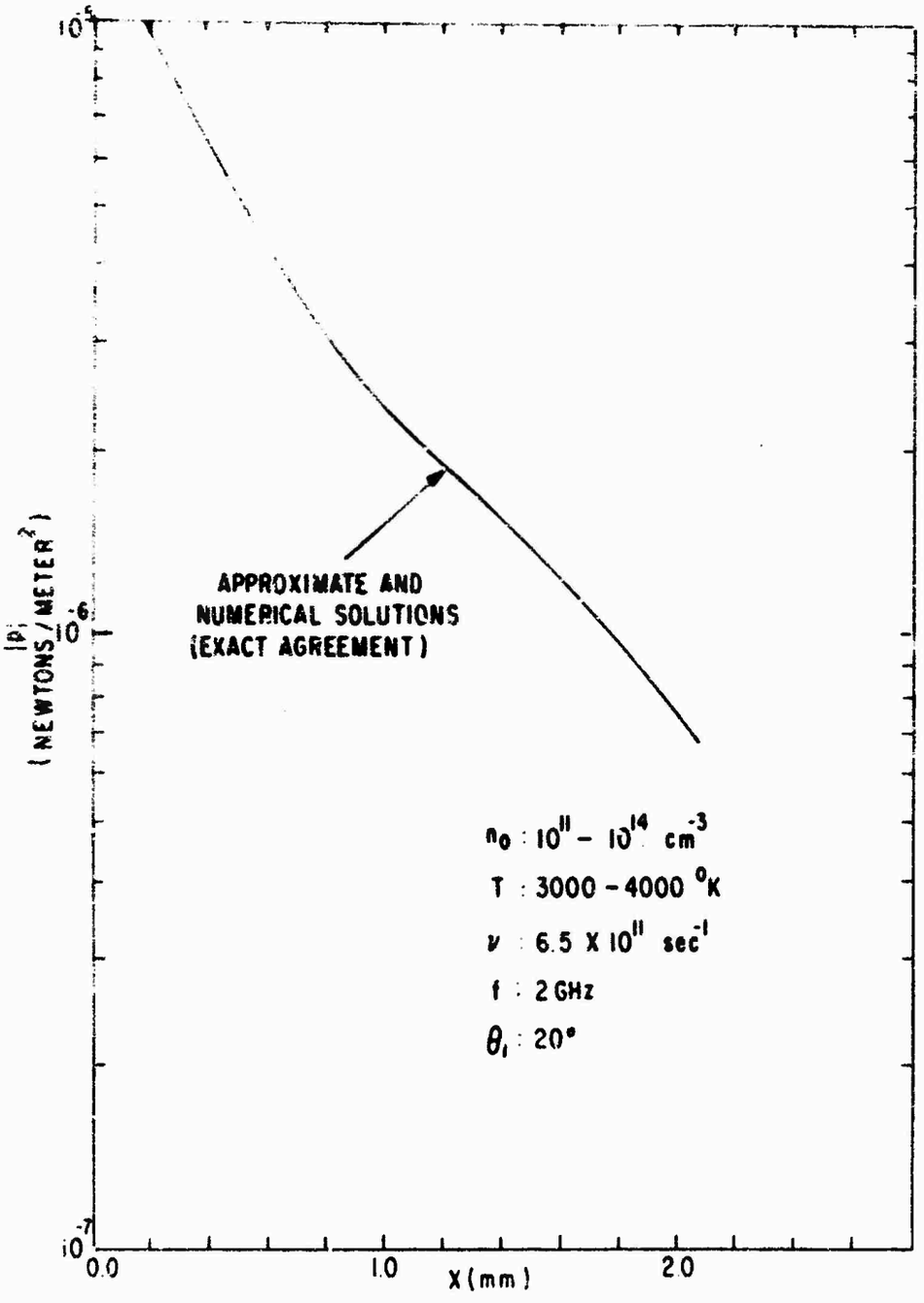

Figure 11. Comparison of Approximate Analytical Solution and Numerical Solution, Pressure Field

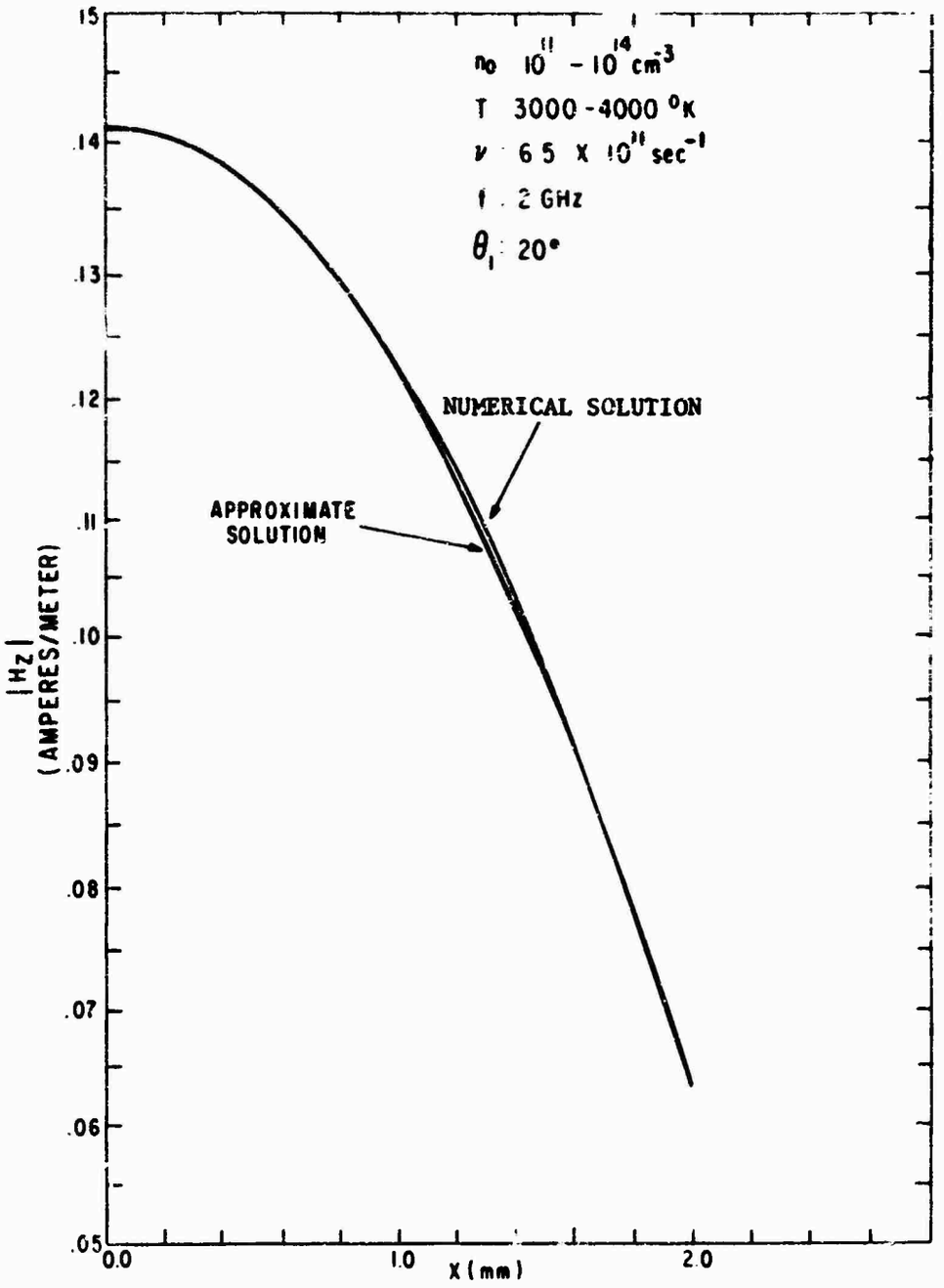

Figure 12. Comparison of Approximate Analytical Solution and Numerical Solution, Magnetic Field

$$\frac{d^2p}{dx^2} + D\frac{dp}{dx} + Ep = g \quad , \tag{119}$$

where $g = FH_z$. The magnetic field H_z can be determined from the first equation. The second equation is now considered in detail. This is an inhomogeneous, second order, ordinary differential equation. The solution will consist of two parts: the homogeneous solution and the particular solution. If D and E are constants (which is not a bad assumption for a linearly increasing electron density profile), the homogeneous solution is

$$p_h = ae^{\gamma_1 x} + be^{\gamma_2 x} \quad , \tag{120}$$

where γ_1 and γ_2 are the two roots of the equation $s^2 + Ds + E = 0$ and a and b are constants. Since $E >> D$, $\gamma_1 \cong j\sqrt{E}$ and $\gamma_2 \cong -j\sqrt{E}$. This is due to the large collision frequency in the plasma (see Eq. (97). The particular solution is calculated as follows:

$$p_p = \int_0^x \frac{g(\beta)\left[ae^{\gamma_1\beta}be^{\gamma_2 x} - ae^{\gamma_1 x}be^{\gamma_2\beta}\right]}{W(\beta)}\,d\beta \quad , \tag{121}$$

where $W(\beta)$ can be determined by calculating the Wronskian

$$W(x) = \begin{vmatrix} p_1(x) & p_2(x) \\ p_1'(x) & p_2'(x) \end{vmatrix} = ab\left(\gamma_2 - \gamma_1\right)e^{\left(\gamma_1+\gamma_2\right)x}$$

$$= ab\left(\gamma_2 - \gamma_1\right) \quad ,$$

where

$$p_1(x) = ae^{\gamma_1 x}$$

and

$$p_2(x) = be^{\gamma_2 x} \quad .$$

Note that since $\gamma_1 = -\gamma_2$,

$$e^{(\gamma_1+\gamma_2)x} = 1 \quad ,$$

and the Wronskian is independent of x. The particular solution is then found to be

$$p_p = \frac{g}{\gamma_1\gamma_2} + \frac{g}{\gamma_2-\gamma_1}\left[\frac{e^{\gamma_2 x}}{\gamma_1} - \frac{e^{\gamma_1 x}}{\gamma_2}\right] \quad ,$$

where it was assumed that the product $FH_z = g$ was constant, allowing the integration of Eq. (121) to be performed easily. The complete solution is just the sum of the homogeneous solution and the particular solution

$$p = ae^{\gamma_1 x} + be^{\gamma_2 x} + \frac{g}{E} - \frac{g}{2E}\left(e^{\gamma_1 x} + e^{\gamma_2 x}\right) \quad ,$$

which can be rewritten

$$p = A'e^{\gamma_1 x} + B'e^{\gamma_2 x} + g/E \quad , \qquad (122)$$

where $\gamma_1\gamma_2 = E$, and $A' = a - g/2E$ and $B' = b - g/2E$ are defined as the new constants of the homogeneous solution (since g and E were considered to be constant). The constants A' and B' can be determined from the two boundary conditions and are found to be functions of both H_z and dH_z/dx at both boundaries. The particular solution has no undetermined

coefficients but depends on the "forcing function" g. The particular solution also is a function of H_z since $g = FH_y$.

The numerical solution yields pressure solutions with approximately the following dependence

$$p = \left(\frac{F}{E}\right) H_z = g/E \quad , \tag{123}$$

and this is just the first part of the particular solution. In the solution, the other terms must be negligible since the x dependence is given by g/E alone and the complete solution is given by the sum of the terms. It is concluded that the "forced solution" (a term in the particular solution) is much larger than the terms in the solution characterizing the acoustic wave propagation in the plasma.

It was noted that changing the acoustic boundary conditions (e.g., setting $p = 0$ at $x = d$) had very little effect on the solution at interior points. This should be expected since the particular solution is not affected by changing the constants A' and B' which depend on the boundary conditions.

Even though the two plasma models considered are simple, there are still eight different parameters which can be changed to affect the solutions. These include: the electron density at the wall, the peak electron density, the temperature at the wall, the temperature at the distance corresponding to the peak electron density, the collision frequency, the distance to the peak, the operating frequency, and the angle of incidence. For the results presented in Figs. 13 to 22, the angle of incidence was fixed at 30°.

In Figs. 13 to 18 the profile of Fig. 5(a) is used. The wall and peak electron densities, the wall and peak temperatures, and the collision frequency are indicated on each figure. Solutions corresponding to different operating frequencies are labelled with the particular frequency. The magnetic field solution for the first density profile is given in Fig. 14 for three different operating frequencies. Since the acoustic modes generated in the plasma are of primary concern, this is the only magnetic field solution presented. Figure 15 gives the pressure field for the same wall and peak electron densities as Fig. 13; however, the distance to the peak in Fig. 15 is only 0.5 mm as compared to 1.0 mm in Fig. 13. This implies that the gradient of the electron density in Fig. 15 is larger than that in Fig. 13. Figure 16 gives pressure solutions for a low electron density at the wall (10^{10} cm^{-3}), while Figs. 17 and 18 give pressure solutions for a high peak electron density (10^{14} cm^{-3}). As given by Eq. (123), the x-dependence of p is just FH_z/E. Since E is almost constant across the plasma layer (see Appendix B) and H_z is slowly varying with no pronounced peaks, the peaks in the curves representing the pressure solutions are due to F. This peak in F can be seen in Fig. 9. The peak occurs at the distance where the electron plasma frequency (determined by the electron density) is equal to the operating frequency. The magnitudes of the pressure solutions for the different density profiles are not significantly different; however, comparing the 30 GHz curve in Fig. 13 to the 30 GHz curve in Fig. 15, it is noted that the pressure magnitude for the larger electron density case (Fig. 15) is slightly larger. The significant result of the pressure solutions given in Figs. 13 to

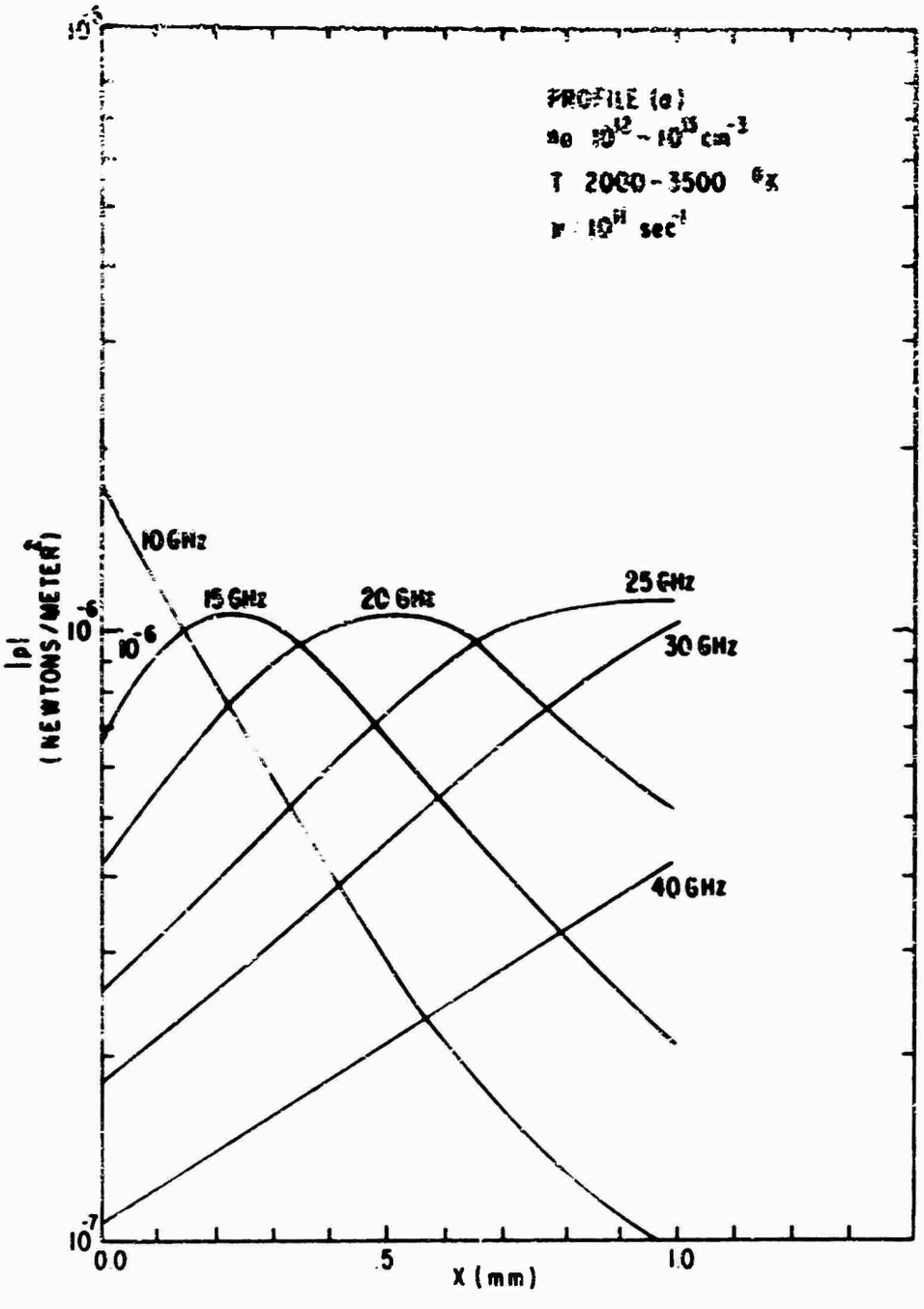

Figure 13. Pressure Field for 10^{12} - 10^{13} cm^{-3} Density Profile (1 mm thick)

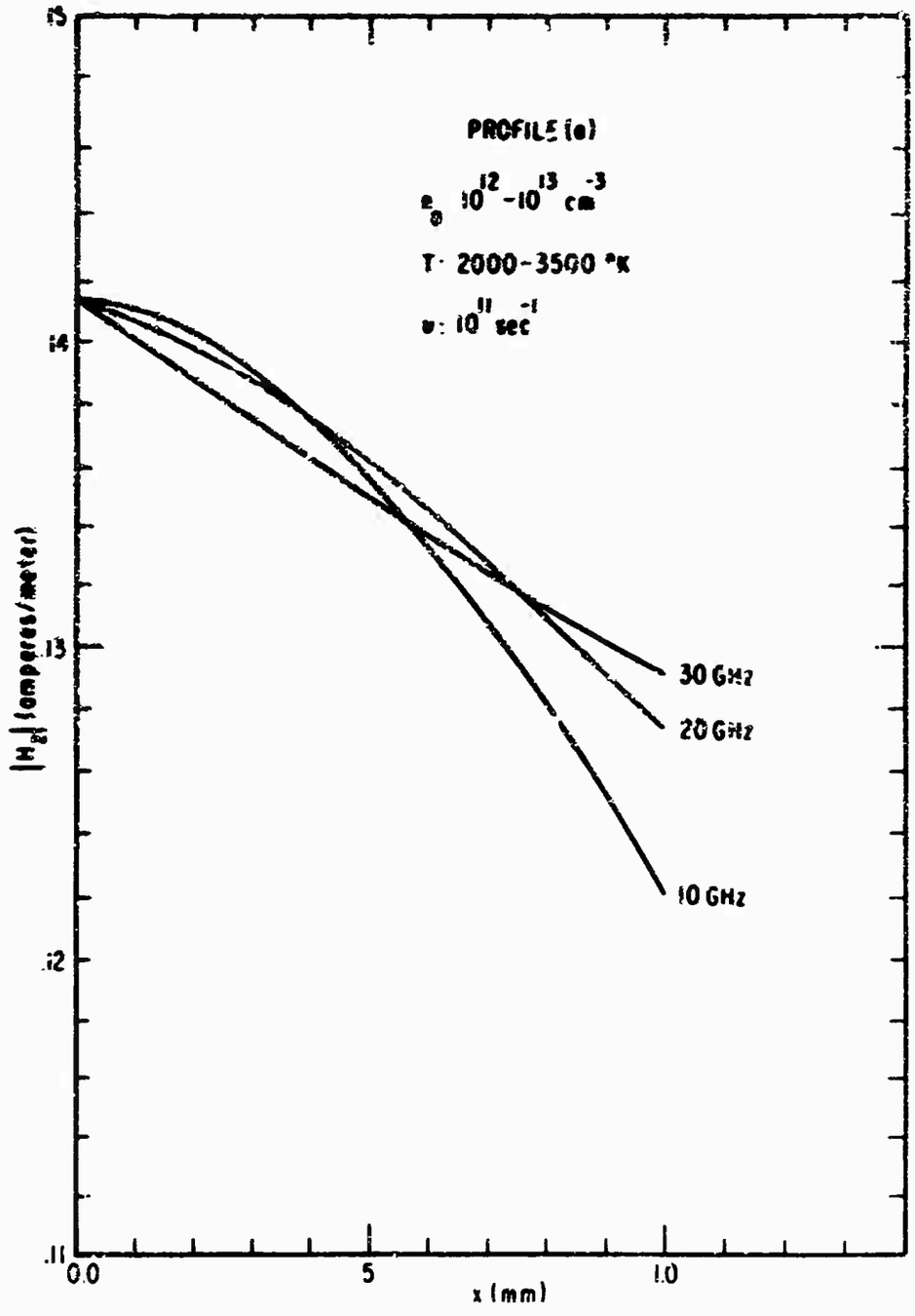

Figure 14. Magnetic Field for 10^{12} - 10^{13} cm^{-3} Density Profile (1 mm thick)

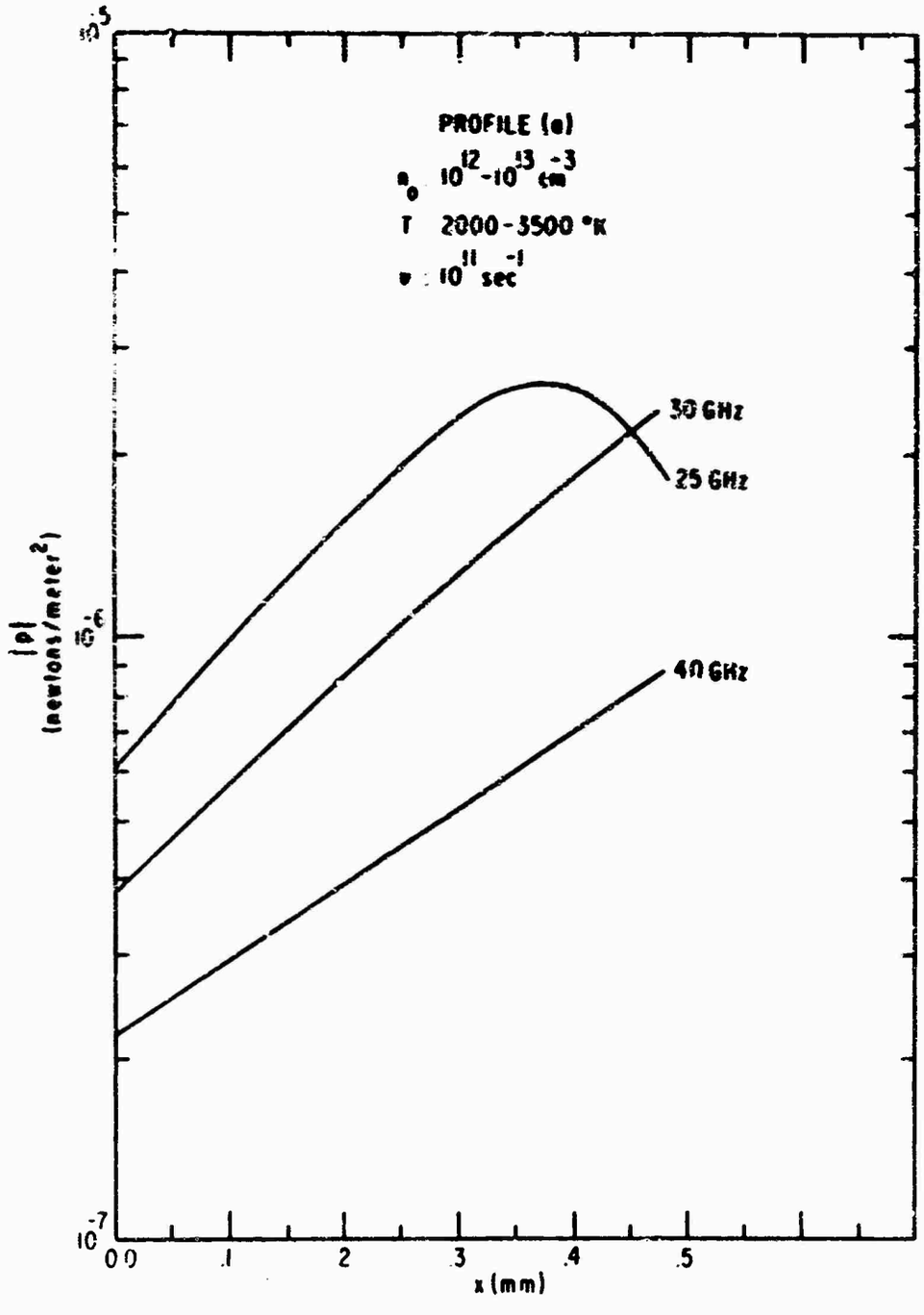

Figure 15. Pressure Field for 10^{12} - 10^{13} cm^{-3} Density Profile (0.5 mm thick)

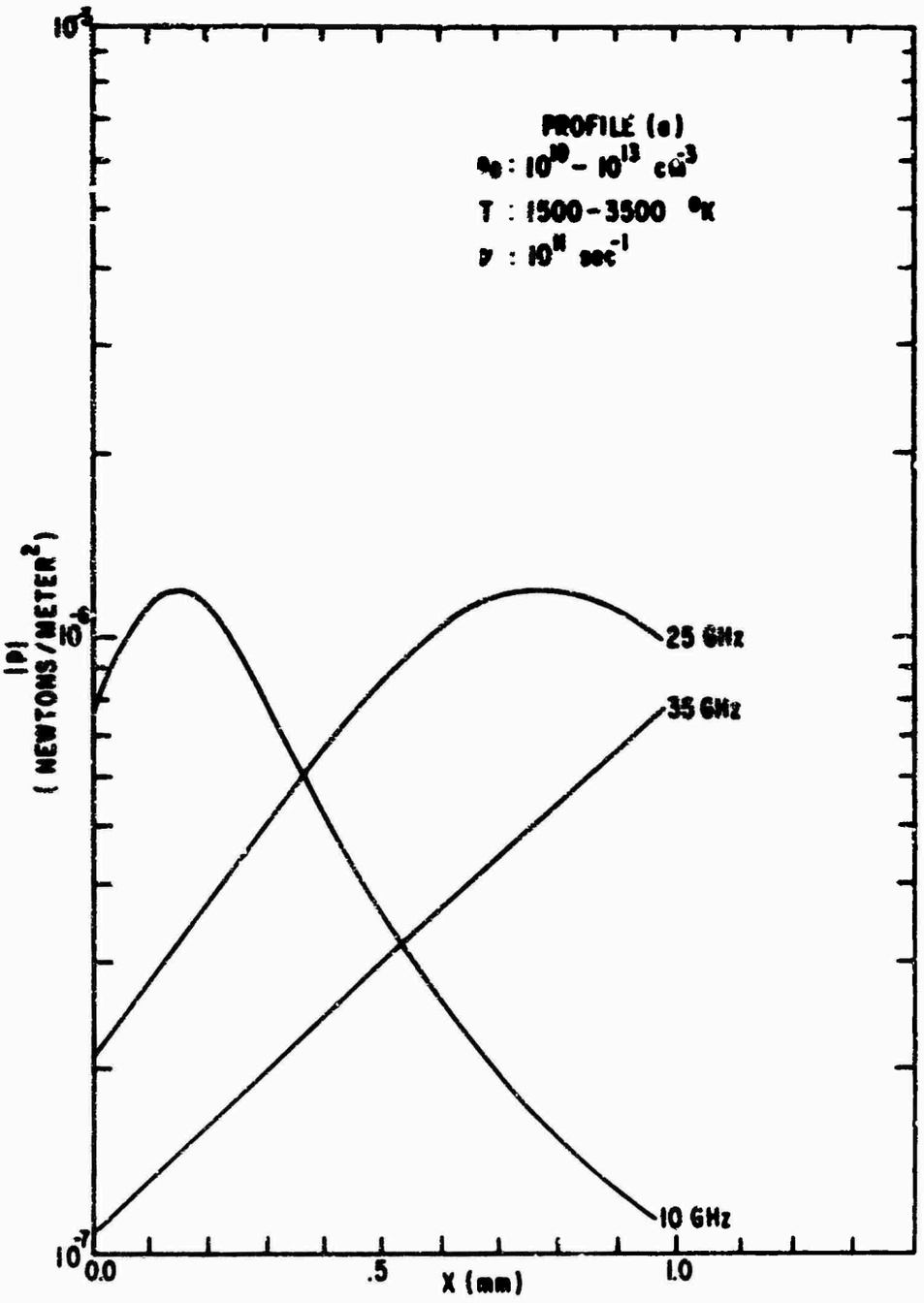

Figure 16. Pressure Field for 10^{10} - 10^{13} cm^{-3} Density Profile

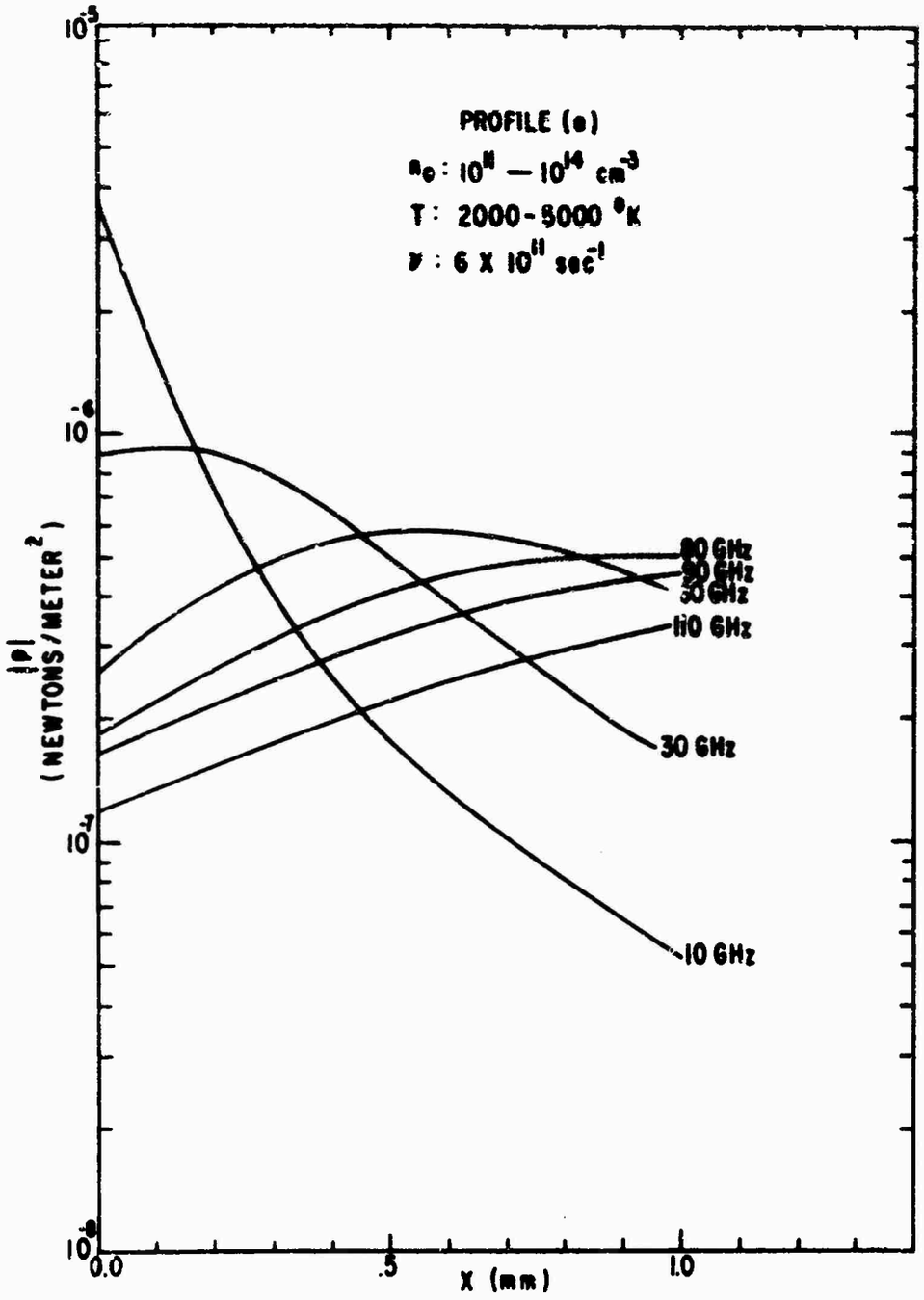

Figure 17. Pressure Field for 10^{11} - 10^{14} cm^{-3} Density Profile

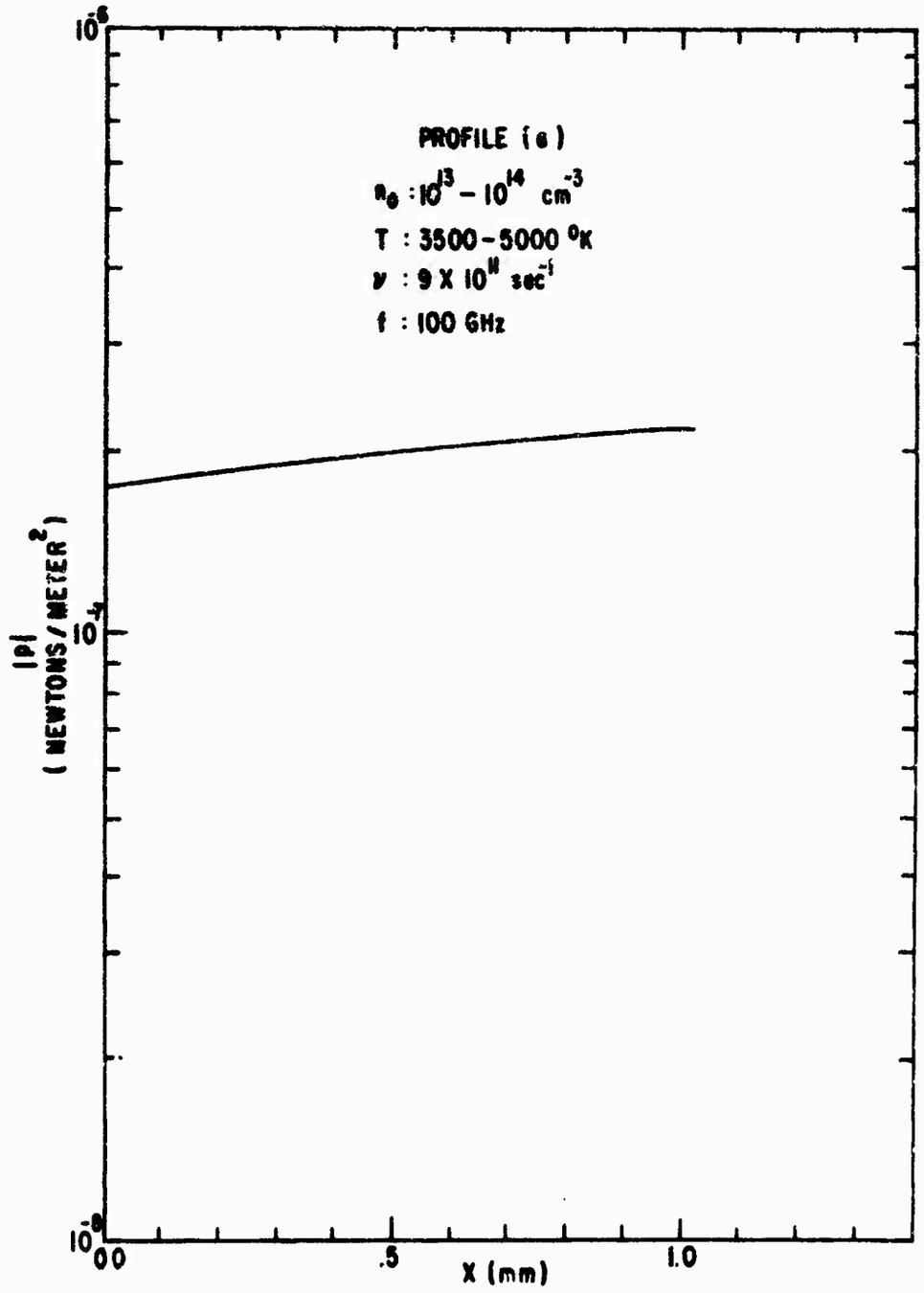

Figure 18. Pressure Field for 10^{13} - 10^{14} cm^{-3} Density Profile (High Collision Frequency)

18, as stated earlier, is that the curve clearly describes a variation given by Eq. (123) with no x-variation of the type given by the two exponential terms in Eq. (122) observable. The influence of these terms (describing acoustic wave propagation) on the "forced solution," Eq. (123), must be negligible. From Figs. 13 to 18, it is observed that the amplitudes of these terms must be of the order of 10^{-8} newtons/meter^2 or smaller. The amplitudes of these terms are discussed further in Chapter V.

In Fig. 19, the pressure field solutions are given for various temperature profiles for a 10^{11} - 10^{13} cm^{-3} electron density profile. The pressure increases as the plasma temperature is increased.

In Fig. 20 the profile of Fig. 5(b) is used. Comparing the 30 GHz curve in Figs. 13 and 20, it is noted that the pressure amplitude for profile (b) is smaller than the amplitude for profile (a). This is due to the fact that H_z is smaller for (b). The same x-dependence (FH_z/E) is present for the pressure solutions in both profiles. The same explanation holds for Fig. 21.

The attenuation of a pressure wave propagating in the positive x direction from x = d in the homogeneous region of profile (b) was calculated by determining the real part of the x component of the propagation constant given by Eq. (130). The pressure amplitude was normalized at x = d and the attenuation is described by

$$\left| \frac{p}{p(d)} \right| = e^{-\alpha(x-d)}$$

where α is the attenuation factor from Eq. (130). The wave is attenuated by a factor of 10^{-4} within a distance of only 0.02 mm from the

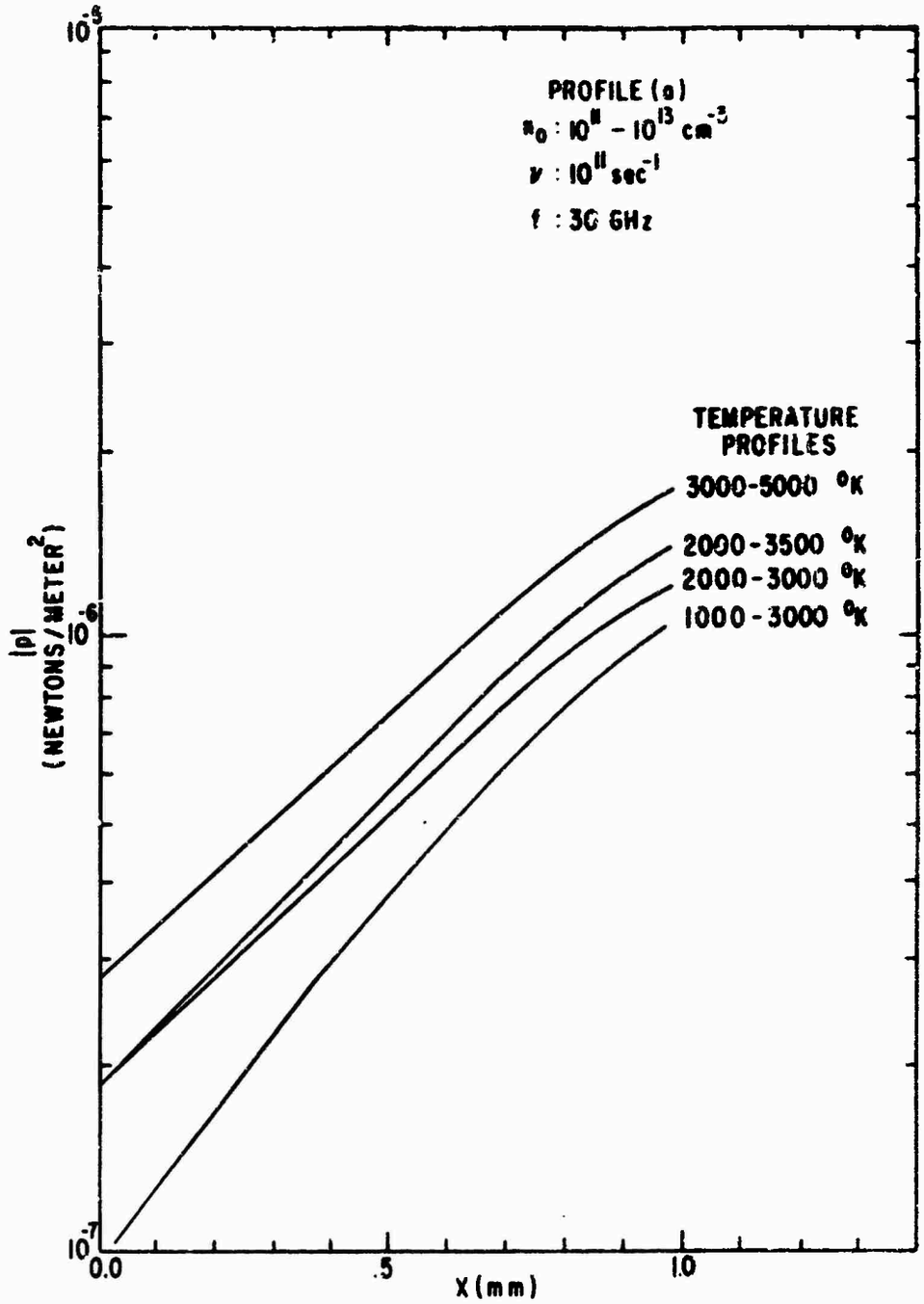

Figure 19. Pressure Field for 10^{11} - 10^{13} cm^{-3} Density Profile with Various Temperature Profiles

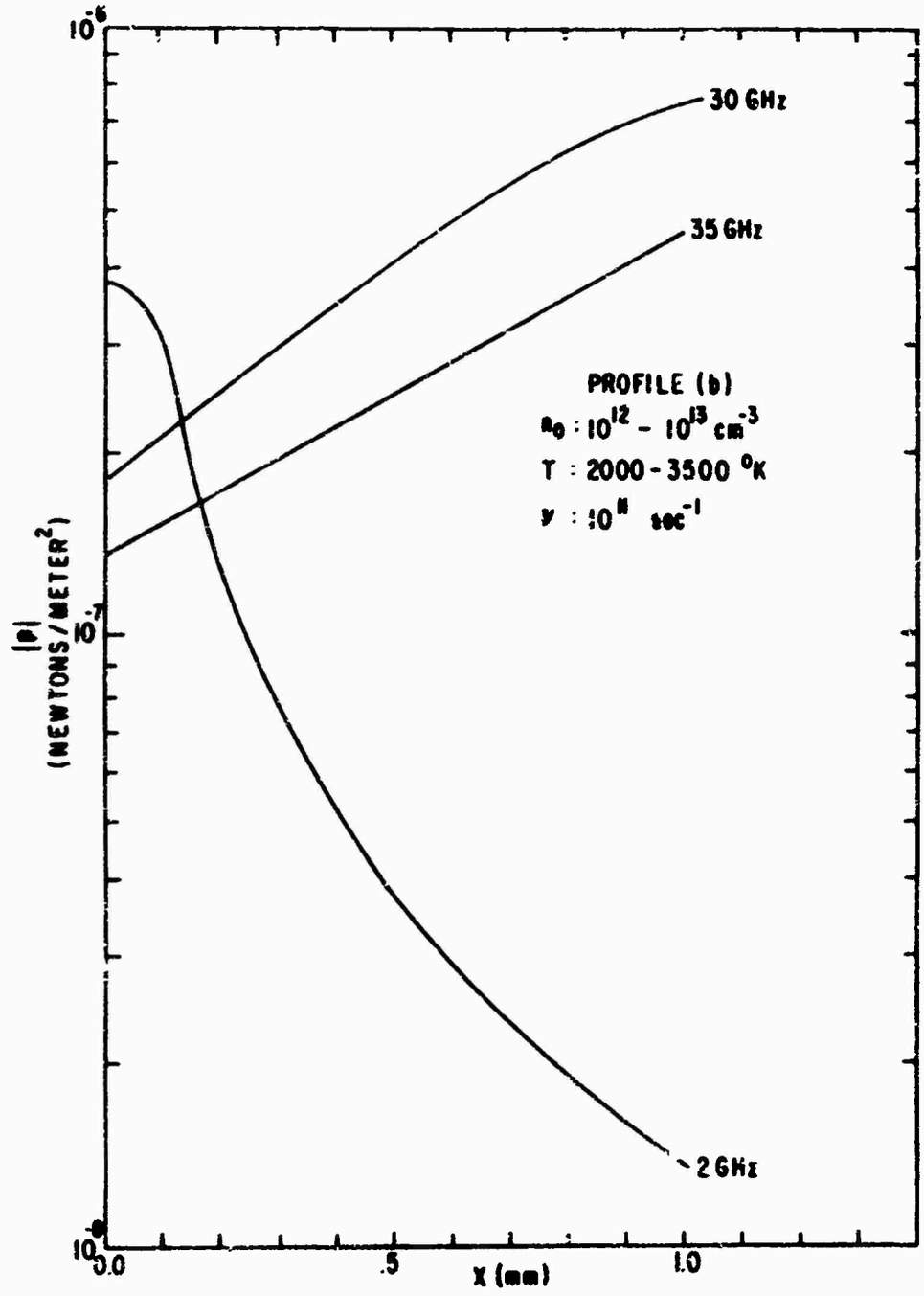

Figure 20. Pressure Field for 10^{12} - 10^{13} cm^{-3} Density Profile

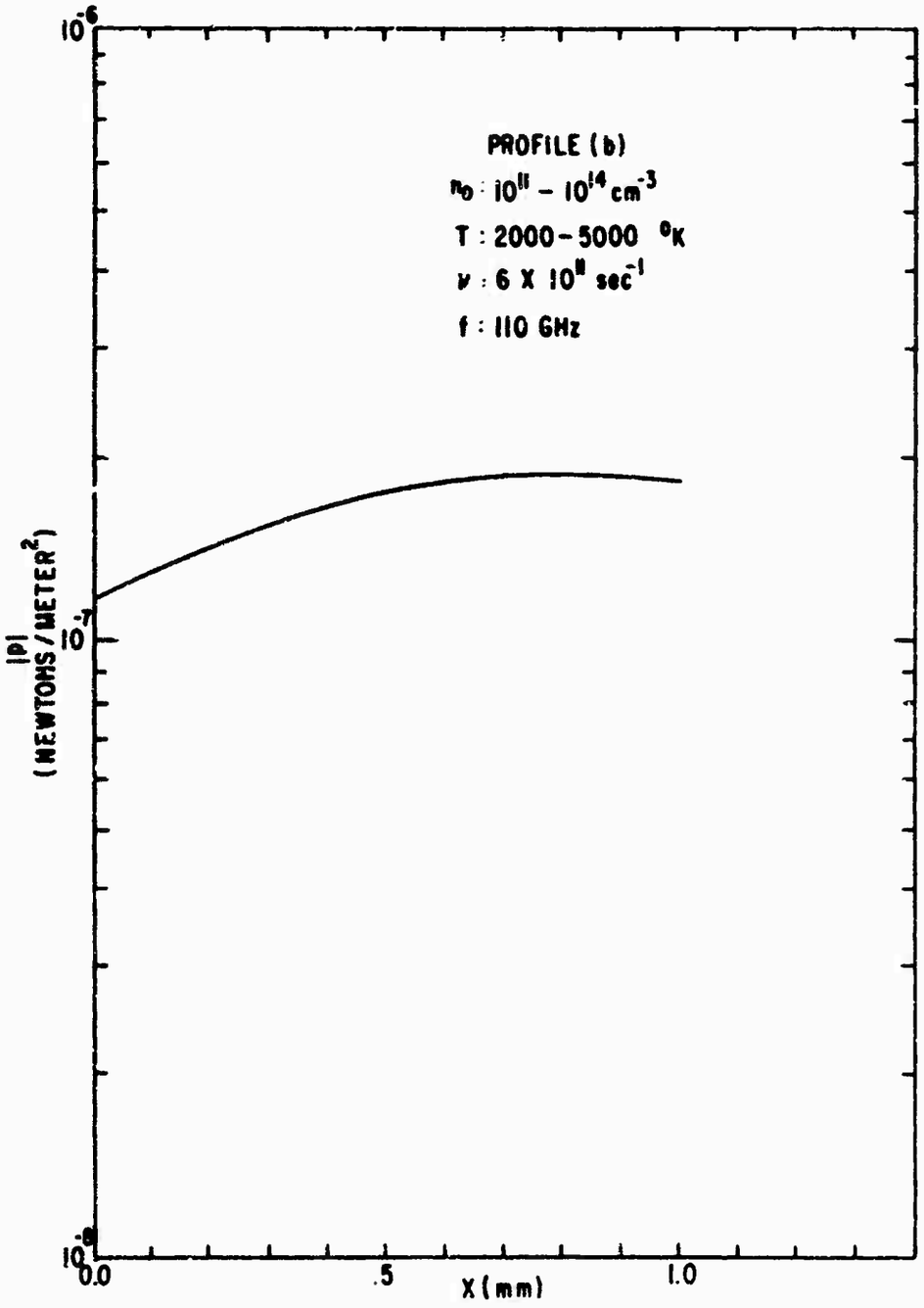

Figure 21. Pressure Field for 10^{11} - 10^{14} cm^{-3} Density Profile

peak (see Fig. 22). The calculations were made at low frequencies (1 GHz and 10 GHz) where the attenuation is less severe. Higher operating frequencies would result in an even more rapid damping of the wave.

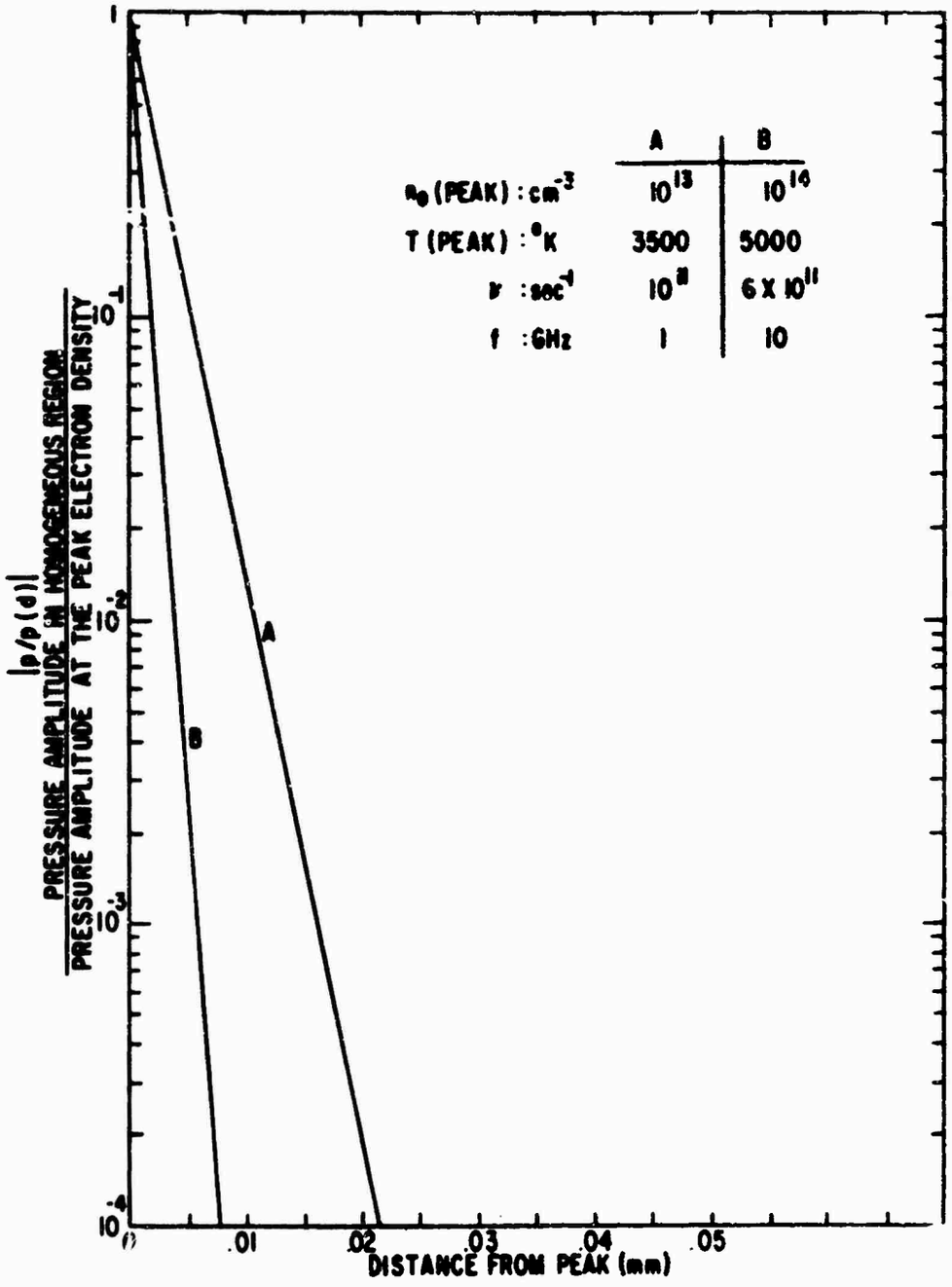

Figure 22. Relative Pressure Amplitude in the Homogeneous Region of the Plasma Model Illustrated in Figure 5(b)

CHAPTER V

CONVERSION EFFICIENCIES AT A DIELECTRIC-PLASMA INTERFACE

Conversion of an Electromagnetic Wave into an Acoustic Wave

It has been shown that the amplitudes of waves associated with the propagating electron acoustic mode are of the order of 10^{-8} newtons/meter^2 or smaller even in a plasma region where there exists coupling between the electromagnetic wave and the acoustic wave. An estimate of the wave amplitudes is made in the section Power Conversion at the end of this chapter. Even though it appears that the amplitude of the reflected acoustic wave is so small as to be undetectable, the conversion efficiencies will be investigated, since very few numerical results seem to be available even for the semi-infinite plasma case of this chapter. For the semi-infinite plasma, the pressure solution simply consists of one of the exponential terms in the homogeneous solution of Chapter IV which corresponds to propagation in the positive x direction.

An electron acoustic wave can be generated at the boundary between a dielectric material and a plasma by an electromagnetic wave which is vertically polarized and obliquely incident from the dielectric material (Ref. 21). It was shown in Chapter III that a vertically polarized electromagnetic wave incident on an inhomogeneous plasma generates a disturbance described by two differential equations implying a coupling between an electromagnetic mode and a plasma mode because of the inhomogeneity of the medium. The modes are also coupled at a boundary, but the coupling in this case is through the boundary

conditions which are both electromagnetic and acoustic. The boundary conditions used are the continuity of the tangential components of the electric and magnetic fields (Ref. 30) and the vanishing of the normal component of the electron velocity (Refs. 12, 13, and 22).

$$H_z(0^-) = H_z(0^+) \tag{124}$$

$$E_y(0^-) = E_y(0^+) \tag{125}$$

$$V_x = 0 \tag{126}$$

The acoustic boundary condition, Eq. (126), implies that none of the electrons penetrates the boundary and is sometimes called the "rigidity boundary condition." This acoustic boundary condition is considered to be valid at a dielectric plasma interface (Refs. 12, 13, 21, and 31); however, at the boundary between a metal and a plasma, a different acoustic boundary condition must be used (Ref. 31) which specifies the ratio of the normal component of the electron velocity to the pressure and is referred to as the "impedance boundary condition."

In this chapter, only homogeneous plasmas are considered so that the spatial dependence of the fields can be explicitly written. Plane wave propagation is considered with harmonic time variation assumed. The objective is to determine numerically the effects of plasma parameters (electron density, temperature, and collision frequency) and the incident electromagnetic wave (frequency and angle of incidence) upon the conversion efficiencies at the boundary.

The conversion of an electromagnetic wave into a pressure wave at a dielectric-plasma half-space interface is shown in Fig. 23. The electromagnetic wave is vertically polarized and incident at some

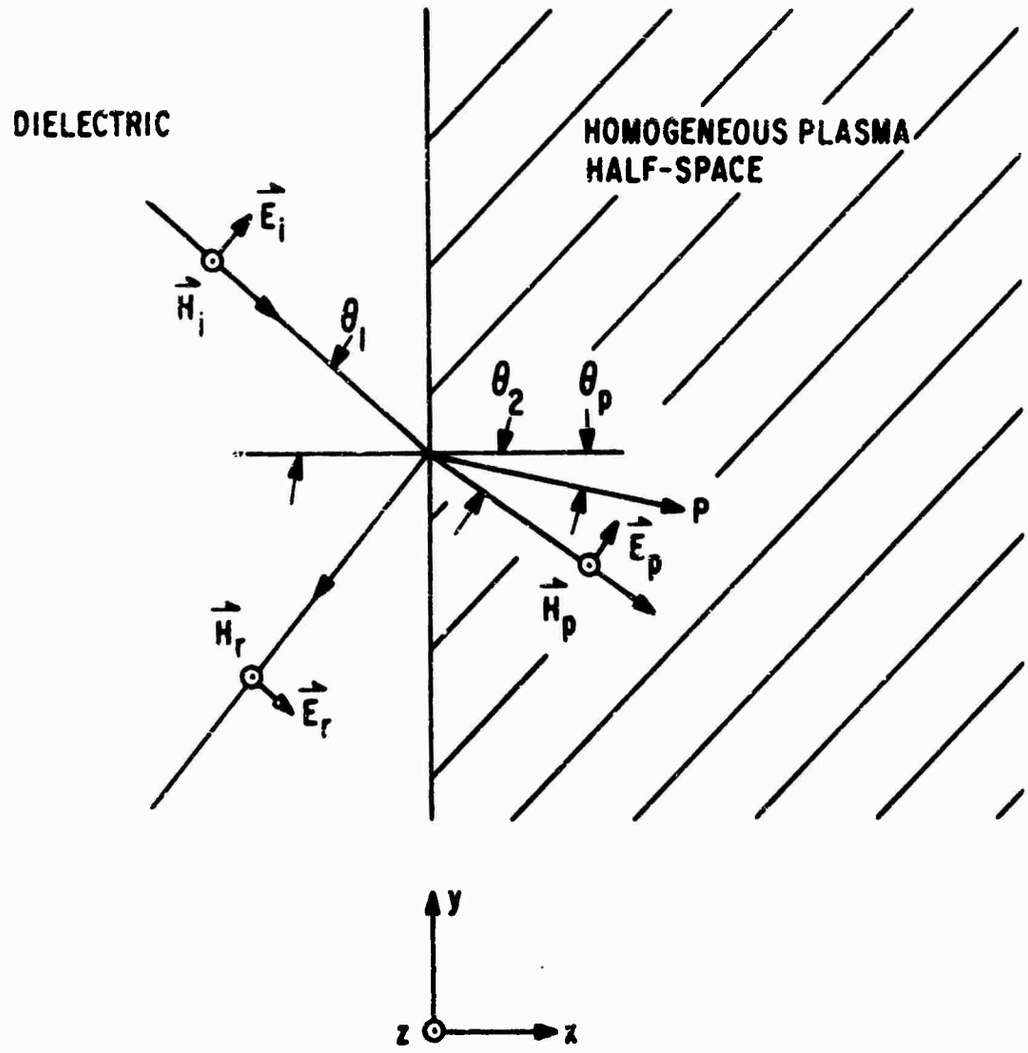

Figure 23. Conversion of an Electromagnetic Wave into an Acoustic Wave

angle θ_1. Part of the wave is transmitted into the plasma and part is reflected at the interface. Due to the coupling at the boundary, part of the electromagnetic wave is converted into an acoustic wave in the plasma. This wave is represented by the scalar pressure p and propagates at some angle θ_p away from the boundary. Since the plasma is homogeneous, Eqs. (61) and (62) become

$$\frac{d^2H_z}{dx^2} - \gamma_{hx}^2 H_z = 0 \tag{127}$$

and

$$\frac{d^2p}{dx^2} - \gamma_{px}^2 p = 0 \quad , \tag{128}$$

where

$$\gamma_{hx}^2 = K_y^2 - K_o^2 \varepsilon_p \tag{129}$$

and

$$\gamma_{px}^2 = K_y^2 - \frac{\omega^2}{u_o^2}\left[1 - \frac{\omega_p^2}{\omega^2} - j\frac{\nu}{\omega}\right] . \tag{130}$$

Both γ_{hx} and γ_{px} are complex numbers. This implies that both types of waves are attenuated in the plasma. Equations (127) and (128) describe wave propagation in the plasma. The electromagnetic and acoustic modes propagate independently. Since the plasma is of infinite extent, there are only outgoing waves and from Eqs. (127) and (128) the fields in the plasma are given by

$$H_z = H_{zo}\, e^{-\gamma_{hx}x}\, e^{jK_y y} \tag{131}$$

and

$$p = p(0)\, e^{-\gamma_{px}x}\, e^{jK_y y} \quad , \tag{132}$$

where the y dependence is the same as that for Eqs. (52) and (53). The value of the pressure wave at the boundary is p(0) and H_{zo} is the value of the transmitted magnetic field at the boundary.

The electromagnetic field in the dielectric is taken to be a superposition of an incident plane wave and a reflected plane wave and is expressed in terms of the magnetic field as

$$H_z = H_o \left(e^{-\gamma_{dx} x} + Re^{\gamma_{dx} x} \right) e^{jK_y y} \tag{133}$$

where H_o is the amplitude of the incident wave and R is defined as the reflection coefficient. The x component of the propagation constant in the dielectric is defined as γ_{dx} and is given by

$$\gamma_{dx}^2 = K_y^2 - \omega^2 \mu_o \varepsilon_o K_d \tag{134}$$

or

$$\gamma_{dx} = j\omega\sqrt{\mu_o \varepsilon_o K_d} \cos \theta_1 \ . \tag{135}$$

The ratio $p(0)/H_o$ will be determined using the three boundary conditions, Eqs. (124), (125), and (126).

From Eq. (124) (H_z continuous at the boundary x = 0),

$$H_o + H_o R = H_{zo} \ . \tag{136}$$

From Eq. (125) (E_y continuous at the boundary x = 0), and using $E_y = -1/j\omega\varepsilon_d \left(dH_z/dx \right)$ in the dielectric along with Eq. (133) and using Eq. (48) for E_y in the plasma along with Eqs. (131) and (132),

$$\frac{H_o \gamma_{dx}}{j\omega\varepsilon_d} \left[1 - R \right] = \frac{\gamma_{hx}}{j\omega\varepsilon} H_{zo} + \frac{eK_y}{\omega\varepsilon Am} p(0) \ . \tag{137}$$

From Eq. (126) ($V_x = 0$ at the boundary $x = 0$), and using Eq. (49) for V_x

$$\frac{eK_y}{\omega\epsilon Am} H_{zo} + \frac{\gamma_{px}\epsilon_o}{\epsilon Amn_o} p(0) = 0 \quad . \tag{138}$$

Equations (136), (137), and (138) can be used to solve for the ratio $p(0)/H_o$, which gives the magnitude of the generated pressure wave at the boundary relative to the amplitude of the incident electromagnetic wave. The result is

$$\frac{p(0)}{H_o} = \frac{\left(\frac{2eK_y}{\omega K_d}\right)\gamma_{dx}\epsilon_p}{j\frac{e^2K_y^2}{\omega Am} - \frac{\gamma_{px}\gamma_{dx}\epsilon_o\epsilon_p}{n_oK_d} - \frac{\gamma_{px}\gamma_{hx}\epsilon_o}{n_o}} \quad . \tag{139}$$

Equation (139) will be used to investigate the conversion of a transverse electromagnetic wave into a pressure wave at a plane dielectric-plasma interface. A computer program was written to solve Eq. (139) for various plasma parameters and incident electromagnetic wave properties. The absolute value of Eq. (139) is used. For simplicity, this value will be designated as $|p/H|$ in the following graphs.

The electromagnetic-to-acoustic conversion efficiency is plotted as a function of electron density in Fig. 24. The temperature and collision frequency will vary for different electron densities. Collision frequencies and temperatures for different electron densities are shown in Table I. These values were taken from case studies made of the plasma sheath surrounding a hypersonic reentry vehicle using a computer code developed by McDonnell Douglas Corporation (Ref. 32).

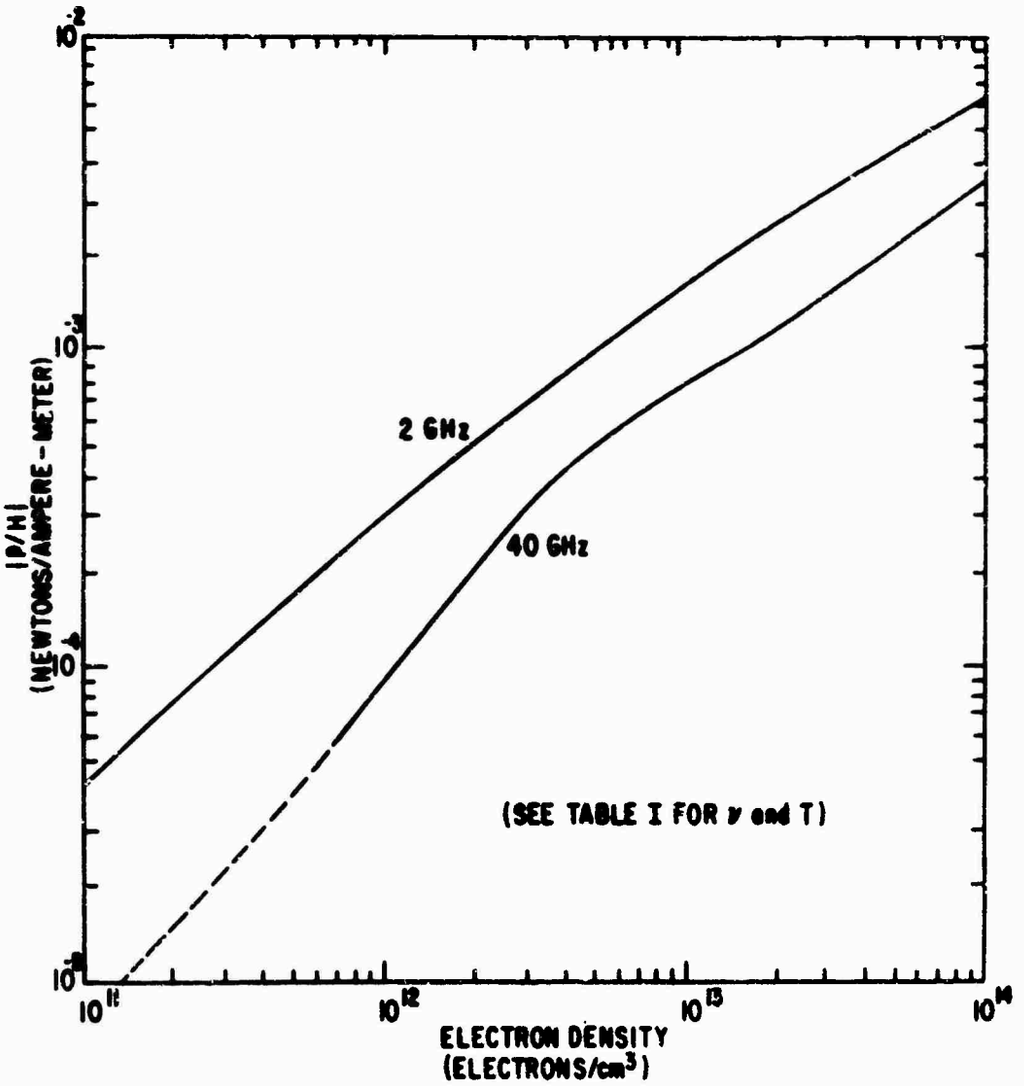

Figure 24. Electromagnetic-to-Acoustic Conversion Efficiency versus Electron Density

Table I

COLLISION FREQUENCIES AND TEMPERATURES

FOR GIVEN ELECTRON DENSITIES (Ref. 32)

Electron density (cm^{-})	Collision frequency (sec^{-})	Temperature (°K)
1.6×10^{11}	10^{11}	2000
3.2×10^{11}	10^{11}	2000
6.4×10^{11}	10^{11}	2000
1.3×10^{12}	10^{11}	3000
2.6×10^{12}	10^{11}	3000
5.1×10^{12}	10^{11}	3000
1.0×10^{13}	10^{11}	4000
2.0×10^{13}	2×10^{11}	4000
4.1×10^{13}	2×10^{11}	4000
8.2×10^{13}	4×10^{11}	4000

The program treats the inviscid flow field, ablation mass loss, and turbulent boundary layer surrounding a spherically blunted conical body. The electron density, temperature, and collision frequency in the turbulent boundary layer are of primary concern in this report. The case studies were made by the Fuzing Environment Branch (WLEE) of the Air Force Weapons Laboratory using the computer code for several advanced reentry vehicles with two different types of heatshield materials and various reentry trajectories. The significant result of Fig. 24 is that the electromagnetic-to-acoustic conversion efficiency increases monotonically, with increasing electron density.

This implies that a more dense plasma would result in a better coupling of electromagnetic energy to acoustic energy at the boundary. The dashed portion of the 40 GHz curve in Fig. 24 indicates the region where the acoustic waves are Landau damped since $\lambda_p \cong \lambda_d$ in this region.

Figure 25 gives the electromagnetic-to-acoustic conversion efficiency as a function of the plasma temperature. It is noted that the conversion efficiency increases as the plasma temperature is increased. This is to be expected since it is the plasma temperature upon which the acoustic waves depend as a propagating mode (see Eq. (33)). The numerical solutions show that the "forced solution" of the pressure field also increases with increasing temperature as illustrated in Fig. 19.

Figures 26, 27, and 28 illustrate the fact that the electromagnetic to acoustic conversion efficiency has a maximum value at a particular angle of incidence. For an electron density of 10^{13} cm^{-3} and a frequency of 40 GHz the efficiency has a peak at approximately 25° (Fig. 26). For a frequency of 31.25 GHZ the peak still occurs at 25° (Fig. 27); however, the efficiency magnitude is larger by an order of magnitude due to the frequency dependence of the efficiency (see Figs. 29 and 30). When the electron density is increased to 10^{14} cm^{-3}, the peak occurs at 45° (Fig. 28).

Figures 29 and 30 illustrate the frequency dependence of the electromagnetic-to-acoustic conversion efficiency. The efficiency is plotted as a function of the dimensionless parameter ω/ω_p, where ω_p is the electron plasma frequency determined by the electron density

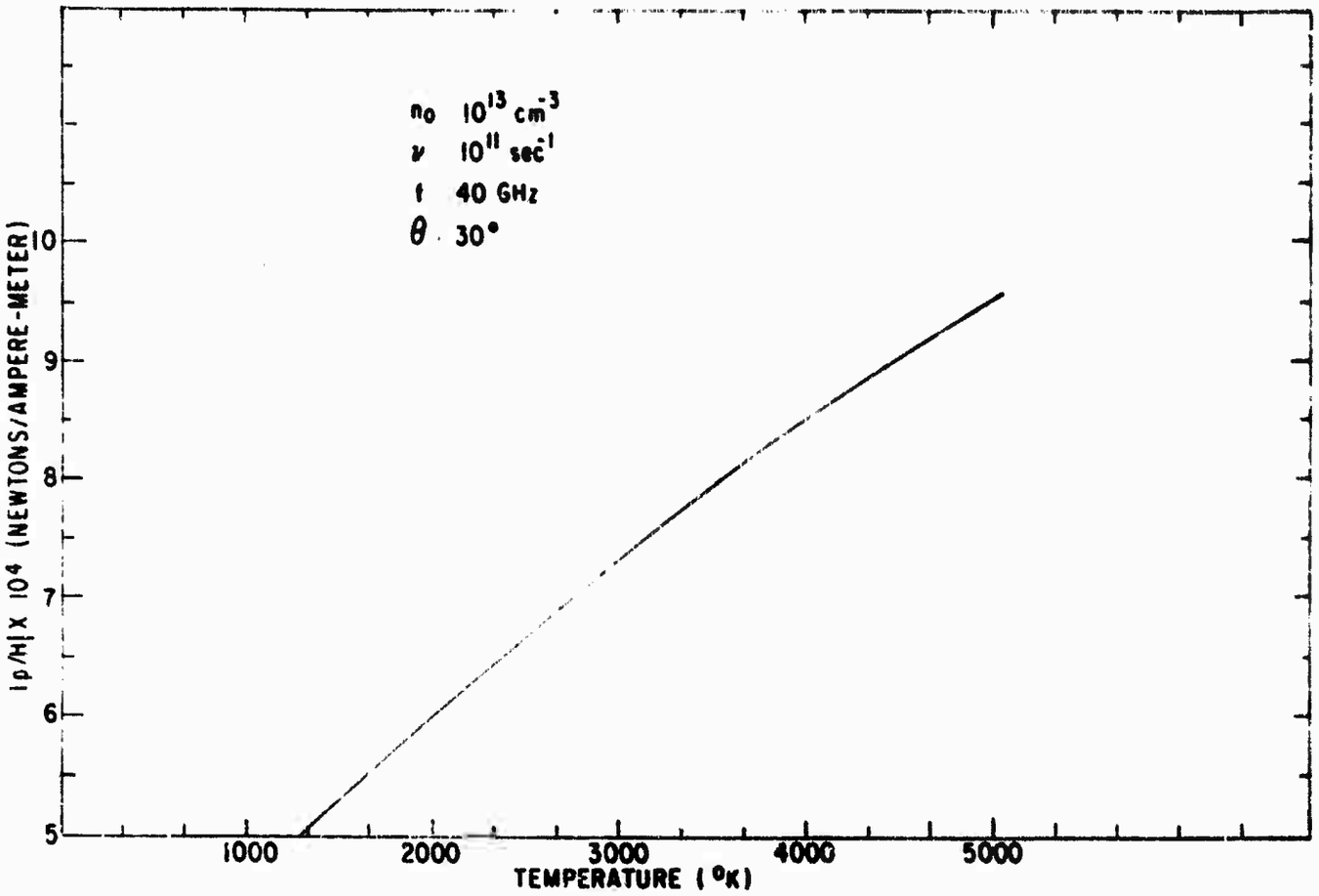

Figure 25. Electromagnetic-to-Acoustic Conversion Efficiency versus Plasma Temperature

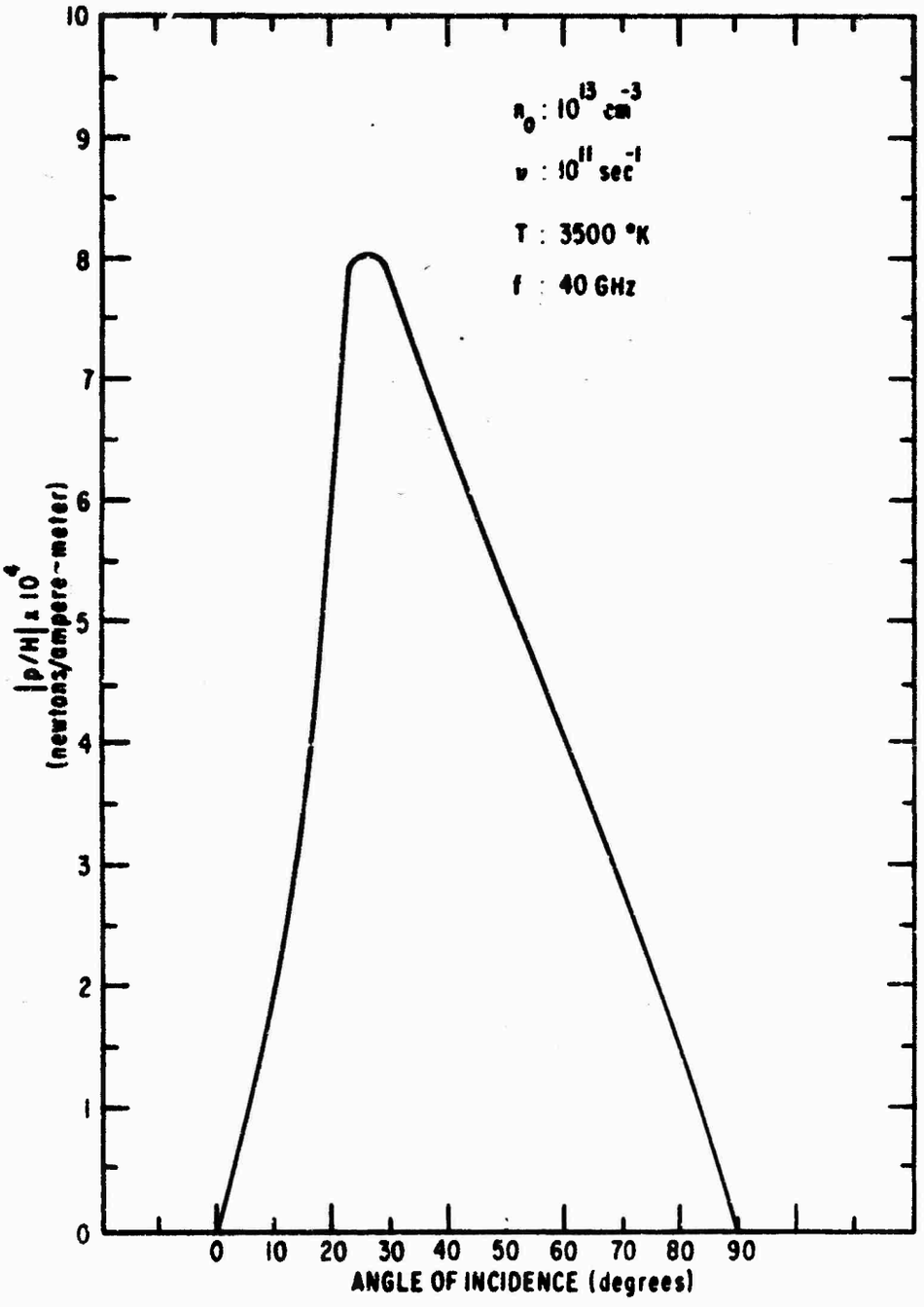

Figure 26. Electromagnetic-to-Acoustic Conversion Efficiency versus Angle of Incidence (f = 40 GHz)

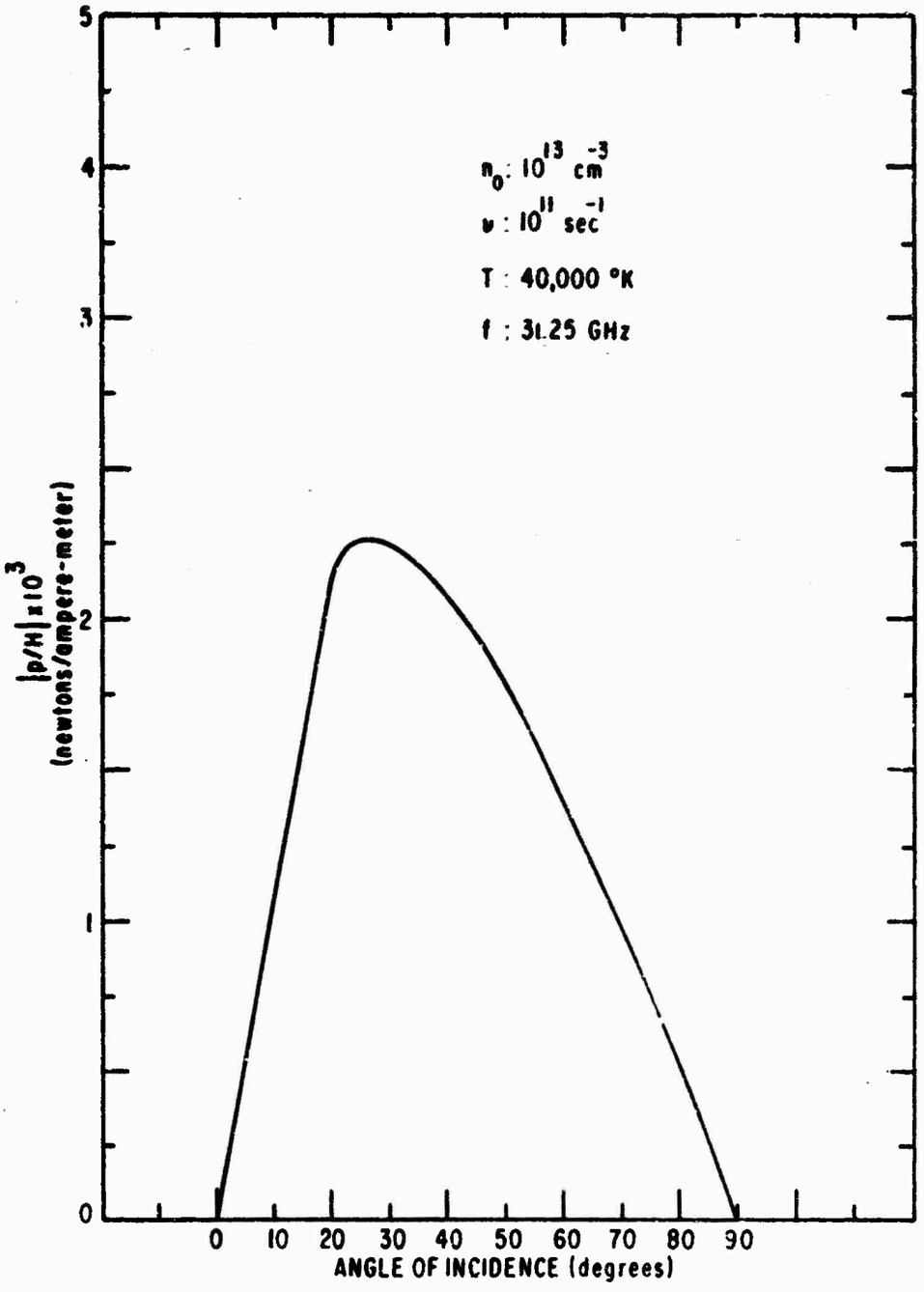

Figure 27. Electromagnetic-to-Acoustic Conversion Efficiency versus Angle of Incidence (f = 31.25 GHz)

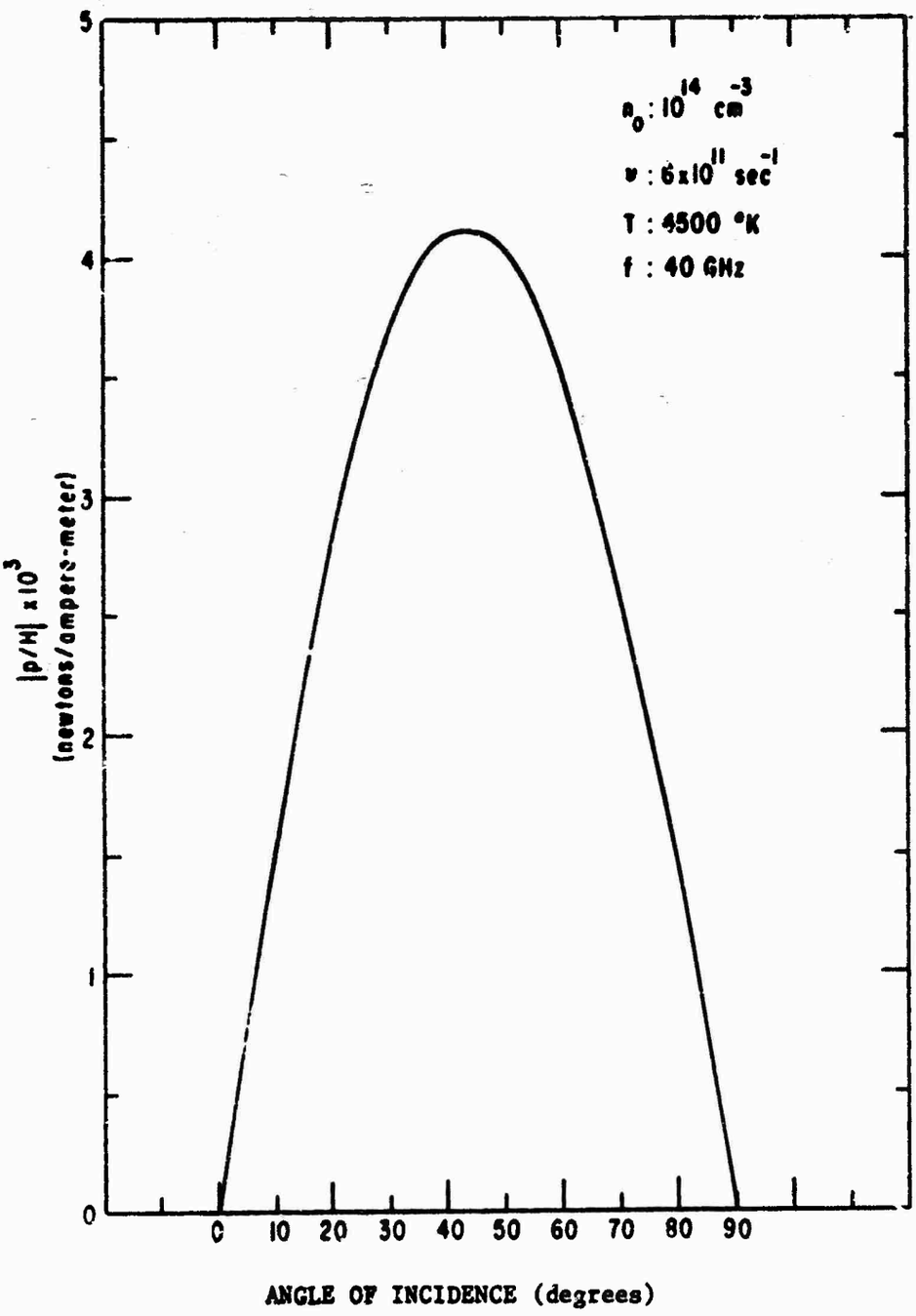

Figure 28. Electromagnetic-to-Acoustic Conversion Efficiency versus Angle of Incidence (Large Electron Density)

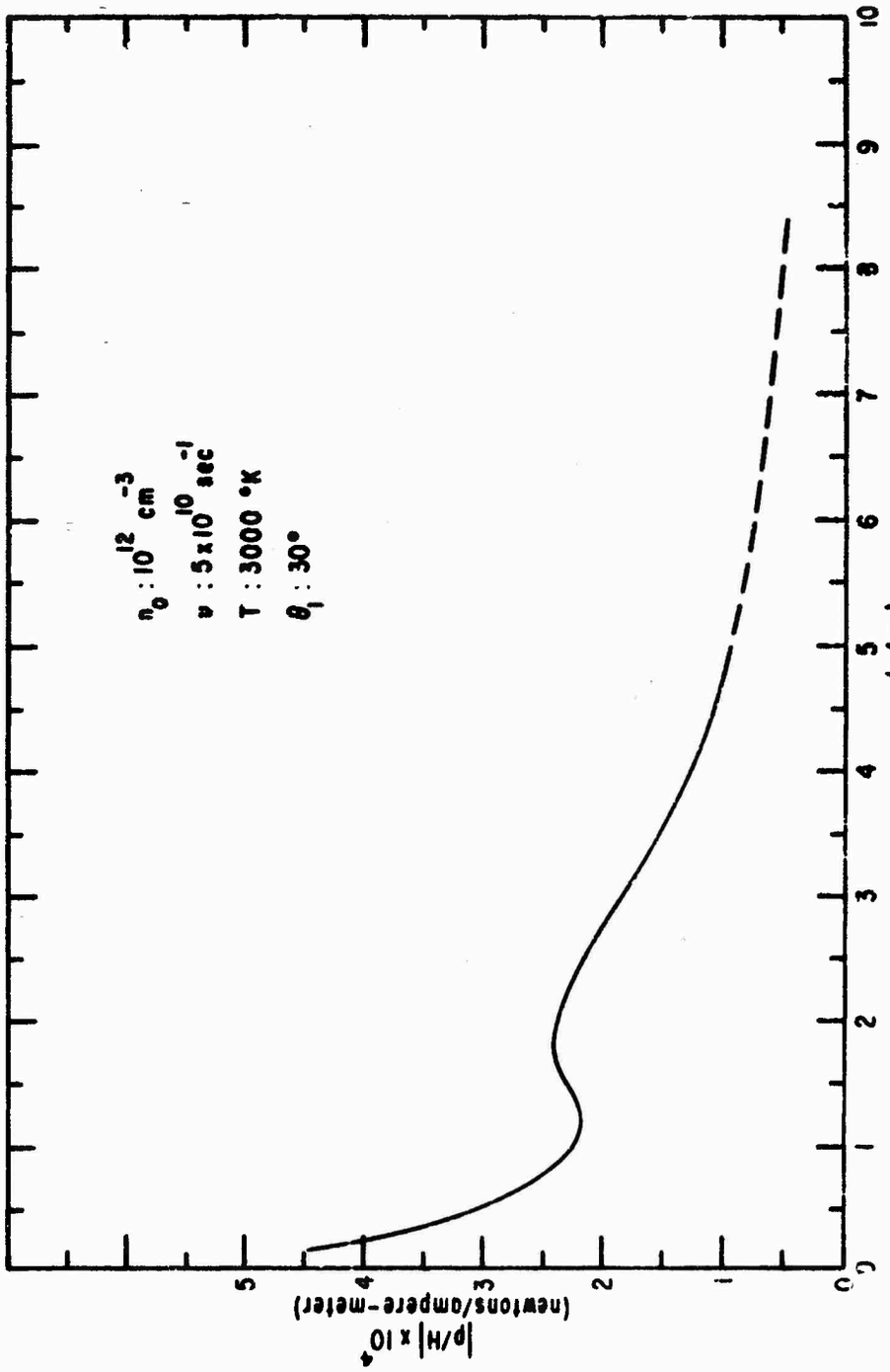

Figure 29. Electromagnetic-to-Acoustic Conversion Efficiency versus (ω/ω_p), $(n_o = 10^{12}$ cm$^{-3})$

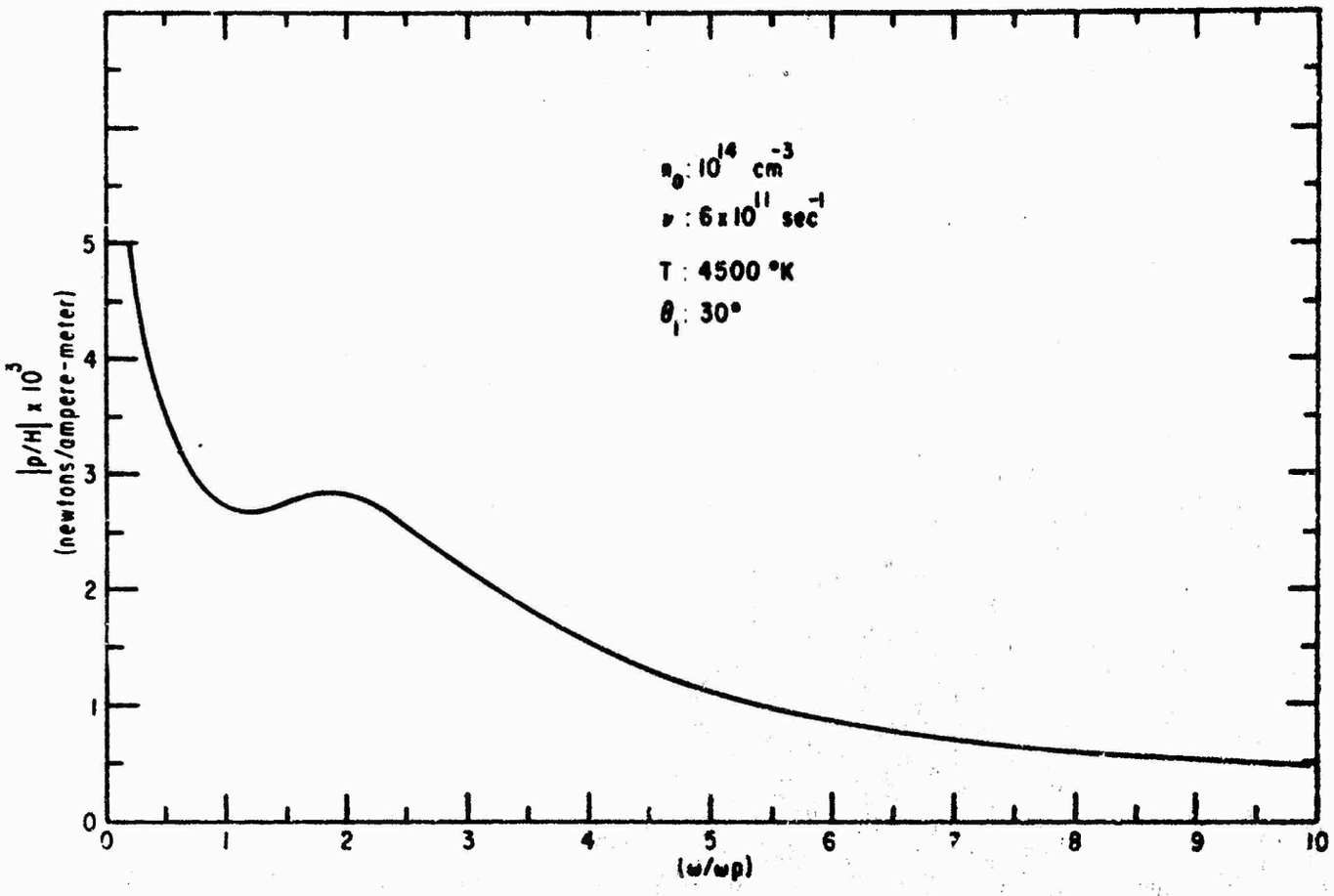

Figure 30. Electromagnetic-to-Acoustic Conversion Efficiency versus (ω/ω_p), $(n_o = 10^{14}\ cm^{-3})$

from Eq. (30). The curves exhibit a minimum at a frequency slightly above the plasma frequency and a steady decrease at frequencies greater than about twice the plasma frequency. The physical explanation for this behavior lies in the interpretation of the electron plasma frequency. At frequencies below the plasma frequency, the electrons can respond to the time variation of the electromagnetic wave and at frequencies above the plasma frequencies the electrons cannot follow the field. Since the pressure wave describes a collective motion of the electrons, a larger response is expected at frequencies below the plasma frequencies. From Eq. (139) it is seen that the efficiency is directly proportional to the relative dielectric constant of the plasma, ϵ_p. For a collisionless plasma, ϵ_p is zero for $\omega = \omega_p$ and the efficiency would be zero. For a plasma with a large collision frequency such as the one considered here, ϵ_p has a minimum for $\omega = \omega_p$ and does not vanish. The dashed portion of the curve in Fig. 29 indicates that Landau damping would destroy any collective motion of the electrons in this frequency range. The efficiency is an order of magnitude smaller for an electron density of 10^{12} cm^{-3} (Fig. 29) as compared to an electron density of 10^{14} cm^{-3} (Fig. 30).

The electromagnetic-to-acoustic conversion efficiency is plotted as a function of the dimensionless parameter ν/ω in Fig. 31. The effect of a large collision frequency is to reduce the amplitude of any organized motion of the electrons considered as a continuum. The effect on the conversion efficiency is therefore a reduction in magnitude of the conversion efficiency. The reduction is fairly small and constant for collision frequencies smaller than the operating (radian)

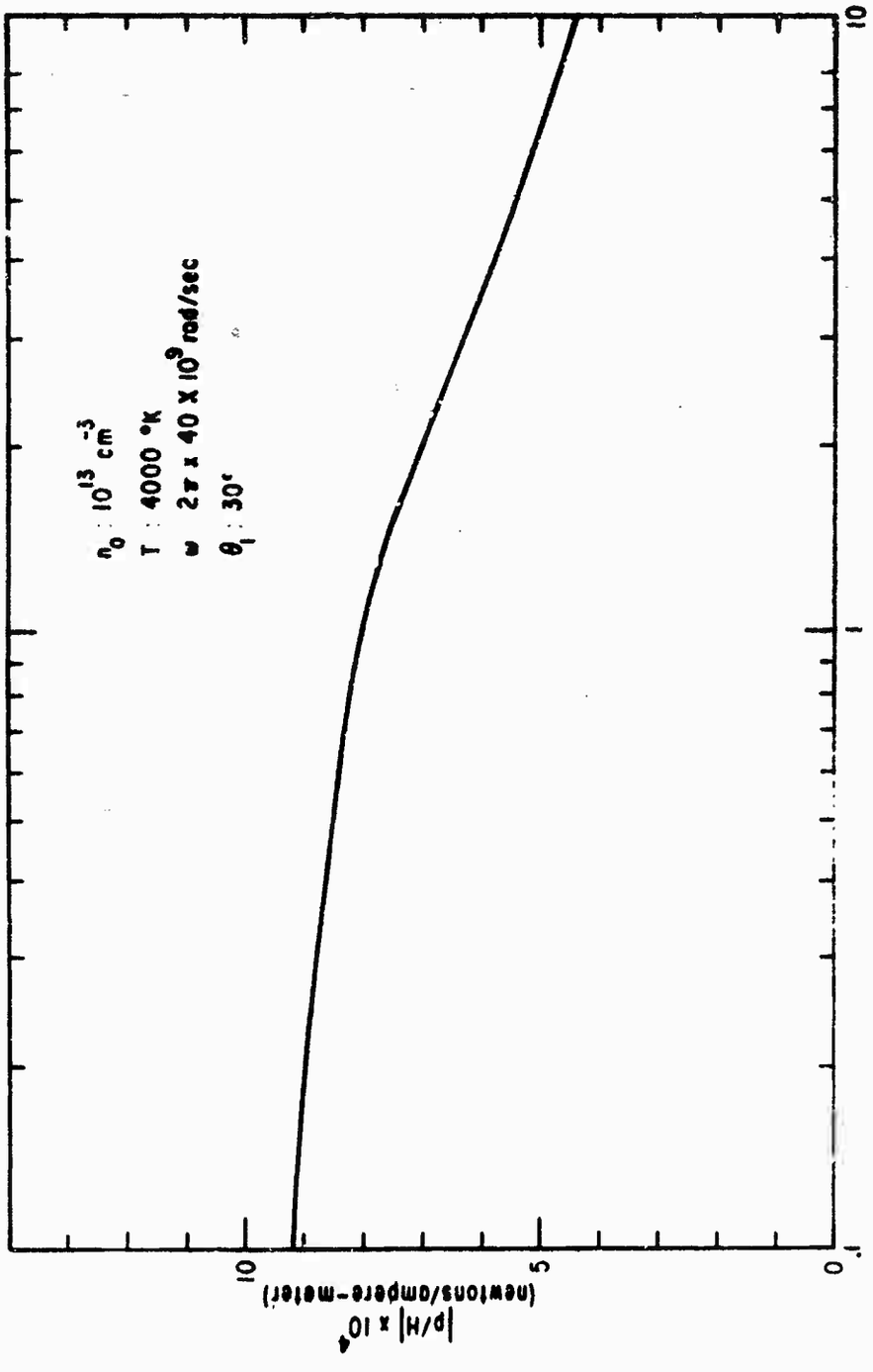

Figure 31. Electromagnetic-to-Acoustic Conversion Efficiency versus (ν/ω)

frequency (Fig. 31); however, the reduction in the efficiency magnitude is greater for collision frequencies larger than the operating (radian) frequency as illustrated in Fig. 31.

Conversion of an Acoustic Wave into an Electromagnetic Wave

An electron acoustic wave incident upon a boundary between a plasma and a dielectric can excite an electromagnetic wave in the dielectric. This is a consequence of the boundary conditions being both electromagnetic and acoustic in nature, Eqs. (124) to (126). The conversion process is illustrated in Fig. 32. In general, there will be both transmitted and reflected electromagnetic waves excited at the boundary. As shown in Chapter III, a pressure wave such as the one shown in Fig. 24 can be excited only by a vertically polarized electromagnetic wave, therefore, a pressure wave of this type will excite only a vertically polarized electromagnetic wave.

The plasma is considered homogeneous so that expressions for the fields can be written explicitly. There is one other assumption which must be made in order to obtain numerical results. The y dependence of all field quantities (including the incident pressure wave) is assumed to be

$$e^{jK_y y} \tag{140}$$

where K_y is given by

$$K_y = \omega\sqrt{\mu_o \varepsilon_o K_d}\,\sin\theta_1 \ . \tag{141}$$

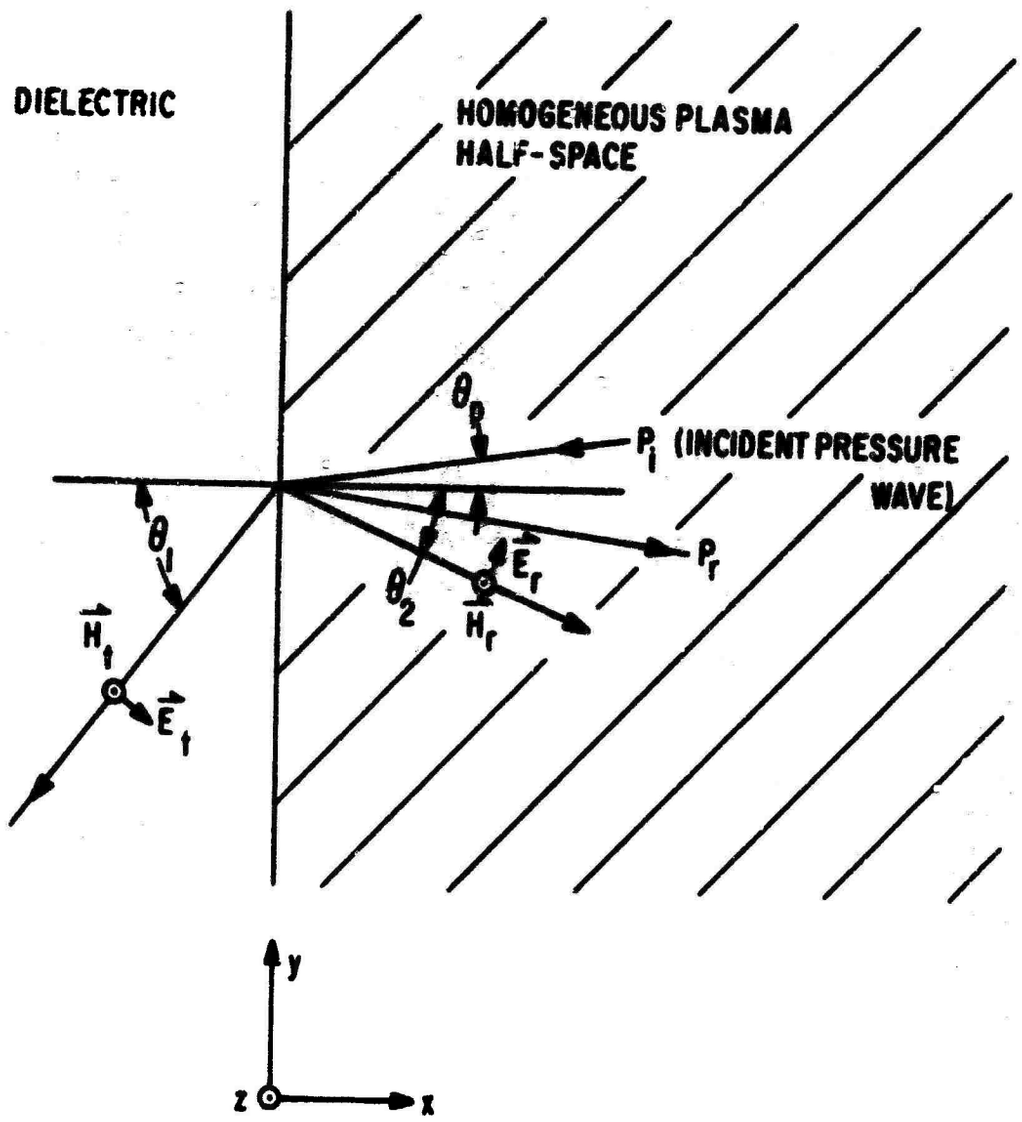

Figure 32. Conversion of an Acoustic Wave into an Electromagnetic Wave

The value of K_y will determine the angle θ_p at which the pressure wave is incident upon the boundary, since K_{px} can be determined from γ_{px} (K_{px} is the imaginary part of γ_{px}) and

$$\theta_p = \tan^{-1}\left[K_y / K_{px}\right] .$$

The spatial variations of the field quantities are determined in the same manner as in the last section. The electromagnetic wave reflected in the positive x direction is described by the magnetic field strength in the plasma

$$H_z = H_{zr}\, e^{-\gamma_{hx} x}\, e^{jK_y y} ,$$

where H_{zr} is the amplitude of the reflected magnetic field strength at $x = 0$ and γ_{hx} is defined by Eq. (129). $\vec{H}$ has only a z component, H_z, for a vertically polarized electromagnetic plane wave. The pressure wave in the plasma is given by

$$p = \left(p_i\, e^{\gamma_{px} x} + p_r\, e^{-\gamma_{px} x}\right) e^{jK_y y} ,$$

where p_i is the amplitude of the incident pressure wave at $x = 0$ and p_r is the amplitude of the reflected pressure wave at $x = 0$ and γ_{px} is defined by Eq. (130). The transmitted electromagnetic wave in the dielectric is described by

$$H_z = H_{zt}\, e^{\gamma_{dx} x}\, e^{jK_y y} ,$$

where H_{zt} is the amplitude of the transmitted magnetic field strength at $x = 0$ and γ_{dx} is defined by Eq. (135).

Applying the boundary condition from Eq. (124) gives

$$H_{zt} = H_{zr} \quad . \tag{142}$$

Applying the boundary condition from Eq. (125) gives

$$-\frac{1}{j\omega\epsilon_d}\gamma_{dx} H_{zt} = -\frac{1}{j\omega\epsilon}\left(-\gamma_{hx} H_{zr}\right) + \frac{eK_y}{\omega\epsilon Am}\left(p_i + p_r\right) \quad . \tag{143}$$

This completes the two electromagnetic boundary conditions.

Applying the acoustic boundary condition from Eq. (126) gives

$$\frac{eK_y}{\omega\epsilon Am} H_{zr} - \frac{\epsilon_o}{\epsilon Am_c}\left(\gamma_{px} p_i - \gamma_{px} p_r\right) = 0 \quad , \tag{144}$$

where Eq. (49) has been used for V_x.

Equations (142), (143), and (144) can be solved for the ratio H_{zt}/p_i which gives the ratio of the amplitude of the electromagnetic field excited in the dielectric to the amplitude of the incident pressure wave. The result is

$$\frac{H_{zt}}{p_i} = \frac{2}{\dfrac{eK_y n_o}{\omega\epsilon_o \gamma_{px}} + j\dfrac{Am}{eK_y}\left[\gamma_{hx} + \dfrac{\gamma_{dx}\epsilon_\rho}{K_d}\right]} \quad . \tag{145}$$

Equation (145) will be used to calculate the conversion of a pressure wave into an electromagnetic wave at a plane dielectric-plasma interface for varying plasma parameters. A computer program

was written to solve Eq. (145). The absolute value of the ratio in Eq. (145) is used. This value will be designated as $|H/p|$ in the following figures.

The acoustic-to-electromagnetic conversion efficiency is plotted as a function of electron density for an operating frequency of 2 GHz in Fig. 33 and for 40 GHz in Fig. 34. The collision frequencies and temperatures corresponding to the electron densities at which the efficiency was computed are given in Table I. The conversion efficiency is larger for lower electron densities. This is desirable, since the conversion process (from a pressure wave into an electromagnetic wave) will occur at the dielectric-plasma interface where the electron density in the boundary layer plasma will be lower than anywhere else in the layer. For the operating frequency of Fig. 33, 2 GHz, the electron density which would result in a plasma frequency equal to the operating frequency is 5×10^{10} electrons/cm^3. For Fig. 34 the operating frequency is 40 GHz and the electron density yielding a plasma frequency equal to the operating frequency is 2×10^{13} electrons/cm^3. In both Figs. 33 and 34 the conversion efficiency decreases for electron densities larger than that electron density which determines a plasma frequency equal to the operating frequency.

The acoustic-to-electromagnetic conversion efficiency is plotted as a function of plasma temperature in Fig. 35. The conversion efficiency (the ratio $|{}^{H}zt/p_i|$) is independent of the temperature. Even though the ratio is constant for varying temperatures, p_i will be smaller for lower temperatures; hence, the effect will be a reduction in the transmitted magnetic field at lower temperatures.

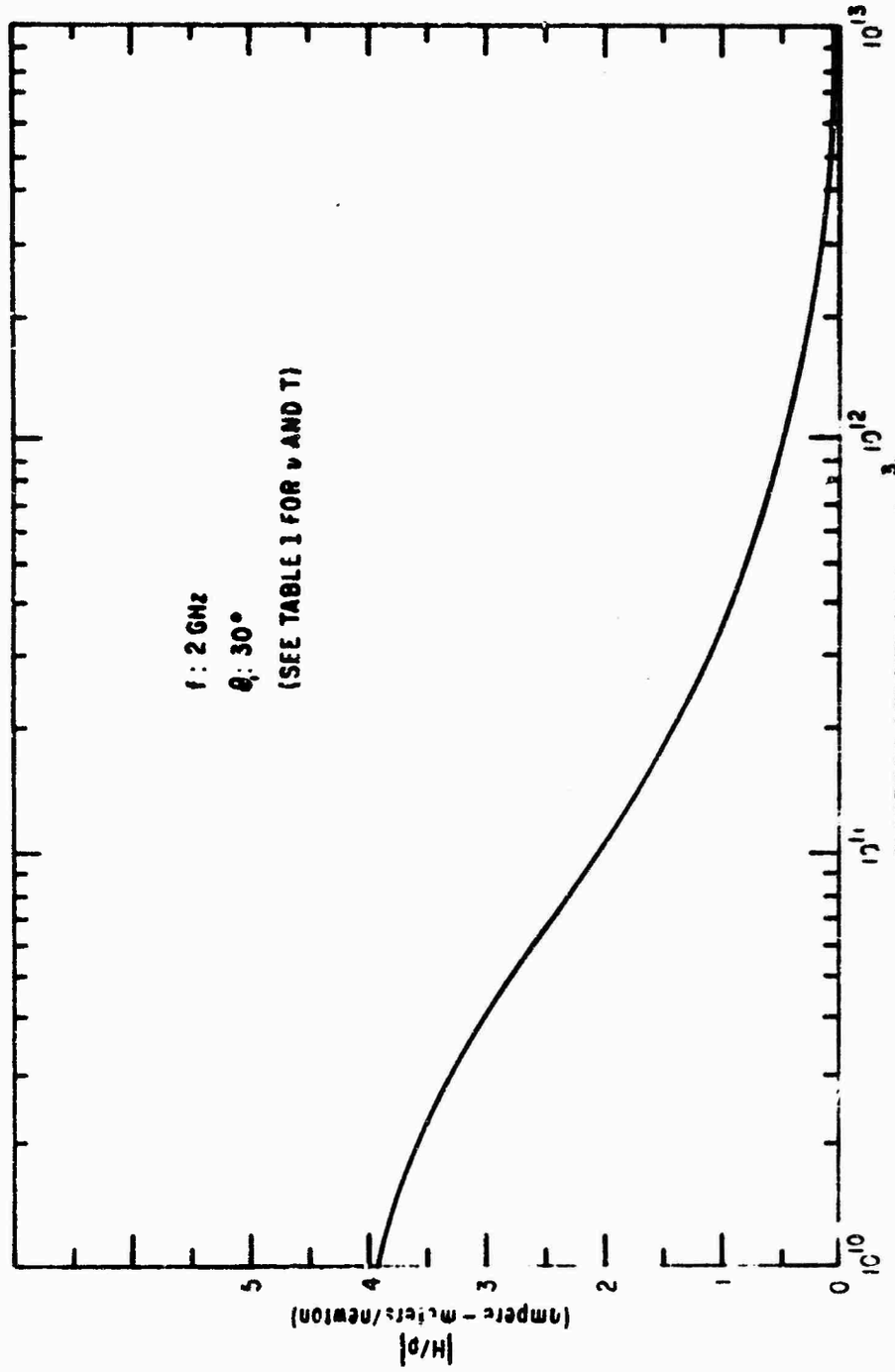

Figure 33. Acoustic-to-Electromagnetic Conversion Efficiency versus Electron Density (f = 2 GHz)

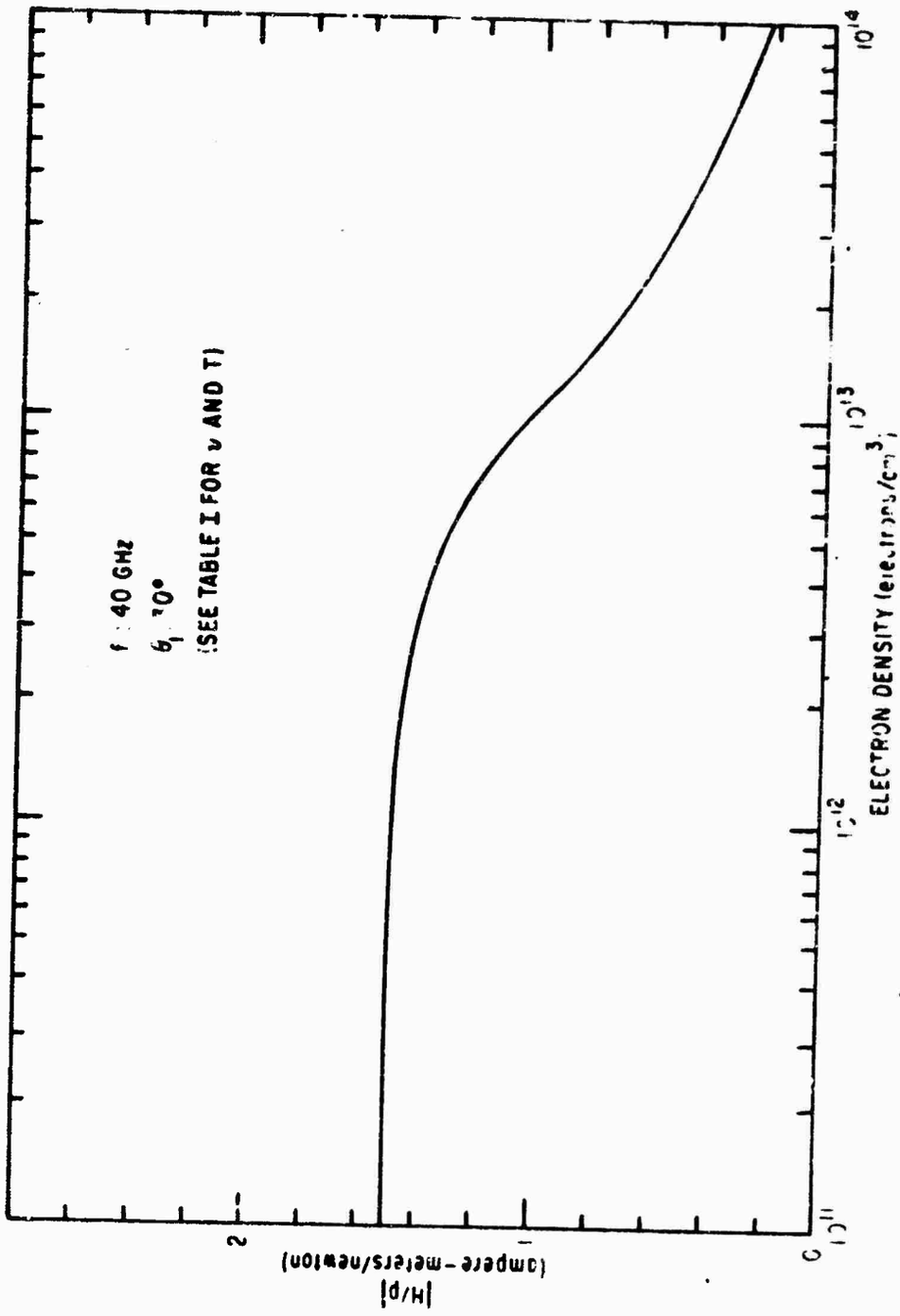

Figure 34. Acoustic-to-Electromagnetic Conversion Efficiency versus Electron Density (f = 40 GHz)

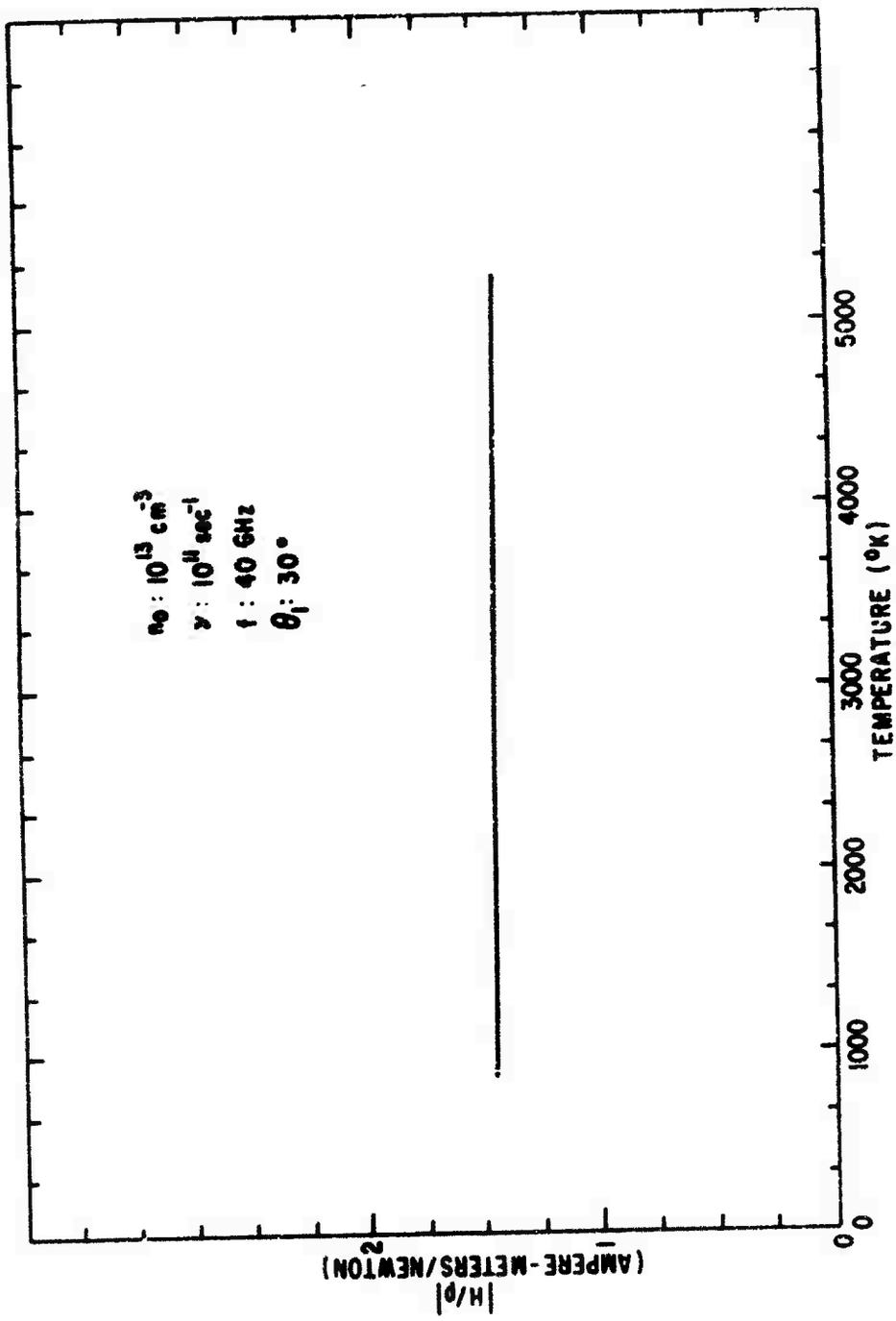

Figure 35. Acoustic-to-Electromagnetic Conversion Efficiency versus Plasma Temperature

The acoustic-to-electromagnetic conversion efficiency is plotted as a function of the dimensionless parameter ω/ω_p in Figs. 36, 37, and 38 for three different electron densities: 10^{12} cm^{-3}, 10^{13} cm^{-3}, and 10^{14} cm^{-3}. There is a maximum in the conversion efficiency at a frequency slightly above the plasma frequency and the efficiency decreases continuously at higher and lower frequencies. It is more difficult to explain the trends of the frequency dependence of the acoustic-to-electromagnetic conversion efficiency by physical reasoning than to explain the frequency dependence of the electromagnetic-to-acoustic conversion efficiency. In the latter case, the electromagnetic wave actually interacts with the plasma in order to excite organized, longitudinal oscillations of the electron gas as a medium. However, in the case of an acoustic wave exciting a transverse electromagnetic wave across a dielectric-plasma boundary, the interaction is more difficult to visualize since the organized oscillations do not exist in the dielectric. Since the conversion of a pressure wave into an electromagnetic wave at a dielectric-plasma interface is the reverse process of the conversion of an electromagnetic wave into a pressure wave at the interface, it would be reasonable to expect the frequency dependencies of the conversion efficiencies to be roughly inverse. This is true at frequencies below the plasma frequencies where electromagnetic-to-acoustic conversion efficiencies increase and acoustic-to-electromagnetic conversion efficiencies decrease. Also, the electromagnetic-to-acoustic conversion efficiencies have a minimum for $\omega \cong \omega_p$, whereas the acoustic-to-electromagnetic conversion efficiencies have

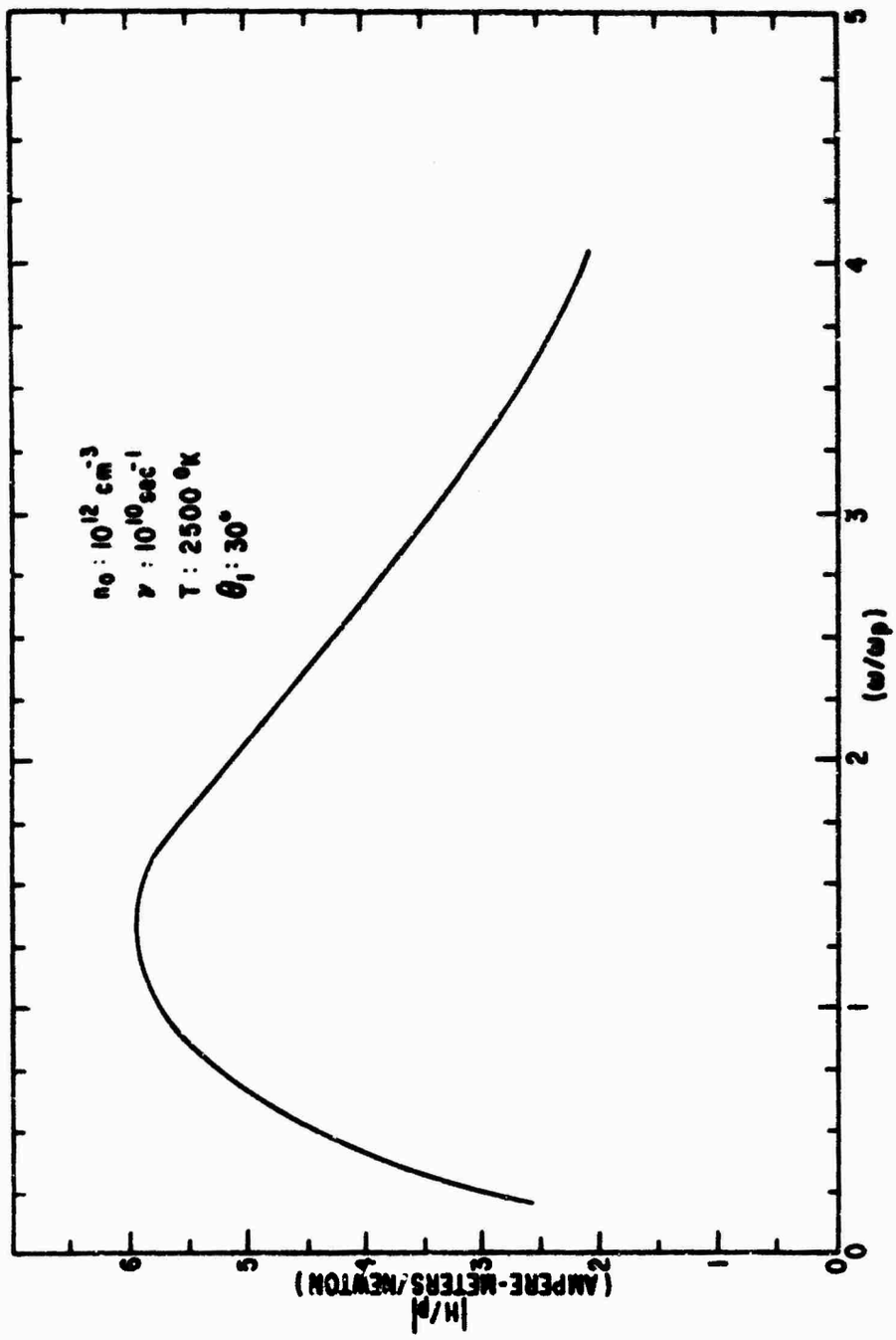

Figure 36. Acoustic-to-Electromagnetic Conversion Efficiency versus (ω/ω_p), $(n_o = 10^{12}\ cm^{-3})$

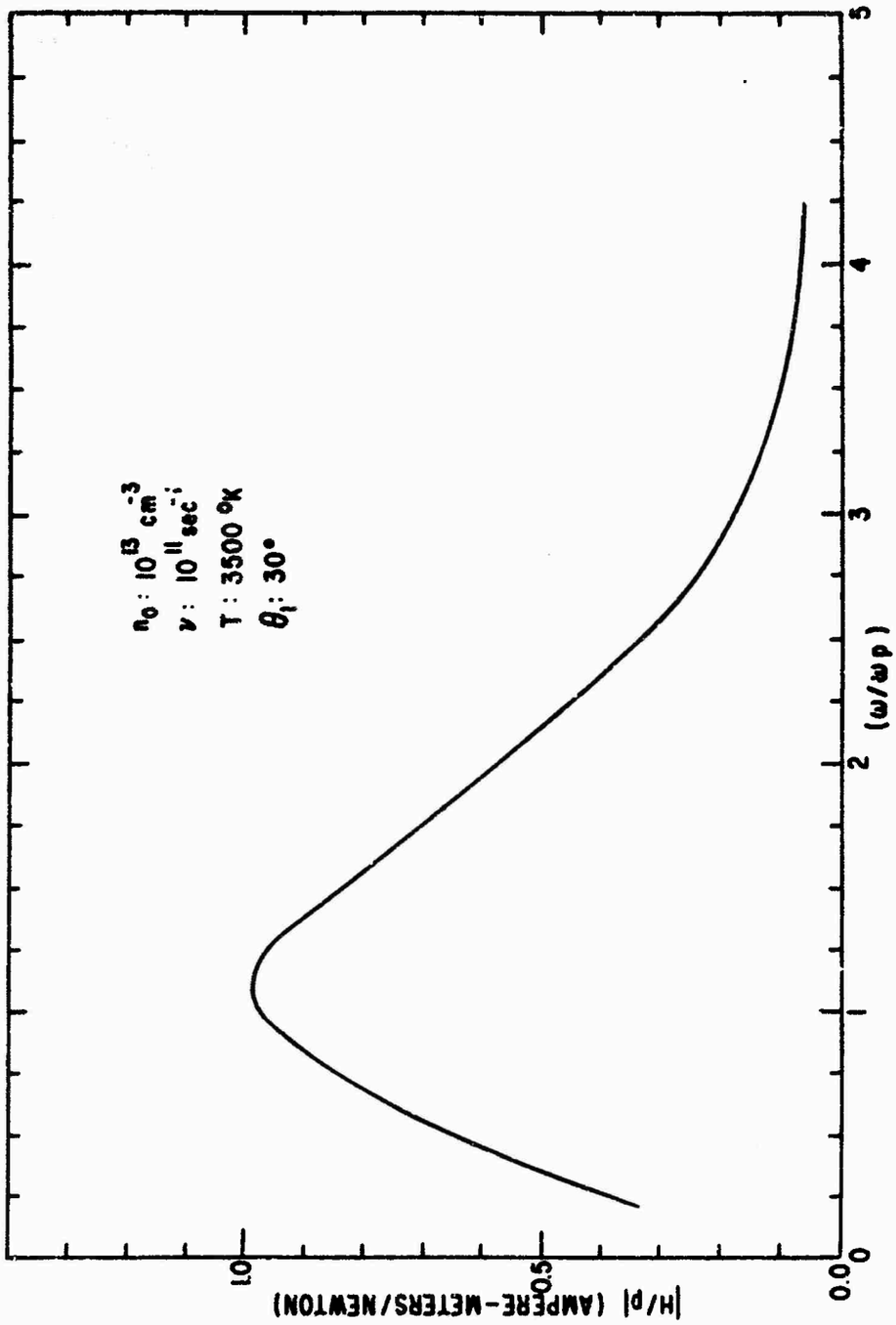

Figure 37. Acoustic-to-Electromagnetic Conversion Efficiency versus (ω/ω_p), $(n_o = 10^{13}\ cm^{-3})$

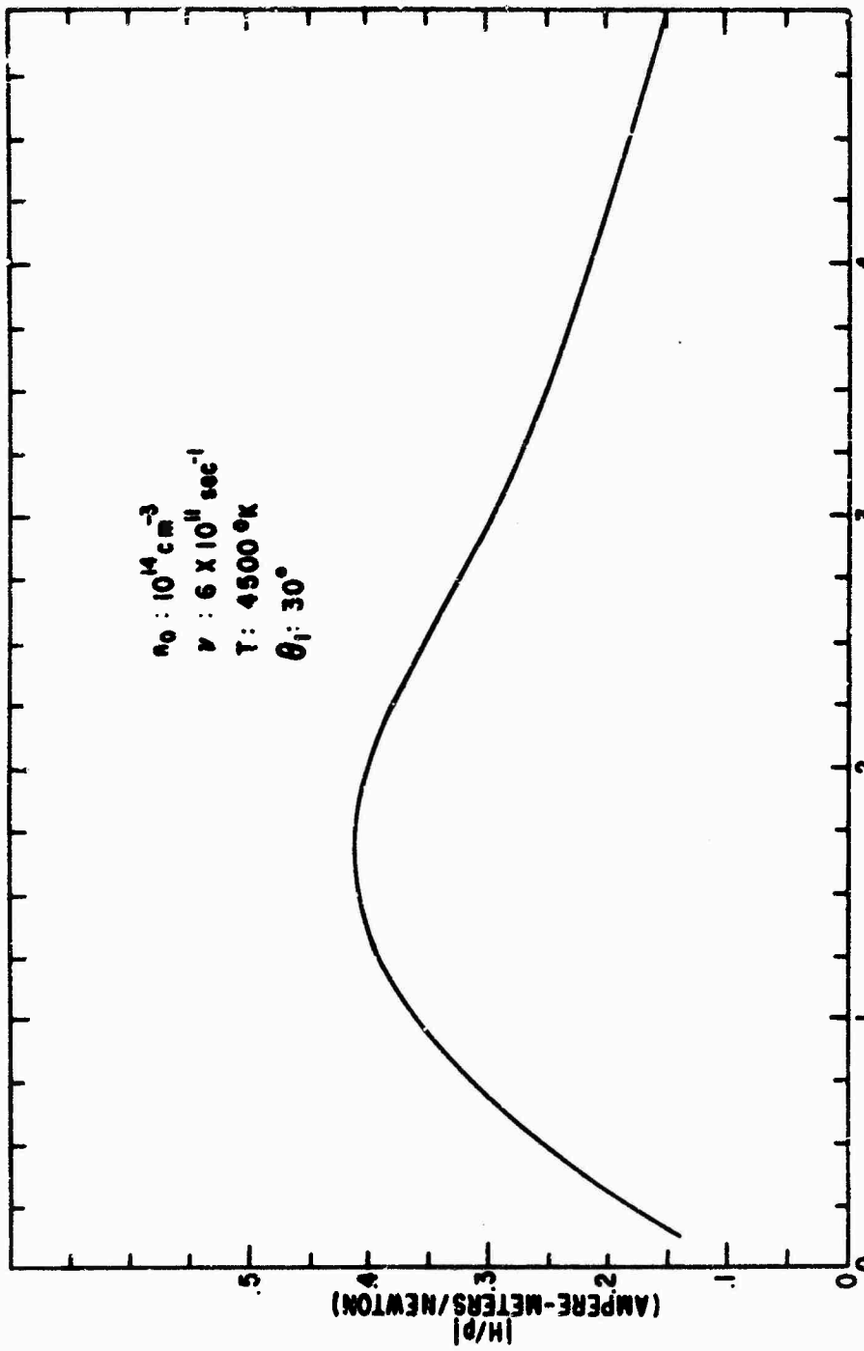

Figure 38. Acoustic-to-Electromagnetic Conversion Efficiency versus (ω/ω_p), $(n_o = 10^{14}\ cm^{-3})$

a maximum for $\omega \cong \omega_p$. A significant result is the fact that both conversion efficiencies decrease for higher frequencies.

The acoustic-to-electromagnetic conversion efficiency is plotted as a function of the dimensionless parameter ν/ω in Fig. 39. The effect of the collision frequency on the efficiency is to reduce the magnitude of the efficiency. From Eq. (145), if $\nu \to \infty$, the conversion efficiency would be zero (note $A = j\omega + \nu$ in Eq. (145)). The effect of the collision frequency upon the acoustic-to-electromagnetic conversion efficiency is even more severe than upon the electromagnetic-to-acoustic conversion efficiency (Fig. 31). The effect of the collision frequency upon the acoustic-to-electromagnetic conversion efficiency begins for collision frequencies well below the operating frequency.

Power Conversion

It was shown in Chapter IV that the amplitudes of any traveling wave pressure solution (or superposition of traveling waves) of the coupled wave equations were negligible compared to the "forced solution," which is dependent mainly upon the coupling term on the right-hand side of Eq. (62). It is these traveling (or propagating) pressure waves with wavelengths of the order of magnitude of one thousandth of a millimeter which are required to obtain the resolution needed in the very short (1 mm) distance from the wall to the peak electron density. It is these waves for which the conversion efficiencies have been calculated in the last two sections. Even though it has been shown that the amplitudes of these waves are negligible compared to the

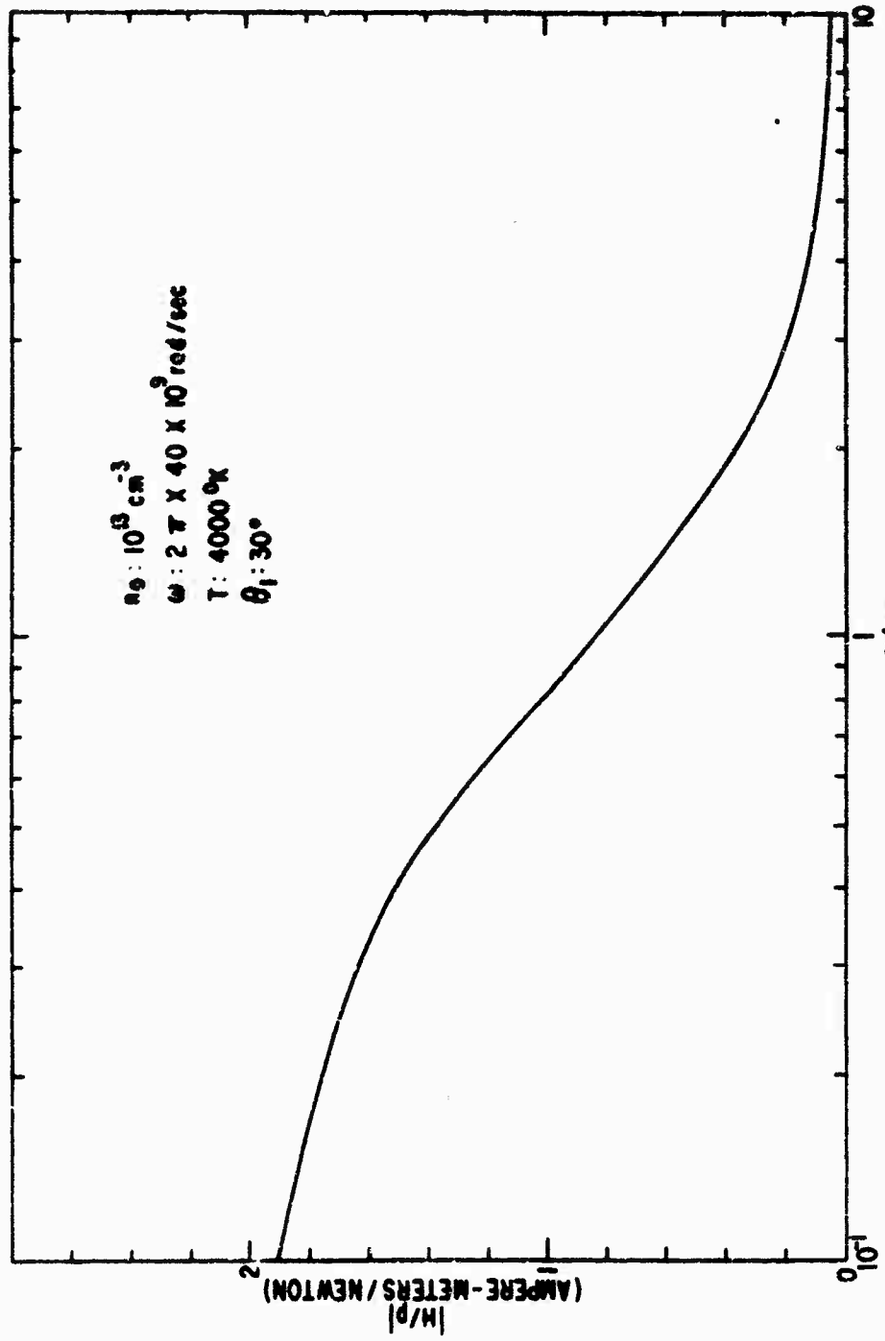

Figure 39. Acoustic-to-Electromagnetic Conversion Efficiency versus (ν/ω)

"forced solution," it is still desirable to obtain some estimate of the order of magnitude of the amplitudes of these waves. It will be shown that the amplitudes are functions of the magnetic field strength; however, the amplitudes are still small and the waves are severely damped.

Using the same assumption about the equation coefficients and g ($g = FH_z$), i.e., that they are all constants, as in the section Solutions of the Coupled Wave Equations in Chapter IV, the complete solution for p is then given by

$$p = A' e^{\gamma_1 x} + B' e^{\gamma_2 x} + g/\mathcal{E} \qquad (146)$$

where

$$\gamma_1 = \alpha + j\beta = j\sqrt{E}$$

and

$$\gamma_2 = -\alpha - j\beta = -j\sqrt{E} \quad ,$$

(α is the attenuation constant and β is the propagation constant) and A' and B' are determined from boundary conditions. The amplitude of the pressure wave traveling in the positive x direction is B' and the amplitude of the reflected pressure wave (the wave traveling in the negative x direction) is A'.

The complex amplitudes A' and B' will be calculated using the two acoustic boundary conditions from Eqs. (88) and (90) for a plasma model like that pictured in Fig. 5(b). It is believed that this model

might actually be more realistic than the one in Fig. 5(a); therefore, the boundary conditions for profile (b) are used in this calculation. The parameters of interest are: n_e (wall) = 10^{11} cm^{-3}, n_e (peak) = 10^{13} cm^{-3}, T (wall) = 2000°K, T (peak) = 5000°K, $\nu = 6 \times 10^{11}$ sec^{-1}, d = 1 mm, and the operating frequency is 30 GHz.

Using Eq. (88) and noting that $\gamma_2 = -\gamma_1$ and that β/k is assumed to be a constant, gives

$$A' - B' = \frac{eK_y n_e(0)}{\gamma_1 \omega \epsilon_0} E_z(0) \quad , \tag{147}$$

where $n_e(0)$ is the electron density at the wall and $E_z(0)$ is fixed at 0.1 + j0.1 amperes/meter.

Using Eq. (89) and noting that $\gamma_{px} \cong \gamma_1$ (since K_y^2 is much smaller than the other terms in Eq. (130)) gives

$$\gamma_1 A' e^{\gamma_1 d} + \gamma_2 B' e^{\gamma_2 d} = -\gamma_1 A' e^{\gamma_1 d} - \gamma_1 B' e^{\gamma_2 d}$$

$$- \gamma_1 (\beta/k)\Big|_{x=d} \quad ,$$

where

$$\frac{d(\beta/k)}{dx}$$

has been assumed to be zero and the complete pressure solution is used in applying the boundary conditions. From the preceding equation

$$A' = -\frac{1}{2} (\beta/k)\Big|_{x=d} e^{-\gamma_1 d}$$

(since $\gamma_2 = -\gamma_1$)

or

$$|A'| = \frac{1}{2} \left|(\mathcal{E}/E)\right|_{x=d} e^{-\alpha d} \quad . \tag{148}$$

Using the plasma parameters given above, the value of

$$(\mathcal{E}/E)\Big|_{x=d}$$

from Fig (17) and assuming $\alpha \cong 10^4$ m^{-1}, Eqs. (147) and (148) become

$$A' - B' \cong 5 \times 10^{-5}$$

and

$$|A| \cong 2.5 \times 10^{-11} \quad .$$

Since $|A'| \ll 5 \times 10^{-5}$,

$$|B'| \cong 5 \times 10^{-5} \quad .$$

Therefore, for this profile, the amplitude of the pressure wave propagating away from the boundary is 5×10^{-5} newtons/m^2 at the boundary. This value is larger than the "forced solutions" at the boundary; however, the propagation constant contains an attenuation factor which causes this wave to be damped out very rapidly in exactly the same manner as for a homogeneous plasma (Fig. 22). The value of α is more likely to be 10^5m^{-1} rather than 10^4m^{-1}, in which case $|A'| \cong 0$ and the wave could be damped out in about one hundredth of a millimeter. For $\alpha \cong 10^4$ m^{-1}, the amplitude of the pressure wave traveling in the negative x direction is 2.5×10^{-11} newtons/m^2 (at $x = 0$). It is this amplitude which would be used in calculating the conversion from a

pressure wave into an electromagnetic wave at the boundary.

It appears that the homogeneous solution (the exponential or propagating wave factor) for the pressure field may be larger (near the boundary) than the "forced solution" due to the boundary conditions. This was the case for the numerical solutions also. In the numerical solutions, the pressure field had a "spike" near x = 0; however, the solution quickly converged (in a very short distance) to the "forced solution" where the effect of the exponential factors of the homogeneous solution was not observable. This is presumed to be caused by the severe damping experienced by the propagating modes. The "spikes" are not shown in any of the figures illustrating pressure solutions (Figs. 13 to 18 and Figs. 20 and 21), where only the "forced solutions" are plotted.

The power in an electromagnetic wave excited in the dielectric by a pressure wave incident from the plasma will now be calculated. The Poynting vector will be calculated at the boundary and the closed surface shown in Fig. 40 will be used to determine the power radiated in the finite two-dimensional geometry. The width (dx) of the volume will be considered to approach zero. The surface area of the volume in the y-z plane is S meter^2.

From Poynting's theorem the time-averaged power is

$$\overline{P} = \iint_{\text{Closed surface}} \frac{1}{2} \operatorname{Re} \left\{ \vec{E}_t \times \vec{H}_t^* \right\} \cdot d\vec{s} \qquad (149)$$

where $d\vec{s} = -\hat{i}\, dydz$ with $\hat{i}$ representing the unit vector in the x direction and the asterisk implies a complex conjugate operation. Figure 32

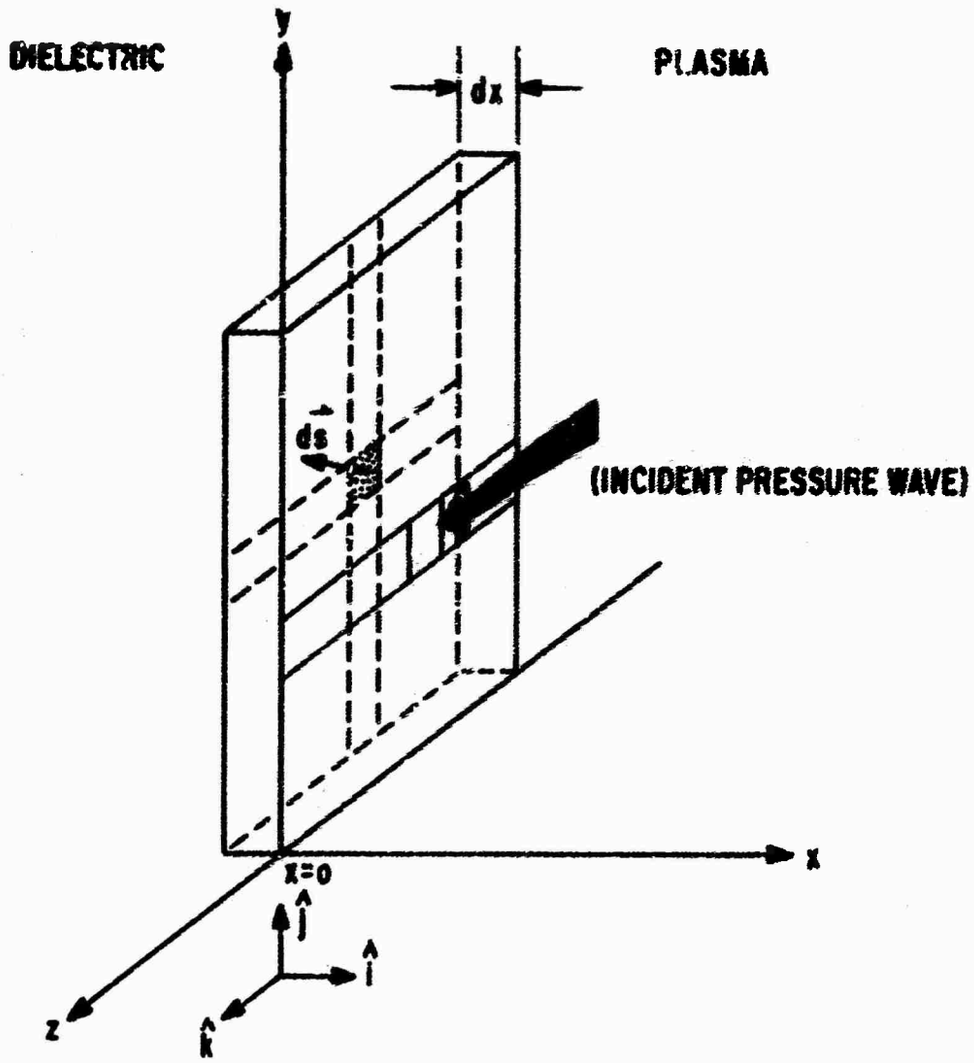

Figure 40. Dielectric Volume Used in the Calculation of the Power in an Electromagnetic Wave Excited by an Incident Plasma Wave

illustrates the incident pressure wave and the excited electromagnetic wave, $\vec{H}_t$, in the dielectric.

For a vertically polarized electromagnetic wave, the electric field in the dielectric, $\vec{E}_t$, has components E_x and E_y and $\vec{H}_t$ has only a z component H_z. For the y dependence of Eq. (140),

$$\vec{E}_t \times \vec{H}_t^* = + \hat{i} E_y H_z^* - \hat{j} E_x H_z^* \quad , \tag{150}$$

where E_y, E_x, and H_z^* are functions of x only since the $e^{jK_y y}$ term will cancel in the operation. Substituting Eq. (150) into Eq. (149) gives

$$\bar{P} = \iint_S \frac{1}{2} \mathrm{Re} \left\{ -\hat{i} E_y H_z^* \right\} dy dz \quad ,$$

since E_y and H_z^* are functions of x only.

$$\bar{P} = \frac{1}{2} \mathrm{Re} \left\{ -E_y H_z^* \right\} S \quad \text{(watts)} \quad . \tag{151}$$

The electric field, E_y, in the dielectric is given by

$$E_y = - \frac{1}{j\omega\epsilon_d} \frac{\partial H_z}{\partial x} \quad ,$$

or

$$E_y = - \frac{H_{zt} \gamma_{dx}}{j\omega\epsilon_d} e^{\gamma_{dx} x} \quad ,$$

where H_{zt} is the amplitude of the excited magnetic field strength at $x = 0$. Using Eq. (135) for γ_{dx} and evaluating E_y at $x = 0^-$ (just inside the dielectric) gives

$$E_y = -H_{zt} \eta_d \cos \theta_1 \quad , \tag{152}$$

where

$$\eta_d = \sqrt{\mu_o/\epsilon_o K_d}$$

is the characteristic impedance of the dielectric.

Substituting Eq. (152) into Eq. (151) gives

$$\bar{P} = \frac{1}{2} \mathrm{Re}\left[E_{xt}\, \eta_d \cos\theta_1 H_z^*\right] S \quad . \tag{153}$$

H_z^* evaluated at $x = 0^-$ is H_{xt}^*. Equation (153) then becomes

$$\bar{P} = \frac{1}{2} \mathrm{Re}\left[\eta_d \cos\theta_1 H_{xt} H_{xt}^*\right] S \quad .$$

Since $H_{xt}H_{xt}^*$ is just $|H_{xt}|^2$ which is a real quantity, the time-averaged power is

$$\bar{P} = \frac{1}{2} \eta_d \cos\theta_1 |H_{xt}|^2 S \quad .$$

From Eq. (145) the ratio $|H_{xt}|^2/|p_i|^2$ can be determined. This ratio will be represented by C^2:

$$C^2 = |H_{xt}|^2/|p_i|^2 \quad .$$

Then $\bar{P}$ can be expressed as

$$\bar{P} = \frac{1}{2} \eta_d \cos\theta_1 C^2 S |p_i|^2 \quad \text{(watts)} \quad . \tag{154}$$

Using Eq. (154), the power in an electromagnetic wave excited by an incident pressure wave will be calculated for the following parameters:

(1) Angle of incidence 30°

(2) Operating frequency 30 GHz

(3)	k_d	3.5
(4)	S (1 in^2)	6.3×10^{-4} meter^2
(5)	Plasma density profile (b)	$10^{11} - 10^{14}$ cm^{-3}
(6)	Plasma temperature profile (b)	1000-5000°K
(7)	Collision frequency	6×10^{11} sec^{-1}
(8)	Distance to the peak electron density	1 m

As stated at the beginning of this section, the appropriate amplitude to be used in acoustic-to-electromagnetic conversion calculations is A', the amplitude of the pressure wave traveling in the negative x direction at $x = 0$. For the parameters given above, the estimate for A' given by Eq. (148) was found to be 2.5×10^{-11} newtons/m^2. Then, $|p_1| = 2.5 \times 10^{-11}$ newtons/m^2. The acoustic-to-electromagnetic conversion efficiency, C in Eq. (154), can be estimated from Figs. 33 and 34. In Fig. 33, C is 2.5 for a frequency of 2 GHz and in Fig. 34, C is 1.5 for a frequency of 40 GHz, where an electron density of 10^{11} cm^{-3} was used to determine C. For an operating frequency of 30 GHz C will be somewhere between 1.5 and 2.5, so let C be equal to 2 as an approximation. All of the factors in Eq. (154) have been determined and the time-averaged steady-state power can be calculated as follows:

$$\overline{P} = (0.5)(202)(0.866)(2)^2(6.3 \times 10^{-4})(2.5 \times 10^{-11})^2$$

which gives

$$\overline{P} = 1.4 \times 10^{-22} \quad \text{watts} \quad .$$

This is an extremely small power level and it would be very hard to distinguish between this signal and background noise due to spectral emission in the plasma layer, etc. In terms of power relative to 1 milliwatt (or dBm) the power level is

$$\bar{P} = -188 \text{ dBm} \quad ,$$

which would require a very sensitive receiver indeed for detection. It must be emphasized that the attenuation factor was assumed to be 10^4 m^{-1}. If the attenuation factor is actually an order of magnitude larger than this (which it more than likely is), the power given by Eq. (154) would be virtually zero.

CHAPTER VI

CONCLUSION

The propagation of electron acoustic waves in an inhomogeneous, warm, lossy plasma layer has been investigated. The coupled wave equations (Eqs. (61) and (62)) have been solved by a finite difference numerical technique in order to determine the degree of coupling between the electromagnetic wave and the electron acoustic wave in the inhomogeneous region of a warm, lossy plasma layer. For the plasma profiles and operating frequencies considered, it was found that the pressure (or acoustic) solutions of the coupled wave equations consisted of two parts: a "forced solution" with an x-variation similar to the coupling coefficient in the pressure equation (Eq. (62)), and a "homogeneous solution" which characterized the propagating electron acoustic wave. It is shown that both parts of the solution are directly dependent upon (or coupled to) the magnetic field in the inhomogeneous plasma (see Eqs. (123), (146), (147) and (148)). It is also shown that for the plasma profiles and operating frequencies considered, the homogeneous solution is negligible compared to the forced solution except possibly near the dielectric-plasma interface. Thus, even though the electron acoustic wave is indeed coupled to the electromagnetic wave, the electron-acoustic wave is severly damped for propagation in either direction in the inhomogeneous plasma. In the approximate analysis it is shown that the "propagation constant" for the electron acoustic wave in the inhomogeneous region is the same as that for a homogeneous,

lossy plasma (Eq. (130)) and the damping effect is due to the large collision frequency of the plasma.

It is also shown in the approximate analysis that the steady-state time-averaged power produced by the conversion of a pressure wave into an electromagnetic wave at a dielectric boundary is of the order of 10^{-22} watts for a typical plasma profile and operating frequency. This result is based on a probe area of 1.0 in^2, an incident electromagnetic power of 10 mw and an operating frequency of 30 GHz. This received power level is too low for reliable detection.

In addition, it is shown that the conversion efficiency for pressure wave-to-electromagnetic wave at a dielectric-plasma boundary is reduced for collision frequencies well below the operating frequency (see Fig. 31). High collision frequencies will, therefore, reduce the detection capability of an acoustic probe system by damping the propagating acoustic wave and by reducing the conversion efficiency. The results of this investigation show that even for an inhomogeneous plasma, the damping effects of high collision frequency on electron-acoustic waves is drastic.

For the plasma profiles considered, and using a steady-state plane wave analysis, the effect of the acoustic solution upon the electromagnetic solution is shown to be negligible. This is true even for a "warm" plasma layer with temperatures as high as 5000°K. Therefore, for the plasma conditions studied, the approximate solution for the pressure given by Eq. (115), used together with Eq. (61) for the magnetic field, adequately treats the effects of

compressibility. This is valid since the approximate solution for p is very good for the plasma parameters considered. Thus the effect of the acoustic portion of the fields in the plasma is taken care of by substituting p from the approximate solution into the right hand side of Eq. (61). In this case, the effect on the electromagnetic fields in the plasma will be determined by solving Eq. (61) rather than the two coupled second order differential equations.

REFERENCES

1. Lustig, C. D. and McBee, W. D., "Proposed Method of Measurement of Electron Density in Re-entry Sheaths by Observation of Electro-acoustic Resonances," Air Force Cambridge Research Laboratories report AFCRL-69-0039, February 1969.

2. Lustig, C. D., Baird, A. W., and Ewald, H. N., "Study of Pulse and Wave Phenomena in Plasmas," Air Force Cambridge Research Laboratory report AFCRL-69-0489, November 1969, p. 17.

3. Bohm, D. and Gross, E. P., "Theory of Plasma Oscillations. A. Origin of Medium-Like Behavior," Physical Review, June 1949, pp. 1851-1864.

4. Oster, L., "Linearized Theory of Plasma Oscillations," Reviews of Modern Physics, January 1960, pp. 141-168.

5. Burman, R., "First-Order Coupled Wave Equations for Propagation in Stratified Compressible Plasmas," Electronics Letters, August 1966, pp. 747-757.

6. Verma, Y. P., "Study of Coupled Electroacoustic and Electromagnetic Waves in an Inhomogeneous and Lossy Plasma," PhD. Thesis, Northeastern University, Boston, Massachusetts, June 1969.

7. Stix, T. H., The Theory of Plasma Waves, New York: McGraw-Hill Book Company, 1962, p. 3.

8. Friedlander, F. G., Sound Pulses, London: Cambridge Press, 1958, Chapter 1.

9. Van Hoven, G., "Observation of Plasma Oscillations," Physical Review Letters, July 1966, pp. 169-172.

10. Derfler, H. and Simonen, T. C., "Landau Waves: An Experimental Fact," Physical Review Letters, July 1966, pp. 172-175.

11. Malmberg, J. H. and Wharton, C. B., "Dispersion of Electron Plasma Waves," Physical Review Letters, July 1966, pp. 175-178.

12. Wait, J. R., "Radiation from Sources Immersed in Compressible Plasma Media," Canadian Journal of Physics, September 1964, pp. 1760-1780.

13. Wait, J. R., "On the Theory of Wave Propagation in a Bounded Compressible Plasma," Canadian Journal of Physics, February 1966, pp. 293-302.

REFERENCES (cont'd)

14. Felsen, L. B., "Equations for Wave Propagation in an Inhomogeneous Compressible Plasma," Electronics Letters, January 1966, pp. 3-4.

15. Burman, R., "Equations for Wave Propagation in an Inhomogeneous Compressible Plasma," Electronics Letters, June 1966, pp. 219-220.

16. Burman, R., "Coupled Wave Equations for Propagation in Inhomogeneous Compressible Plasmas," Proceedings of the Cambridge Philosophical Society, 1967, pp. 1229-1246.

17. Wait, J. R., "Modes of Propagation in a Bounded Compressible Plasma," Electronics Letters, September 1965, pp. 193-194.

18. Yeh, Y. S., "Boundary Conditions at a Dielectric-Plasma Interface," Electronics Letters, August 1967, pp. 367-368.

19. Wait, J. R., "On Assumed Boundary Conditions at an Interface Between a Dielectric and a Compressible Plasma," Electronics Letters, July 1967, pp. 317-318.

20. Sancer, M. I., "Boundary Conditions for a Unique Solution to the Linearized Warm-Plasma Equations," Radio Science, September 1966, pp. 1067-1072.

21. Bessel, A., Marcuvitz, N., and Shmoys, J., "Conversion of Transverse Electromagnetic Waves into a Longitudinal Wave at a Dielectric-Plasma Boundary," IEEE Transactions on Antennas and Propagation (Communications), January 1964, pp. 130-132.

22. Wait, J. R., "On Radiation of Electromagnetic and Electroacoustic Waves in a Plasma," Applied Scientific Research, 1964, pp. 423-432.

23. Kuehl, H. H., "Resistance of a Short Antenna in a Warm Plasma," Radio Science, August 1966, pp. 971-976.

24. Rasmer, H. R., "A Mathematical Model for Analysis of Wave Propagation in a Linearized Vertically Nonuniform Partially Ionized Gas," Canadian Journal of Physics, 1966, pp. 1047-1065.

25. Jackson, J. D., Classical Electrodynamics, New York: John Wiley and Sons, Inc., 1962, Chapter 10.

26. Budden, K. G., Radio Waves in the Ionosphere, London: Cambridge University Press, 1967, Chapter 18.

27. Clemmow, P. C. and Heading, J., "Coupled Forms of the Differential Equations Governing Radio Propagation in the Ionosphere," Proceedings of the Cambridge Philosophical Society, 1953, pp. 319-333.

REFERENCES (cont'd)

28. Kantorovich, L. V. and Krylov, V. I., Approximate Methods of Higher Analysis, New York: Interscience Publishers, Inc., 1958, Chapter 3.

29. Smith, G. D., Numerical Solution of Partial Differential Equations, New York: Oxford University Press, 1965, Chapter 2.

30. Jordan, E. C. and Balmain, K. G., Electromagnetic Waves and Radiating Systems, Englewood Cliffs, New Jersey: Prentice Hall, Inc., 1968, Chapter 4.

31. Cohen, M. H., "Radiation in a Plasma. III. Metal Boundaries," Physical Review, April 1962, pp. 398-404.

32. Fivel, B. J. and Schaffer, M. J., Turbulent Boundary Layer Program (REBOUND), AFWL-TR-67-141, Vol V, Air Force Weapons Laboratory, Kirtland Air Force Base, New Mexico, May 1969.

This page intentionally left blank.

APPENDIX A: APPROXIMATIONS INVOLVED IN THE APPROXIMATE SOLUTION

The approximations used in obtaining the approximate solution will be investigated here for the following parameters:

n_o: $10^{11} - 10^{14}$ cm^{-3}

T: 3000 - 4000°K

ν: 6.5×10^{11} sec^{-1}

f: 2 GHz

θ_1: 20°

The coefficients for the differential equations were computed and their maximum or minimum absolute values are listed below:

$$|A| \geq 6.0 \times 10^2$$

$$|B| \leq 2.0 \times 10^4$$

$$|C| \leq 1.5 \times 10^5$$

$$|D| \leq 6.0 \times 10^5$$

$$|E| \leq 1.8 \times 10^{12}$$

$$|F| \leq 2.0 \times 10^5$$

The characteristic length of the plasma inhomogeneity is just the width which was 2mm. The approximation will improve as d is decreased.

Using Eqs. (108) and (109) gives

$$(2.5 \times 10^5 + 3 \times 10^5 + 2 \times 10^4)\ H_z = 1.5 \times 10^5\ p$$

and

$$(2.5 \times 10^5 + 3 \times 10^8 + 1.8 \times 10^{12})\ p = 2 \times 10^6\ H_z$$

From the first equation, it is observed that the first two terms in the parentheses are much larger than the last. In the second equation

the third term in the parentheses completely dominates the first two. In the approximate solution, only the dominant terms are retained.

It is now necessary to compare CF/E with $1/d^2$ and A/d. For the profile and operating frequency, $|E|$ minimum = 8×10^{10} and the maximum absolute values for C and F have been given.

$$\left|\frac{CF}{E}\right|_{max.} = 3.75 \times 10^2$$

$$\frac{1}{d^2} = 2.50 \times 10^5$$

$$\frac{|A|_{min.}}{d} = 4.00 \times 10^6$$

Therefore CF/E is much smaller than the other two terms and is neglected in the approximate solution. In the approximate form, the equations then become

$$\left(\frac{1}{d^2} + \frac{A}{d} \right) H_z = 0$$

and

$$p = \left(\frac{F}{E} \right) H_z$$

Some general remarks can be made about the validity of the approximate solution. The approximation is more accurate at lower frequencies. The accuracy is also improved as the electron density is increased or the plasma thickness is decreased.

APPENDIX B: COEFFICIENTS OF THE COUPLED WAVE EQUATIONS FOR A PARTICULAR CASE

The real and imaginary parts of the coefficients of the coupled wave equations are given in Table II for the following plasma profile:

n_o: $10^{12} - 10^{13}$ cm^{-3}

T: 2000 - 3500°K

d: 1.0 mm

ν: 10^{11} sec^{-1}

θ_1: 30°

f: 26 GHz

The coefficients change, of course, for different plasma profiles, angles of incidence and operating frequencies.

NOTE: R(A) means the real part of coefficient A and I(A) means the imaginary part; the same notation applies for the other coefficients.

Table II

COEFFICIENTS OF THE COUPLED WAVE EQUATIONS FOR A PARTICULAR CASE

x (mm)	R(A)	I(A)	R(B)	I(B)	R(C)	I(C)
0.0	8.2×10^2	5.7×10^2	1.1×10^4	-1.6×10^4	-1.9×10^5	-4.3×10^5
0.1	8.5×10^2	6.8×10^2	-1.2×10^4	-3.0×10^4	-1.8×10^5	-4.8×10^5
0.2	8.7×10^2	8.0×10^2	-3.5×10^4	-4.4×10^4	-1.5×10^5	-5.3×10^5
0.3	8.7×10^2	9.6×10^2	-5.8×10^4	-5.8×10^4	-1.1×10^5	-6.0×10^5
0.4	8.4×10^2	1.1×10^3	-8.1×10^4	-7.3×10^4	-5.7×10^4	-6.6×10^5
0.5	7.5×10^2	1.3×10^3	-1.0×10^5	-8.7×10^4	2.7×10^4	-7.1×10^5
0.6	5.9×10^2	1.5×10^3	-1.3×10^5	-1.0×10^5	1.4×10^5	-7.5×10^5
0.7	3.5×10^2	1.7×10^3	-1.5×10^5	-1.2×10^5	2.7×10^5	-7.6×10^5
0.8	6.3×10^1	1.8×10^3	-1.7×10^5	-1.3×10^5	4.0×10^5	-7.1×10^5
0.9	-2.4×10^2	1.7×10^3	-2.0×10^5	-1.4×10^5	5.2×10^5	-6.3×10^5
1.0	-5.0×10^2	1.6×10^3	-2.2×10^5	-1.6×10^5	5.9×10^5	-5.1×10^5

Table II (cont'd)

x (mm)	R(D)	I(D)	R(E)	I(E)	R(F)	I(F)
0.0	8.2×10^{2}	5.7×10^{2}	2.6×10^{11}	-1.8×10^{11}	-5.5×10^{5}	-3.2×10^{4}
0.1	8.5×10^{2}	6.8×10^{2}	2.1×10^{11}	-1.7×10^{11}	-6.0×10^{5}	-7.2×10^{4}
0.2	8.7×10^{2}	8.0×10^{2}	1.7×10^{11}	-1.6×10^{11}	-6.5×10^{5}	-1.3×10^{5}
0.3	8.7×10^{2}	9.6×10^{2}	1.3×10^{11}	-1.5×10^{11}	-6.9×10^{5}	-2.0×10^{5}
0.4	8.4×10^{2}	1.1×10^{3}	1.0×10^{11}	-1.4×10^{11}	-7.3×10^{5}	-2.9×10^{5}
0.5	7.5×10^{2}	1.3×10^{3}	7.3×10^{10}	-1.3×10^{11}	-7.4×10^{5}	-4.1×10^{5}
0.6	5.9×10^{2}	1.5×10^{3}	4.8×10^{10}	-1.2×10^{11}	-7.2×10^{5}	-5.5×10^{5}
0.7	3.5×10^{2}	1.7×10^{3}	2.5×10^{10}	-1.2×10^{11}	-6.5×10^{5}	-6.9×10^{5}
0.8	6.3×10^{1}	1.8×10^{3}	4.1×10^{9}	-1.1×10^{11}	-5.4×10^{5}	-8.1×10^{5}
0.9	-2.4×10^{2}	1.7×10^{3}	-1.5×10^{10}	-1.1×10^{11}	-3.9×10^{5}	-8.8×10^{5}
1.0	-5.0×10^{2}	1.6×10^{3}	-3.2×10^{10}	-1.0×10^{11}	-2.2×10^{5}	-9.0×10^{5}

APPENDIX C: APPROXIMATION FOR THE DERIVATIVE OF H_z AT THE FAR BOUNDARY

The expression for the derivative of H_z at the outer boundary for the plasma-free space condition is given by

$$\left.\frac{dH_z}{dx}\right|_{x=d} = j\left(\frac{eK_y}{Am}\, p(d) - \epsilon_p(d)\, K_{ox}\, H_{zd}\right) ,$$

where $p(d)$ and H_{zd} are the values of p and H_z at the boundary. It is necessary now to compare the two terms on the right-hand side of the equation above.

$$\frac{eK_y}{Am}\, p(d) \overset{?}{\leq} \epsilon_p(d)\, K_{ox}\, H_{zd} .$$

Substituting typical values for the variables above (and choosing them so that the left-hand side would be as large as possible and the right-hand side would be as small as possible) gives

$$\frac{10^{-19}\ 10^{3}}{10^{11}\ 10^{-30}}\, p(d) \overset{?}{\leq} (0.1)(10)^{3}\, H_{zd}$$

or

$$10\ p(d) \overset{?}{\leq} H_{zd} .$$

From the section Solutions of the Coupled Wave Equations it is seen that $p(d)$ is always at least four orders of magnitude below H_{zd}, therefore the inequality above holds and we have

$$\frac{eK_y}{Am} p(d) << \varepsilon_p(d) K_{ox} H_{zd} ,$$

and to a very good approximation,

$$\left.\frac{dH_z}{dx}\right|_{x=d} = -j\varepsilon_p(d) K_{ox} H_{zd} .$$

APPENDIX D: ACOUSTIC WAVELENGTHS COMPARED TO THE DEBYE LENGTH AND THE INTER-PARTICLE SPACING

The acoustic wavelength in the inhomogeneous plasma will be computed as the equivalent wavelength in a lossy, homogeneous plasma with the same electron density and temperature. This, of course, is only an approximation since a definite wavelength cannot be found for a plasma wave in an inhomogeneous medium. The wave length is computed as follows:

$$\gamma_{px} = \sqrt{K_y^2 - \frac{\omega^2}{u_o^2} + \frac{\omega_p^2}{u_o^2} + j\frac{\omega^2}{u_o^2}\frac{\nu}{\omega}} \quad ,$$

where γ_{px} consists of a real part and an imaginary part and is just the x component of the complex propagation constant of the plasma wave in a homogeneous plasma. The plasma wavelength in the x direction is

$$\lambda_p = 2\pi \Big/ \mathrm{Im}\left\{\gamma_{px}\right\} \quad ,$$

where Im indicates that the imaginary part of γ_{px} is to be used.

The purpose of computing a plasma wavelength is to determine if the plasma wavelength is larger or smaller than the Debye length in the plasma. The Debye length is computed from the following expression:

$$\lambda_d = \sqrt{\frac{\epsilon_o K_B T}{n_o e^2}}$$

The plasma wavelength is also compared to the inter-particle spacing which is given by $n_o^{-1/3}$.

The three quantities described above (plasma wavelength, Debye length, and inter-particle spacing) were computed as functions of the distance into the plasma layer in Figs. 42 to 44 for the four plasma profiles of interest.

It is noted that in Figs. 42 and 45, the plasma wavelength is smaller than the Debye length in a very narrow region close to the wall. This is due to the low electron densities in this region. In Fig. 43 it is observed that a decrease in operating frequency can increase the plasma wavelength to a value larger than the Debye length. The plasma wavelength is larger than the inter-particle spacing in all cases.

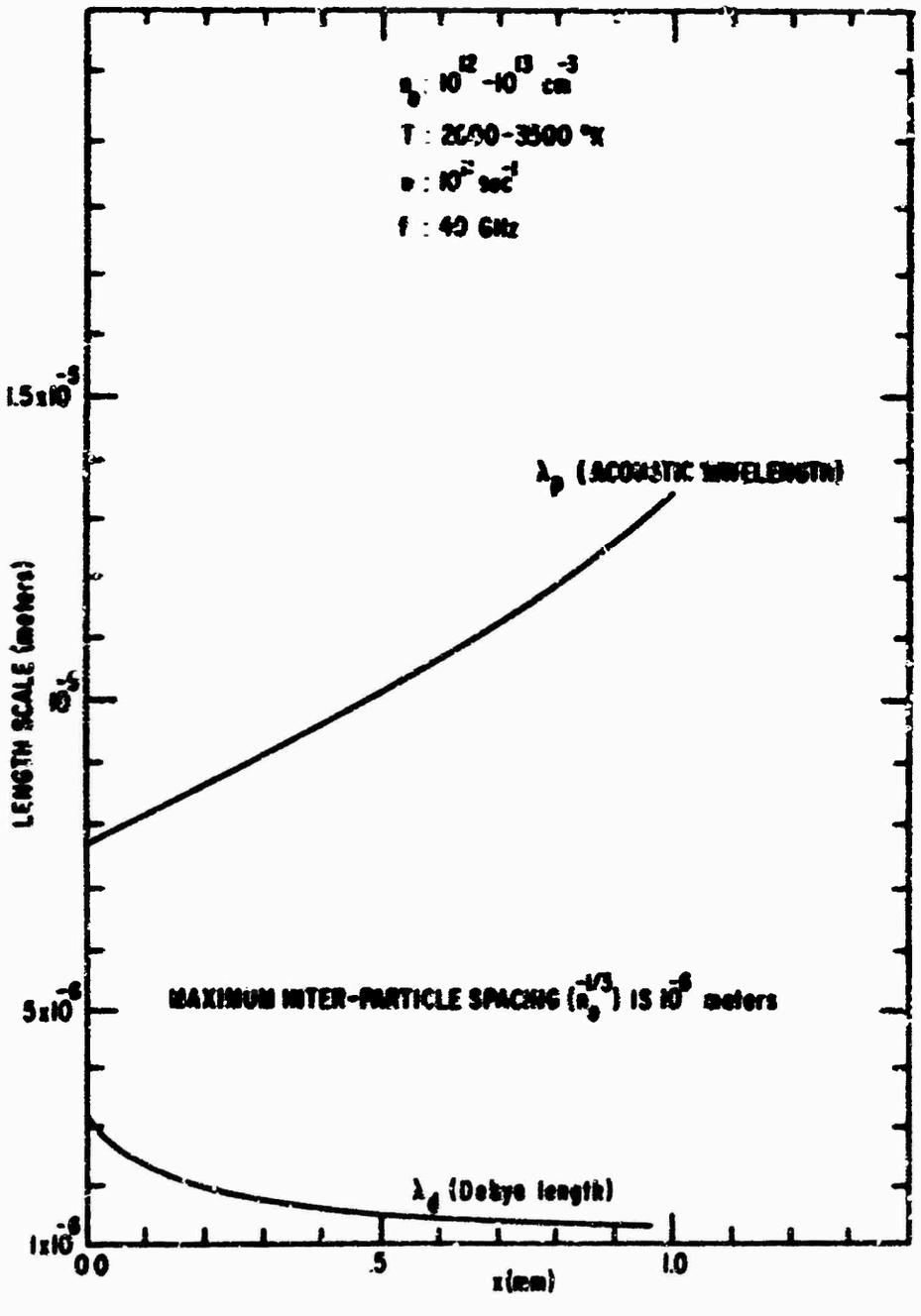

Figure 41. Acoustic Wavelength, Debye Length and Inter-Particle Spacing (n_o: 10^{12} to 10^{13} cm^{-3})

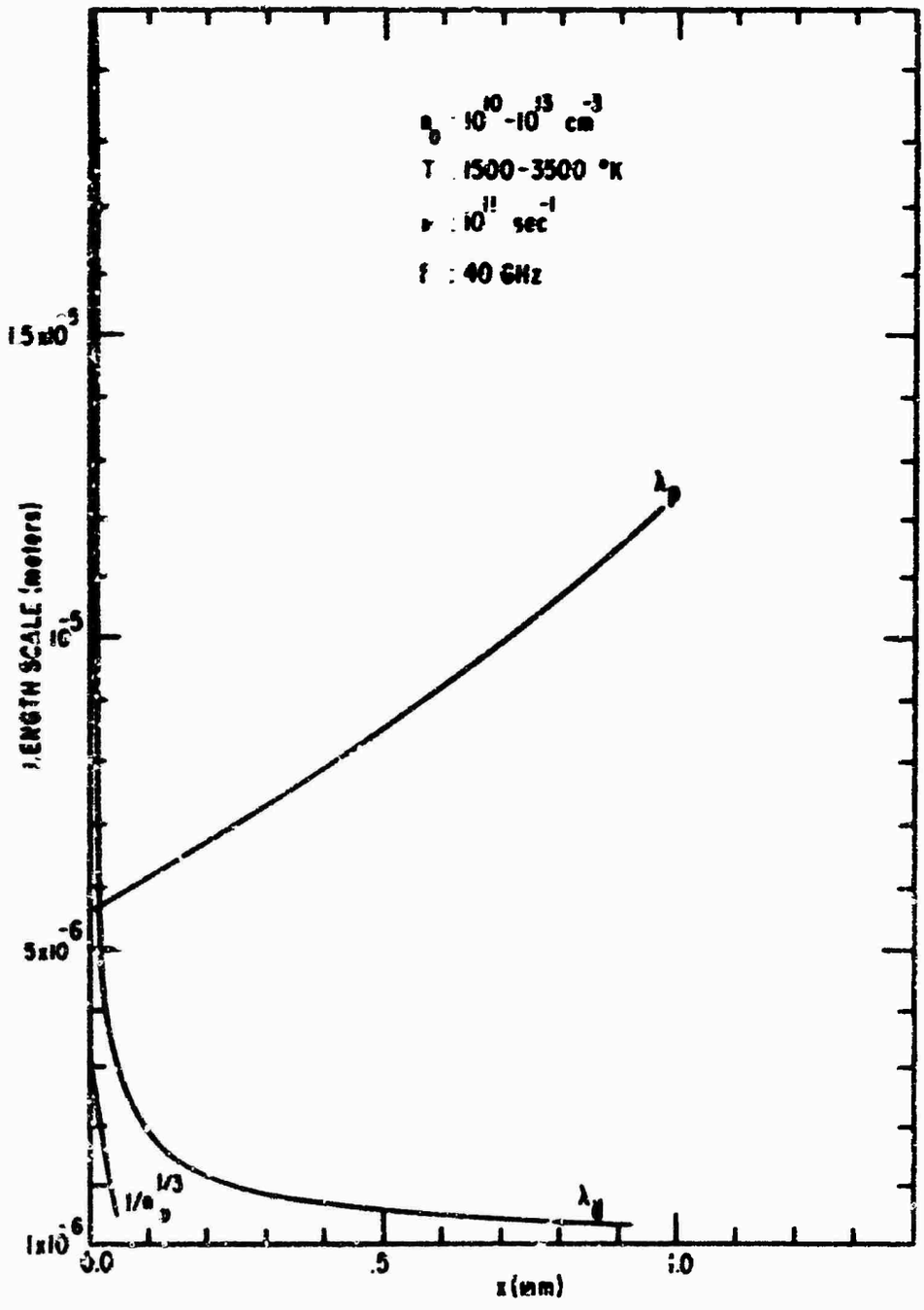

Figure 42. Acoustic Wavelength, Debye Length and Inter-Particle Spacing (n_o: 10^{10} to 10^{13} cm^{-3})

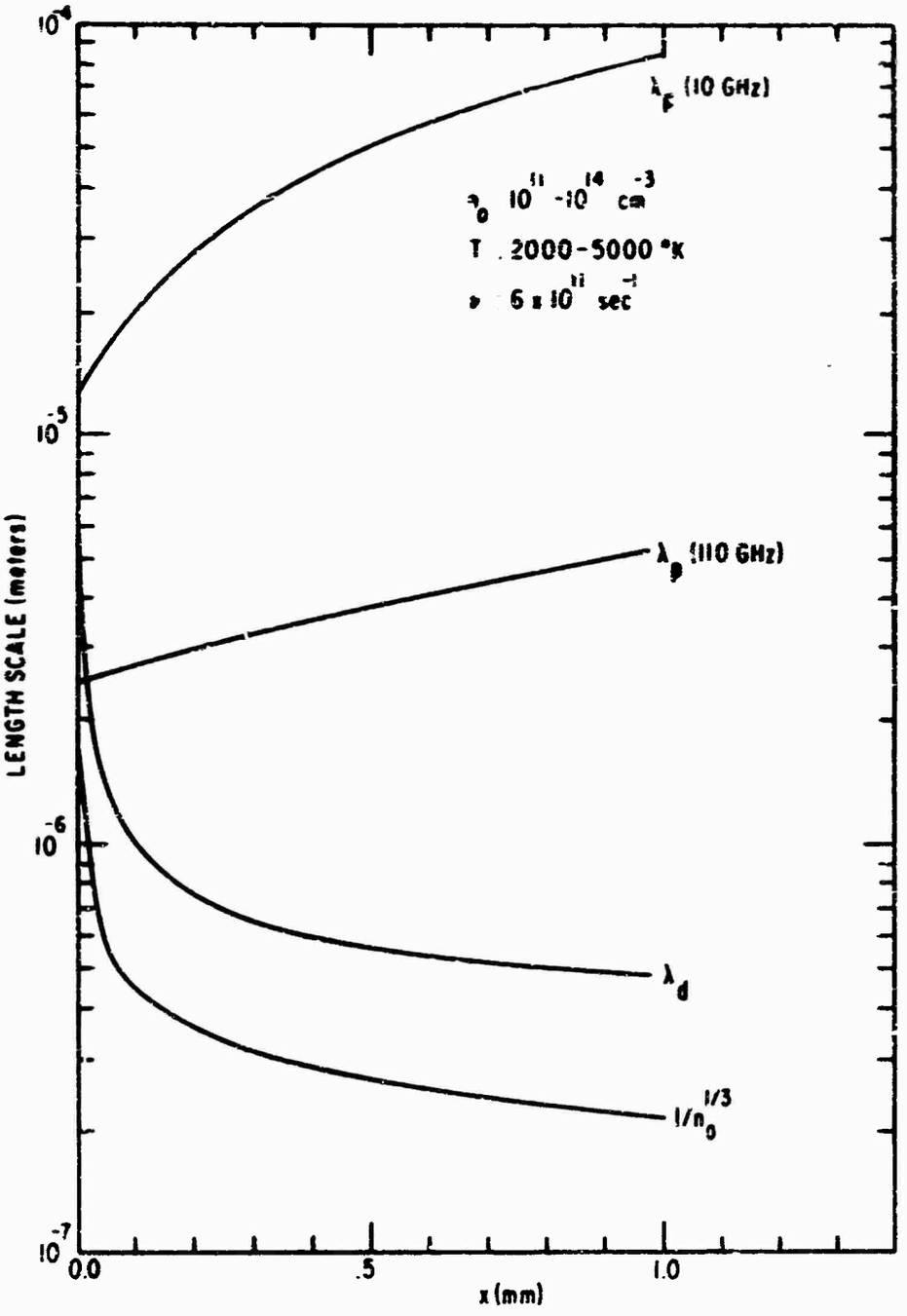

Figure 43. Acoustic Wavelength, Debye Length and Inter-Particle Spacing (n_o: 10^{11} to 10^{14} cm^{-3})

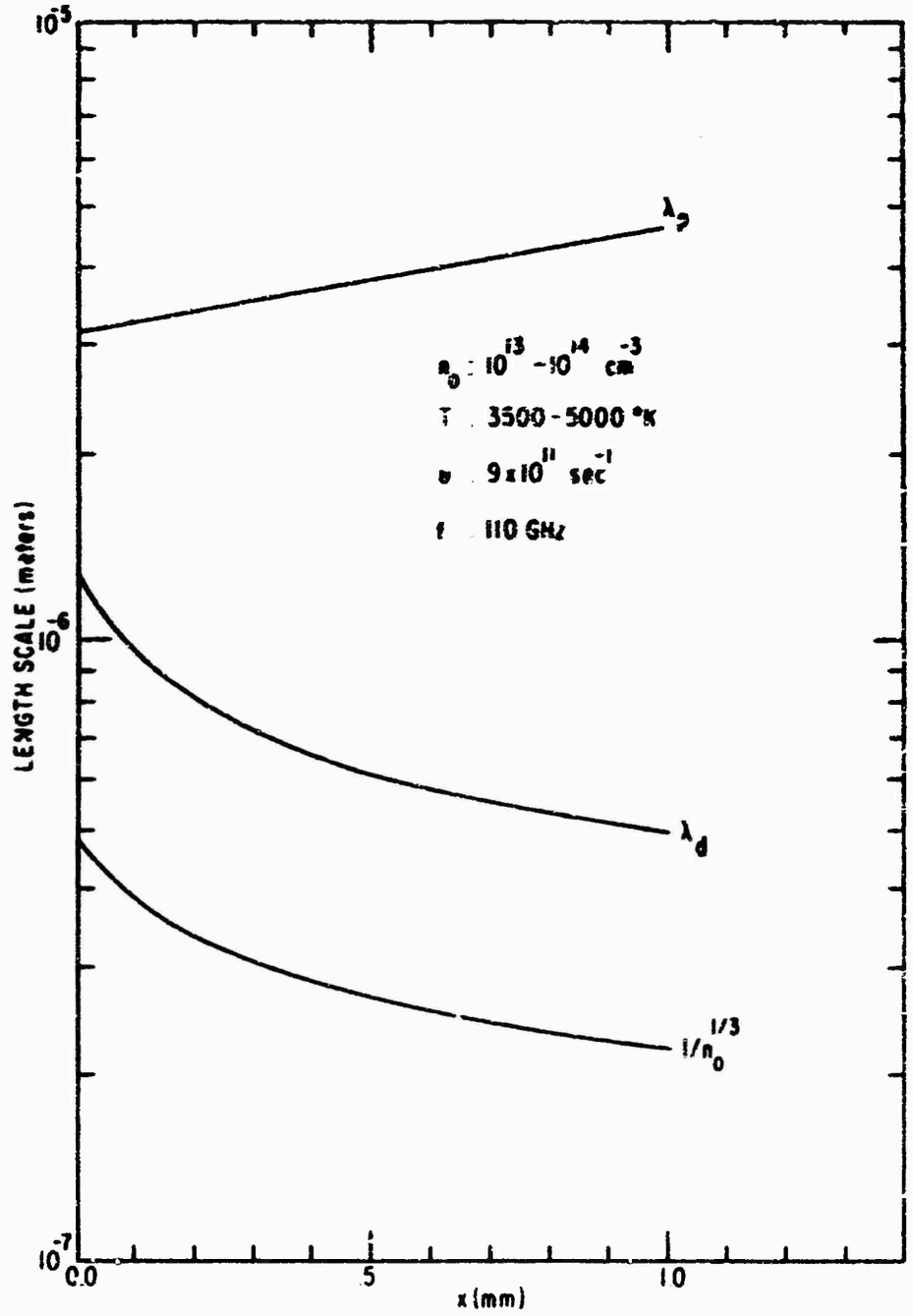

Figure 44. Acoustic Wavelength, Debye Length and Inter-Particle Spacing (n_o: 10^{13} to 10^{14} cm^{-3})

APPENDIX B: DIGITAL COMPUTER PROGRAM

Calculations of the electromagnetic and pressure fields in the inhomogeneous plasma sheath were performed on the CDC 6600 computer at the Air Force Weapons Laboratory, Kirtland AFB, New Mexico. Based on these calculations for various plasma sheaths with large peak electron densities and high collision frequencies, it was concluded in this study that the small wavelength propagating acoustic waves were damped so severely that reliable detection of the reflected acoustic waves would be impossible. For less dense plasmas or for plasmas with much lower collision frequencies, reflected acoustic waves may provide valuable diagnostic information. The computer program developed for this work would apply equally well for these types of plasmas and the program is included for this reason. A FORTRAN listing of the program and subroutines, along with sample input and output data, are given in this appendix.

Program ESCDE1 uses the finite difference numerical solution process described in Chapter IV to solve the two equations:

$$\frac{d^2H}{dx^2} + A\frac{dH}{dx} + BH = C_p$$

$$\frac{d^2p}{dx^2} + D\frac{dp}{dx} + E_p = FH$$

where A, B, C, D, E and F are functions of the plasma medium and vary with distance x. The program is divided into subroutines which:

(1) calculate the boundary conditions;

(2) calculate the coefficients;

(3) calculate the initial "guesses" for H and p;

(4) iterate the numerical solution;

(5) set the output data format;

(6) calculate the reflection coefficient.

There is one basic restriction on the program as it is presently written. The electron density profile must be linearly increasing from a value at the wall to a peak value at some distance from the wall. Both of the models in Fig. 5 can be used if appropriate boundary conditions at the location of the peak electron density are used in the subroutine calculating the boundary conditions.

Listed below are the FORTRAN names assigned to the input and output variables of Program NSCDE1, along with their definitions and units.

INPUT

FORTRAN NAME	DEFINITION	UNITS
AKD	Relative dielectric constant of the dielectric material.	Dimensionless
AN1	Electron density at the wall.	electrons/m^3
AN2	Peak electron density.	electrons/m^3
ANU	Collision frequency.	sec^{-1}
BLD	Distance from the wall to the peak electron density.	meters
DEGREE	Angle of incidence (θ_1).	degrees
FREQ	Frequency of electromagnetic wave.	Hz

FORTRAN NAME	DEFINITION	UNITS
MAXIT	Maximum number of iterations.	integer
NPTS	Number of points on the x-axis for the numerical solution.	integer
TE1	Electron temperature at the wall.	^{o}K
TE2	Electron temperature at x = BLD	^{o}K

Note: AN1, AN2, ANU, TE1 and TE2 are defined in the program under PROFILE DEFINITION. The variables AKD, BLD, FREQ and DEGREE are read into the program under FORMAT HE20.2. The variable NPTS is read into the program under the FORMAT I10.

OUTPUT

FORTRAN NAME	DEFINITION	UNITS
ABSH(I)	|H|, magnitude of magnetic intensity intensity at point I.	amperes/meter
ABSP(I)	|p|, magnitude of pressure field at point I.	newtons/meter^2
H(I)	Magnetic intensity at point I, a complex variable.	ampere/meter
I	Point along x-axis, I = 1, 2,...NPTS.	integer
P(I)	Pressure field amplitude at point I, a complex variable.	newtons/meter^2
XA(I)	Distance value, x, at point I.	meters

The program will also print out the coefficients of the coupled differential equations as functions of I. In this printout, R(A) represents the real part of coefficient A and I(A) its imaginary part. A similar notation is used for the other coefficients. In the

output listing, x is XA(I), R(H) is the real part of H(I), I(H) is the imaginary part of H(I), R(P) is the real part of P(I), I(P) is the imaginary part of P(I), ABSH is the absolute value of H(I) and ABSP is the absolute value of P(I).

```
      PROGRAM NSCOEF1 (INPUT,OUTPUT)
      COMMON/1/ XA(201),H(201),P(201),ABSH(201),ABSP(201)
      COMMON/2/ ER,RPM,DPO
      COMMON/3/ AN1,ANN,EMO,TE1,TEM,SUM,RAN,AKO,AKY,EC,W,ANU,GAM,AK,EM,
     1EO
      COMMON/4/A,B,C,D,E,F
      COMMON/5/ HO(201),PO(201)
      COMMON/6/ AKOX,AND,ALO

      COMMON/8/ ANG
      COMMON/CONST/DX,NPTS,MAXIT,IPR(6)
      DATA (IPR(N),N=1,6)/30,60,300,600,1000,1300/
      COMPLEX A,B,C,D,E,F,H,P,ER
      COMPLEX HO,PO

      READ 400, NPTS
  400 FORMAT(I10)
      READ 1,FREQ,DEGREE,AKO,ALO
    1 FORMAT(4F20.?)

      MAXIT = 1500
      DX = ALO/FLOAT(NPTS-1)
C     LIST OF CONSTANTS
      GAM = 1.0
      EC = -1.602E-19
      EM = 9.11E-31
      AK = 1.38E-23
      EO = 8.854E-12
      AMU = 1.257E-06
      EMO = (EC*EC)/(EM*EO)
C     PROFILE DEFINITIONS
      AN1 = 1.0E+10
      AN2 = 1.0E+19
      AND = AN2
      ANN = (AN2-AN1)/ALO
      ANU = 1.0E+11
      TE1 = 2.0E+03
      TE2 = 3.5E+03
      TEM = (TE2-TE1)/ALO
C     CONVERSION
      ANG = (DEGREE)/(57.295779)
      W = 6.2831A*FREQ
C     CONSTANT FACTORS
      AKO = W*SQRT(AMU*EO)
      AKY = AKO*SQRT(AKO)*SIN(ANG)
      AKOX = SQRT(AKO*AKO-AKY*AKY)
      SUM = W*W + ANU*ANU
      RAN = ANU/W
C     FILL XA ARRAY WITH X VALUES
C        X GOES FROM 0.0 TO ALO  ( IN METERS )
      XA(1) = 0.0
      DO 101 J=2,NPTS
  101 XA(J) = XA(J-1) + DX
      LINE = 1
      PRINT 107
      DO 105 I=1,NPTS
      CALL COEFF (I)
      LINE = LINE + 1
      IF(LINE-60) 105,105,106
  106 PRINT 107
  107 FORMAT(1H1,3X,1HI,3X,4HR(A),5X,4HI(A),5X,4HR(B),5X,4HI(B),
     15X,4HR(C),5X,4HI(C),5X,4HR(D),5X,4HI(D),5X,4HR(E),5X,4HI(E),
     15X,4HR(F),5X,4HI(F),5X)
```

```
      LINE = 0
  1 0 PRINT 1 8,I,A,B,C,D,E,F
  1 8 FORMAT (1X,I4,12F 3.1)
C     CALCULATE COEFFICIENTS FOR DHXO ( DP/DX AT X = XLD )
      EPRO = 1.0-((EMO*ANO)/SUM)
      EPIO = (-DAM*EMO*ANO)/SUM
      EP = CMPLX(AKOX*EPIO,-AKOX*EPRO)
C     CALCULATE DP/DX COEFFICIENT  (DPH)
      DPH = (EO*ANO*AKY)/(H*EO)
      DPO = (EO*AKY*AMO)/(H*EO)
      CALL INITIAL
      CALL OUTPUT(6,0,0,0,0)
      CALL  IFPAT
      END
```

```
      SUBROUTINE BC (HOM,CDDP,KORH)
      COMPLEX EP,H,P
      COMMON/1/ YA(201),H(201),P(201)
      COMMON/2/ EP,DOM,DPO
      COMMON/CONST/DY,NPTS
      H(1) = CMPLX(0.1,0.1)
      P(1) = -(2.0/3.0)*DY*DPH*H(1) - (1.0/3.0)*P(3) + (4.0/3.0)*P(2)
      H(NPTS) = (4.0*H(NPTS-1) - H(NPTS-2))/(3.0 - 2.0*DX*ER)
      P(NPTS) = (2.0*DX*DPO*H(NPTS) + 4.0*P(NPTS-1) - P(NPTS-2))/3.0
      RETURN
      END
```

```
      SUBROUTINE COEFF (T)
      COMPLEX A,B,C,D,E,F
      COMMON/1/ VA(201)
      COMMON/2/ AN1,AN4,EN0,TE1,TEN,SUP,RAN,AKO,AKY,EC,W,ANU,GAN,AK,EM,
     1EO
      COMMON/6/A,B,C,D,E,F
      V = VA(T)
      AK = AN1 + AN4*V
      DN = ANN
      T = TE1+TEN*V
      UO2 = (GAM*AK*T)/EM
      WP2 = EN*AN
C     CALCULATE COEFFICIENT A
      EPR = 1.0 - (WP2/SUM)
      EPI = (-RAN*WP2)/SUM
      EPRO = EPR/(EPR*EPR + EPI*EPI)
      EPIO = -EPI/(EPR*EPR + EPI*EPI)
      DVR = (-EN0*DN)/SUM
      DVI = (-RAN*EN0)*DN)/SUM
      AR = EPRO*DVR - EPIO*DVI
      AI = EPRO*DVI + EPIO*DVR
      A = CMPLX(-AR,-AI)
C     CALCULATE B
      BR = AKO*AKO*EPR - AKY*AKY
      BI = AKO*AKO*EPI
      B = CMPLX(BR,BI)
C     CALCULATE C
      CN = (-EC*AKY)/(W*EM)
      CNR = CN/(1.0 + RAN*RAN)
      CNI = (CN*RAN)/(1.0 + RAN*RAN)
      CNRR = CNR*AR - CNI*AI
      CNII = CNR*AI + CNI*AR
      C = CMPLX(CNRR,CNII)
C     CALCULATE D
      D = A
C     CALCULATE E
      ER = (W*W)/UO2 - WP2/UO2 - AKY*AKY
      EI = (-RAN*W*W)/UO2
      E = CMPLX(ER,EI)
C     CALCULATE F
      FN = (EC*AKY)/(W*EO)
      FR1 = -FN*AN*AR
      FI = -FN*AN*AI
      FR2 = FN*DN
      FR = FR1 + FR2
      F = CMPLX(FR,FI)
      RETURN
      END
```

```
      SUBROUTINE INITIAL
      COMPLEX H,P,HO,PO,A,B,C,D,E,F,FS,EP,EPD,AINE,AK1
      COMMON/1/ XA(201),H(201),P(201),ABSH(201),ABSP(201)
      COMMON/2/ ER,DPM,DPC
      COMMON/3/ AN1,ANM,EMO,TE1,TEM,SUM,PAN,AKO,AK/,EC,W,AMU,GAM,AK,EM,
     1EC
      COMMON/4/A,B,C,D,E,F
      COMMON/5/ HO(201),PO(201)
      COMMON/6/ AKOY,AMO,BLD
      COMMON/CONST/DX,NPTS,MAXIT,IPR(6)
      H(1) = CMPLX(0.1,0.1)
      A1 = (EMO*AN1)/SUM
      A2 = (EMO*ANM)/SUM
      A3 = (PAN*EMO*AN1)/SUM
      A4 = (PAN*EMO*ANM)/SUM
      EPP = 1.0 - A1 - A2*BLD
      EPI = -A3 - A4*BLD
      EPD = CMPLX(EPP,EPI)
      AIR = [illegible] - A1*BLD - (A2/2.0)*BLD*BLD
      AII = -A3*BLD - (A4/2.0)*BLD*BLD
      AINE = CMPLX(AIR,AII)
      AK1 = ( (ER*H(1))/EPD )/(1.0 - (ER/EPD)*AINE)
      AK1R = REAL(AK1)
      AK1I = AIMAG(AK1)
      DO 190 I=1,NPTS
      X = XA(I)
      AER = X - A1*X - (A2/2.0)*X*X
      AEI = -A3*X - (A4/2.0)*X*X
      HR = AK1R*AER - AK1I*AEI + REAL(H(1))
      HI = AK1I*AER + AK1R*AEI + AIMAG(H(1))
      H(I) = CMPLX(HR,HI)
      AN = AN1 + ANM*X
      DN = ANM
      HP2 = EMO*AN
      EPR = 1.0-(HP2/SUM)
      EPI = (-PAN*HP2) /SUM
      EPPD = EPR/(EPR*EPR+EPI*EPI)
      EPIO = -EPI/(EPR*EPR+EPI*EPI)
      DPR = (-EMO/SUM)*DN
      DPI = ((-PAN*EMO)/SUM)*DN
      AR = EPRO*DPR-EPIO*DPI
      AI = EPRO*DPI+DPR*EPIO
      P(I) = (E/F)*H(I)
      ABSH(I) = CABS(H(I))
      ABSP(I) = CABS(P(I))
190   CONTINUE
      DO 210 K=1,NPTS
      HO(K) = H(K)
210   PO(K) = P(K)
      RETURN
      END
```

```
      SUBROUTINE ITERAT
      COMPLEX A,B,C,D,E,F,H,P
      COMPLEX HO,PO
      COMMON/1/ XA(201),H(201),P(201),ABSH(201),ABSP(201)
      COMMON/47 A,B,C,D,E,F
      COMMON/5/ HO(201),PO(201)
      COMMON/CONST/DX,NPTS,MAXIT,IPR(6)
      NPR=NPTS-1
      DXX=DY*DX
      NPR=1
      ITP=IPR(1)
      DO 3 IT=1,MAXIT
      DO 1 I=2,NPR
      CALL COEFF(I)
      IM=I-1
      IP=I+1
      H(I) = (-DXX*C*PO(I) + (1.0 + (DX*A)/2.0)*HO(IP)
     1 + (1.0 - (DY*A)/2.0)*HO(IM))/(2.0 - DXX*B)
      P(I) = (-DXX*F*HO(I) + (1.0 + (DX*D)/2.0)*PO(IP)
     1 + (1.0 - (DY*D)/2.0)*PO(IM))/(2.0 - DXX*E)
      ERRH = CABS((HO(I) - H(I))/HO(I))
      ERRP = CABS((PO(I) - P(I))/PO(I))
      ERRH1 = CABS((HO(IM) - H(IM))/HO(IM))
      ERRP1 = CABS((PO(IM) - P(IM))/PO(IM))
      IF(ERRP.GT.ERRP1) GO TO 4
      ERRP = ERRP1
      GO TO 6
    4 ERRP = ERRP
    6 IF(ERRH.GT.ERRH1) GO TO 5
      ERRH = ERRH1
      GO TO 1
    5 ERRH = ERRH
    1 CONTINUE
      CALL BC (NPR,ERRP,ERRH)
      DO 127 K=1,NPTS
      ABSH(K) = CABS(H(K))
  127 ABSP(K) = CABS(P(K))
      DO 54 K=1,NPTS
      PO(K) = P(K)
   54 HO(K) = H(K)
      IF (IT-ITP) 3,2,3
2     CALL OUTPUT (IT,ERRP,ERRH)
      NPR=NPR+1
      IF (NPR.LT.7) ITP=IPR(NPR)
3     CONTINUE
      CALL OUTPUT (MAXIT,ERRP,ERRH)
      RETURN
      END
```

```
      SUBROUTINE OUTPUT (IT,ERRP,ERRH)
      COMPLEX R
      COMPLEX P,H
      COMMON/1/ A(201),H(201),P(201),ABSH(201),ABSP(201)
      COMMON/2/ P,PC
      COMMON/CONST/DX,NPTS
      CALL DEFL
      PRINT 1,IT
    1 FORMAT (1H1,50X,16HITERATION NUMBER,I5)
      PRINT 2,ERRH,ERRP
    2 FORMAT(/45X,20HMAXIMUM ERROR IN H = ,E12.5/45X,20HMAXIMUM ERROR IN
     * P = ,E12.5/)
      PRINT 3
    3 FORMAT (9X,1HI,7X,1HX,11X,4HR(H),10X,4HI(H),10X,4HR(P),10X,
     *4HI(P),13X,4HABSH,17X,4HABSP)
    4 FORMAT(1X,I4,7E14.6)
    5 FORMAT (1H1)
      LINE=6
      DO 7 I=1,NPTS
      LINE=LINE+1
      IF (LINE-60) 7,7,6
    6 PRINT 5
      PRINT 3
      LINE=3
    7 PRINT 4, I,A(I),H(I),P(I),ABSH(I),ABSP(I)
      PRINT 11, P,PC
   11 FORMAT(1H1,2E15.5,E20.6)
      RETURN
      END
```

I	P(A)	T(A)	R(B)	I(B)	R(C)	I(C)	R(D)	I(D)	P(E)	I(E)	R(F)	I(F)
1	1.1E+03	1.1E+03	2.9E+02	-1.7E+04	-7.9E+04	-6.9E+05	1.1E+03	1.1E+03	1.4E+11	-1.4E+11	-5.7E+	-6.4E+04
2	1.1E+03	1.2E+03	-3.6E+03	-2.0E+04	-6.5E+04	-7.0E+05	1.1E+03	1.2E+03	1.3E+11	-1.4E+11	-5.8E+	-7.9E+04
3	1.1E+03	1.2E+03	-7.5E+03	-2.3E+04	-4.9E+04	-7.2E+05	1.1E+03	1.2E+03	1.2E+11	-1.3E+11	-6.0E+	-9.6E+04
4	1.1E+03	1.3E+03	-1.1E+04	-2.7E+04	-3.1E+04	-7.4E+05	1.1E+03	1.3E+03	1.1E+11	-1.3E+11	-6.1E+	-1.1E+05
5	1.1E+03	1.4E+03	-1.5E+04	-3.0E+04	-1.2E+04	-7.6E+05	1.1E+03	1.4E+03	1.1E+11	-1.3E+11	-6.2E+	-1.3E+05
6	1.1E+03	1.4E+03	-1.9E+04	-3.3E+04	9.7E+03	-7.7E+05	1.1E+03	1.4E+03	1.0E+11	-1.3E+11	-6.3E+	-1.5E+05
7	1.1E+03	1.5E+03	-2.3E+04	-3.6E+04	3.3E+04	-7.9E+05	1.1E+03	1.5E+03	9.3E+10	-1.3E+11	-6.4E+	-1.7E+05
8	1.1E+03	1.6E+03	-2.7E+04	-3.9E+04	5.4E+04	-8.1E+05	1.1E+03	1.6E+03	8.6E+10	-1.3E+11	-6.4E+	-2.0E+05
9	1.0E+03	1.6E+03	-3.1E+04	-4.2E+04	4.5E+04	-8.2E+05	1.0E+03	1.6E+03	7.9E+10	-1.2E+11	-6.5E+	-2.2E+05
10	1.0E+03	1.7E+03	-3.5E+04	-4.5E+04	1.1E+05	-8.3E+05	1.0E+03	1.7E+03	7.2E+10	-1.2E+11	-6.6E+	-2.5E+05
11	9.6E+02	1.8E+03	-3.9E+04	-4.8E+04	1.5E+05	-8.5E+05	9.6E+02	1.8E+03	6.6E+10	-1.2E+11	-6.6E+	-2.8E+05
12	9.1E+02	1.8E+03	-4.3E+04	-5.1E+04	1.9E+05	-8.6E+05	9.1E+02	1.8E+03	6.0E+10	-1.2E+11	-6.6E+	-3.1E+05
13	8.6E+02	1.9E+03	-4.7E+04	-5.5E+04	2.2E+05	-8.6E+05	8.6E+02	1.9E+03	5.3E+10	-1.2E+11	-6.6E+	-3.4E+05
14	8.0E+02	2.0E+03	-5.0E+04	-5.8E+04	2.5E+05	-8.7E+05	8.0E+02	2.0E+03	4.6E+10	-1.2E+11	-6.6E+	-3.7E+05
15	7.3E+02	2.0E+03	-5.4E+04	-6.1E+04	2.9E+05	-8.7E+05	7.3E+02	2.0E+03	4.2E+10	-1.1E+11	-6.5E+	-4.0E+05
16	6.6E+02	2.1E+03	-5.8E+04	-6.4E+04	3.3E+05	-8.7E+05	6.6E+02	2.1E+03	3.6E+10	-1.1E+11	-6.5E+	-4.3E+05
17	5.8E+02	2.1E+03	-6.2E+04	-6.7E+04	3.7E+05	-8.7E+05	5.8E+02	2.1E+03	3.1E+10	-1.1E+11	-6.4E+	-4.6E+05
18	4.9E+02	2.2E+03	-6.6E+04	-7.0E+04	4.1E+05	-8.6E+05	4.9E+02	2.2E+03	2.5E+10	-1.1E+11	-6.2E+	-5.0E+05
19	4.0E+02	2.2E+03	-7.0E+04	-7.3E+04	4.5E+05	-8.5E+05	4.0E+02	2.2E+03	2.0E+10	-1.1E+11	-6.0E+	-5.3E+05
20	3.1E+02	2.3E+03	-7.4E+04	-7.6E+04	5.0E+05	-8.3E+05	3.1E+02	2.2E+03	1.5E+10	-1.1E+11	-5.8E+	-5.6E+05
21	2.1E+02	2.3E+03	-7.8E+04	-7.9E+04	5.3E+05	-8.2E+05	2.1E+02	2.3E+03	9.7E+09	-1.1E+11	-5.6E+	-5.9E+05
22	1.0E+02	2.4E+03	-8.2E+04	-8.2E+04	5.7E+05	-7.9E+05	1.0E+02	2.3E+03	4.8E+09	-1.1E+11	-5.4E+	-6.1E+05
23	1.2E+00	2.3E+03	-8.6E+04	-8.6E+04	6.1E+05	-7.7E+05	1.2E+00	2.3E+03	5.2E+07	-1.0E+11	-5.1E+	-6.4E+05
24	-1.0E+02	2.4E+03	-8.9E+04	-8.9E+04	6.4E+05	-7.4E+05	-1.0E+02	2.3E+03	-4.6E+09	-1.0E+11	-4.8E+	-6.6E+05
25	-2.0E+02	2.3E+03	-9.3E+04	-9.2E+04	6.7E+05	-7.0E+05	-2.0E+02	2.3E+03	-9.2E+09	-1.0E+11	-4.9E+	-6.8E+05
26	-3.0E+02	2.2E+03	-9.7E+04	-9.5E+04	7.0E+05	-6.7E+05	-3.0E+02	2.2E+03	-1.4E+10	-1.0E+11	-4.1E+	-6.9E+05
27	-4.0E+02	2.2E+03	-1.0E+05	-9.8E+04	7.2E+05	-6.3E+05	-4.0E+02	2.2E+03	-1.0E+10	-9.9E+10	-3.8E+	-7.1E+05
28	-4.9E+02	2.2E+03	-1.1E+05	-1.0E+05	7.5E+05	-6.0E+05	-4.9E+02	2.2E+03	-9.8E+10	-2.2E+10	-3.9E+	-7.2E+05
29	-5.8E+02	2.1E+03	-1.1E+05	-1.0E+05	7.6E+05	-5.6E+05	-5.8E+02	2.1E+03	-2.7E+10	-9.7E+10	-3.1E+	-7.2E+05
30	-6.6E+02	2.1E+03	-1.1E+05	-1.1E+05	7.7E+05	-5.2E+05	-6.6E+02	2.1E+03	-3.1E+10	-9.6E+10	-2.8E+	-7.3E+05
31	-7.3E+02	2.0E+03	-1.2E+05	-1.1E+05	7.8E+05	-4.8E+05	-7.3E+02	2.0E+03	-3.5E+10	-9.5E+10	-2.4E+	-7.3E+05
32	-8.0E+02	2.0E+03	-1.2E+05	-1.1E+05	7.9E+05	-4.4E+05	-8.0E+02	2.0E+03	-3.9E+10	-9.4E+10	-2.1E+	-7.3E+05
33	-8.6E+02	1.9E+03	-1.2E+05	-1.2E+05	7.9E+05	-4.0E+05	-8.6E+02	1.9E+03	-4.3E+10	-9.3E+10	-1.8E+	-7.2E+05
34	-9.1E+02	1.8E+03	-1.3E+05	-1.2E+05	7.9E+05	-3.7E+05	-9.1E+02	1.8E+03	-4.6E+10	-9.2E+10	-1.9E+	-7.1E+05
35	-9.6E+02	1.8E+03	-1.3E+05	-1.2E+05	7.9E+05	-3.3E+05	-9.6E+02	1.8E+03	-5.0E+10	-9.2E+10	-1.2E+	-7.1E+05
36	-1.0E+03	1.7E+03	-1.4E+05	-1.3E+05	7.9E+05	-3.0E+05	-1.0E+03	1.7E+03	-5.4E+10	-9.1E+10	-9.6E+	-7.0E+05
37	-1.0E+03	1.6E+03	-1.4E+05	-1.3E+05	7.9E+05	-2.7E+05	-1.0E+03	1.6E+03	-5.7E+10	-9.0E+10	-7.2E+	-6.8E+05
38	-1.1E+03	1.6E+03	-1.4E+05	-1.3E+05	7.7E+05	-2.4E+05	-1.1E+03	1.6E+03	-6.1E+10	-8.9E+10	-4.8E+	-6.7E+05
39	-1.1E+03	1.5E+03	-1.5E+05	-1.4E+05	7.6E+05	-2.1E+05	-1.1E+03	1.5E+03	-6.4E+10	-8.8E+10	-2.8E+	-6.6E+05
40	-1.1E+03	1.4E+03	-1.5E+05	-1.4E+05	7.5E+05	-1.8E+05	-1.1E+03	1.4E+03	-6.8E+10	-8.7E+10	-0.5E+	-6.5E+05
41	-1.1E+03	1.4E+03	-1.6E+05	-1.4E+05	7.4E+05	-1.6E+05	-1.1E+03	1.4E+03	-7.1E+10	-8.6E+10	9.3E+	-6.3E+05
42	-1.1E+03	1.3E+03	-1.6E+05	-1.4E+05	7.3E+05	-1.4E+05	-1.1E+03	1.3E+03	-7.4E+10	-8.6E+10	2.5E+	-6.2E+05
43	-1.1E+03	1.2E+03	-1.6E+05	-1.5E+05	7.1E+05	-1.2E+05	-1.1E+03	1.2E+03	-7.7E+10	-8.5E+10	4.8E+	-6.0E+05
44	-1.1E+03	1.2E+03	-1.7E+05	-1.5E+05	7.0E+05	-9.5E+04	-1.1E+03	1.2E+03	-8.0E+10	-8.4E+10	5.4E+	-5.9E+05
45	-1.1E+03	1.1E+03	-1.7E+05	-1.5E+05	6.9E+05	-7.7E+04	-1.1E+03	1.1E+03	-8.3E+10	-8.3E+10	6.6E+	-5.7E+05
46	-1.1E+03	1.1E+03	-1.8E+05	-1.6E+05	6.7E+05	-6.1E+04	-1.1E+03	1.1E+03	-8.6E+10	-8.3E+10	7.7E+	-5.6E+05
47	-1.1E+03	1.0E+03	-1.8E+05	-1.6E+05	6.6E+05	-4.5E+04	-1.1E+03	1.0E+03	-8.9E+10	-8.2E+10	8.7E+	-5.4E+05
48	-1.1E+03	9.9E+02	-1.8E+05	-1.6E+05	6.5E+05	-3.1E+04	-1.1E+03	9.9E+02	-9.2E+10	-8.1E+10	9.5E+	-5.3E+05
49	-1.1E+03	9.5E+02	-1.9E+05	-1.7E+05	6.3E+05	-1.9E+04	-1.1E+03	9.5E+02	-9.5E+10	-8.0E+10	1.0E+	-5.2E+05
50	-1.1E+ 3	9.1E+02	-1.9E+05	-1.7E+05	6.2E+05	-6.4E+03	-1.1E+03	9.1E+02	-9.8E+10	-8.0E+10	1.1E+	-5.0E+05
51	-1.1E+03	8.7E+02	-1.9E+05	-1.7E+05	6.0E+05	4.5E+03	-1.1E+03	8.7E+02	-1.0E+11	-7.9E+10	1.2E+	-4.9E+05

ITERATION NUMBER = 1

MAXIMUM ERROR IN H = 0.
MAXIMUM ERROR IN P = 0.

I	X	H(H)	I(H)	P(P)	I(P)	ABSH	ABSP
1	0.	1.000000E-01	1.000000E-01	-1.930676E-07	5.214439E-07	1.414214E-01	5.560176E-07
2	2.000000E-05	1.001960E-01	9.972447E-02	-1.917613E-07	5.216915E-07	1.413655E-01	5.557941E-07
3	4.000000E-05	1.003912E-01	9.945159E-02	-1.904190E-07	5.219032E-07	1.413039E-01	5.555598E-07
4	6.000000E-05	1.005865E-01	9.917946E-02	-1.891607E-07	5.220749E-07	1.412396E-01	5.552911E-07
5	8.000000E-05	1.007819E-01	9.890906E-02	-1.879264E-07	5.222186E-07	1.411634E-01	5.550032E-07
6	1.000000E-04	1.009774E-01	9.863939E-02	-1.867162E-07	5.223223E-07	1.410849E-01	5.546923E-07
7	1.200000E-04	1.011731E-01	9.837243E-02	-1.855299E-07	5.223900E-07	1.409993E-01	5.543579E-07
8	1.400000E-04	1.013689E-01	9.810721E-02	-1.843577E-07	5.224217E-07	1.409041E-01	5.539999E-07
9	1.600000E-04	1.015630E-01	9.784371E-02	-1.832294E-07	5.224174E-07	1.408110E-01	5.536181E-07
10	1.800000E-04	1.017728E-01	9.758193E-02	-1.821152E-07	5.223771E-07	1.407078E-01	5.532122E-07
11	2.000000E-04	1.019710E-01	9.732188E-02	-1.810250E-07	5.223007E-07	1.405984E-01	5.527822E-07
12	2.200000E-04	1.021693E-01	9.706355E-02	-1.799580E-07	5.221884E-07	1.404828E-01	5.523277E-07
13	2.400000E-04	1.023678E-01	9.680695E-02	-1.789166E-07	5.220401E-07	1.403610E-01	5.518487E-07
14	2.600000E-04	1.025663E-01	9.655207E-02	-1.778984E-07	5.218559E-07	1.402329E-01	5.513450E-07
15	2.800000E-04	1.027650E-01	9.629891E-02	-1.769043E-07	5.216354E-07	1.400984E-01	5.508164E-07
16	3.000000E-04	1.029639E-01	9.604749E-02	-1.759341E-07	5.213791E-07	1.399576E-01	5.502627E-07
17	3.200000E-04	1.031628E-01	9.579777E-02	-1.749880E-07	5.210860E-07	1.398104E-01	5.496837E-07
18	3.400000E-04	1.033619E-01	9.554979E-02	-1.740659E-07	5.207564E-07	1.396567E-01	5.490795E-07
19	3.600000E-04	1.035611E-01	9.530354E-02	-1.731679E-07	5.203941E-07	1.394965E-01	5.484497E-07
20	3.800000E-04	1.037605E-01	9.505900E-02	-1.722937E-07	5.199937E-07	1.393298E-01	5.477943E-07
21	4.000000E-04	1.039599E-01	9.481619E-02	-1.714436E-07	5.195574E-07	1.391565E-01	5.471131E-07
22	4.200000E-04	1.041595E-01	9.457511E-02	-1.706175E-07	5.190850E-07	1.389767E-01	5.464061E-07
23	4.400000E-04	1.043593E-01	9.433575E-02	-1.698155E-07	5.185767E-07	1.387902E-01	5.456730E-07
24	4.600000E-04	1.045591E-01	9.409811E-02	-1.690374E-07	5.180323E-07	1.385972E-01	5.449139E-07
25	4.800000E-04	1.047591E-01	9.386220E-02	-1.682834E-07	5.174529E-07	1.383974E-01	5.441285E-07
26	5.000000E-04	1.049592E-01	9.362802E-02	-1.675533E-07	5.168356E-07	1.381909E-01	5.433168E-07
27	5.200000E-04	1.051595E-01	9.339555E-02	-1.668473E-07	5.161833E-07	1.379778E-01	5.424787E-07
28	5.400000E-04	1.053598E-01	9.316481E-02	-1.661653E-07	5.154949E-07	1.377579E-01	5.416142E-07
29	5.600000E-04	1.055603E-01	9.293580E-02	-1.655073E-07	5.147705E-07	1.375312E-01	5.407230E-07
30	5.800000E-04	1.057610E-01	9.270851E-02	-1.648734E-07	5.140101E-07	1.372978E-01	5.398052E-07
31	6.000000E-04	1.059617E-01	9.248295E-02	-1.642634E-07	5.132130E-07	1.370575E-01	5.388607E-07
32	6.200000E-04	1.061626E-01	9.225911E-02	-1.636775E-07	5.123814E-07	1.368105E-01	5.378894E-07
33	6.400000E-04	1.063636E-01	9.203699E-02	-1.631155E-07	5.115130E-07	1.365566E-01	5.368913E-07
34	6.600000E-04	1.065647E-01	9.181660E-02	-1.625776E-07	5.106086E-07	1.362959E-01	5.358663E-07
35	6.800000E-04	1.067661E-01	9.159793E-02	-1.620637E-07	5.096682E-07	1.360284E-01	5.348143E-07
36	7.000000E-04	1.069675E-01	9.138099E-02	-1.615738E-07	5.086918E-07	1.357539E-01	5.337354E-07
37	7.200000E-04	1.071691E-01	9.116577E-02	-1.611079E-07	5.076795E-07	1.354727E-01	5.326295E-07
38	7.400000E-04	1.073709E-01	9.095227E-02	-1.606660E-07	5.066311E-07	1.351845E-01	5.314966E-07
39	7.600000E-04	9.998646E-02	9.074050E-02	-1.602482E-07	5.055467E-07	1.348895E-01	5.303366E-07
40	7.800000E-04	9.959937E-02	9.053046E-02	-1.598543E-07	5.044263E-07	1.345875E-01	5.291496E-07
41	8.000000E-04	9.921420E-02	9.032214E-02	-1.594845E-07	5.032699E-07	1.342787E-01	5.279355E-07
42	8.200000E-04	9.882901E-02	9.011554E-02	-1.591306E-07	5.020775E-07	1.339631E-01	5.266943E-07
43	8.400000E-04	9.844291E-02	8.991067E-02	-1.588168E-07	5.008490E-07	1.336405E-01	5.254261E-07
44	8.600000E-04	9.805590E-02	8.970752E-02	-1.585190E-07	4.995846E-07	1.333110E-01	5.241308E-07
45	8.800000E-04	9.766791E-02	8.950609E-02	-1.582452E-07	4.982842E-07	1.329747E-01	5.228085E-07
46	9.000000E-04	9.727893E-02	8.930639E-02	-1.579954E-07	4.969470E-07	1.326315E-01	5.214592E-07
47	9.200000E-04	9.688896E-02	8.910842E-02	-1.577697E-07	4.955754E-07	1.322815E-01	5.200829E-07
48	9.400000E-04	9.649801E-02	8.891217E-02	-1.575679E-07	4.941670E-07	1.319246E-01	5.186797E-07
49	9.600000E-04	9.610645E-02	8.871764E-02	-1.573902E-07	4.927225E-07	1.315608E-01	5.172496E-07
50	9.800000E-04	9.571366E-02	8.852484E-02	-1.572365E-07	4.912421E-07	1.311903E-01	5.157927E-07
51	1.000000E-03	9.531990E-02	8.833376E-02	-1.571067E-07	4.897257E-07	1.308129E-01	5.143090E-07

ITERATION NUMBER 500

MAXIMUM ERROR IN H = 3.11492E-05
MAXIMUM ERROR IN P = 3.12217E-05

I	X	R(H)	I(H)	R(P)	I(P)	ABSH	ABSP
1	0.	1.000000E-01	1.000000E-01	7.537825E-05	7.297921E-05	1.414214E-01	1.049183E-04
2	2.000000E-05	1.002369E-01	9.961799E-02	9.809380E-06	-1.440344E-06	1.413191E-01	1.842540E-06
3	4.000000E-05	1.004582E-01	9.923384E-02	7.707169E-06	-4.467495E-07	1.412105E-01	4.534855E-07
4	6.000000E-05	1.006654E-01	9.886553E-02	1.217298E-07	-4.828871E-07	1.410954E-01	4.972184E-07
5	8.000000E-05	1.008543E-01	9.849504E-02	1.543446E-07	-5.039572E-07	1.409740E-01	5.278027E-07
6	1.000000E-04	1.010371E-01	9.812934E-02	1.915223E-07	-5.244377E-07	1.408462E-01	5.583151E-07
7	1.200000E-04	1.012019E-01	9.776540E-02	2.332017E-07	-5.429355E-07	1.407121E-01	5.908998E-07
8	1.400000E-04	1.013529E-01	9.740619E-02	2.795275E-07	-5.586954E-07	1.405716E-01	6.247208E-07
9	1.600000E-04	1.014903E-01	9.705069E-02	3.305326E-07	-5.708629E-07	1.404248E-01	6.596086E-07
10	1.800000E-04	1.016142E-01	9.669887E-02	3.861050E-07	-5.784917E-07	1.402716E-01	6.955869E-07
11	2.000000E-04	1.017249E-01	9.635170E-02	4.459516E-07	-5.805633E-07	1.401120E-01	7.320781E-07
12	2.200000E-04	1.018221E-01	9.600614E-02	5.095625E-07	-5.760204E-07	1.399462E-01	7.690602E-07
13	2.400000E-04	1.019064E-01	9.566516E-02	5.761798E-07	-5.638128E-07	1.397739E-01	8.061439E-07
14	2.600000E-04	1.019777E-01	9.532773E-02	6.447724E-07	-5.429578E-07	1.395953E-01	8.429322E-07
15	2.800000E-04	1.020362E-01	9.499342E-02	7.140370E-07	-5.126122E-07	1.394102E-01	8.788882E-07
16	3.000000E-04	1.020818E-01	9.466340E-02	7.824041E-07	-4.721539E-07	1.392188E-01	9.138381E-07
17	3.200000E-04	1.021144E-01	9.433642E-02	8.488816E-07	-4.212638E-07	1.390209E-01	9.469458E-07
18	3.400000E-04	1.021353E-01	9.401207E-02	9.091217E-07	-3.600027E-07	1.388165E-01	9.778058E-07
19	3.600000E-04	1.021432E-01	9.369271E-02	9.635159E-07	-2.888699E-07	1.386057E-01	1.005007E-06
20	3.800000E-04	1.021387E-01	9.337590E-02	1.009312E-06	-2.080335E-07	1.383885E-01	1.030865E-06
21	4.000000E-04	1.021219E-01	9.306243E-02	1.044744E-06	-1.213254E-07	1.381647E-01	1.051765E-06
22	4.200000E-04	1.020929E-01	9.275227E-02	1.060361E-06	-2.019257E-08	1.379345E-01	1.060732E-06
23	4.400000E-04	1.020517E-01	9.244539E-02	1.079139E-06	6.938931E-08	1.376978E-01	1.081304E-06
24	4.600000E-04	1.019984E-01	9.214179E-02	1.076567E-06	1.660421E-07	1.374547E-01	1.089298E-06
25	4.800000E-04	1.019332E-01	9.184146E-02	1.068588E-06	2.623264E-07	1.372051E-01	1.092637E-06
26	5.000000E-04	1.018561E-01	9.154438E-02	1.032060E-06	3.548929E-07	1.369491E-01	1.091379E-06
27	5.200000E-04	1.017673E-01	9.125057E-02	9.917791E-07	4.416208E-07	1.366867E-01	1.085693E-06
28	5.400000E-04	1.016667E-01	9.096003E-02	9.413118E-07	5.207382E-07	1.364179E-01	1.075748E-06
29	5.600000E-04	1.015546E-01	9.067200E-02	8.824178E-07	5.908581E-07	1.361429E-01	1.061967E-06
30	5.800000E-04	1.014310E-01	9.038689E-02	8.170169E-07	6.510947E-07	1.358617E-01	1.044721E-06
31	6.000000E-04	1.012960E-01	9.010436E-02	7.470667E-07	7.009000E-07	1.355743E-01	1.024442E-06
32	6.200000E-04	1.011499E-01	8.982425E-02	6.744545E-07	7.404605E-07	1.352809E-01	1.001590E-06
33	6.400000E-04	1.009924E-01	8.955763E-02	6.009120E-07	7.698701E-07	1.349816E-01	9.765248E-07
34	6.600000E-04	1.008240E-01	8.929758E-02	5.279597E-07	7.897769E-07	1.346764E-01	9.499948E-07
35	6.800000E-04	1.006446E-01	8.902119E-02	4.568658E-07	8.009868E-07	1.343656E-01	9.221204E-07
36	7.000000E-04	1.004545E-01	8.875955E-02	3.906419E-07	8.044290E-07	1.340492E-01	8.933916E-07
37	7.200000E-04	1.002537E-01	8.849179E-02	3.240483E-07	8.010984E-07	1.337274E-01	8.641562E-07
38	7.400000E-04	1.000424E-01	8.824503E-02	2.636126E-07	7.920015E-07	1.334004E-01	8.347203E-07
39	7.600000E-04	9.982067E-02	8.799441E-02	2.076590E-07	7.791138E-07	1.330683E-01	8.053467E-07
40	7.800000E-04	9.958866E-02	8.774900E-02	1.563397E-07	7.603502E-07	1.327314E-01	7.762567E-07
41	8.000000E-04	9.934651E-02	8.750622E-02	1.096679E-07	7.395450E-07	1.323894E-01	7.476322E-07
42	8.200000E-04	9.909436E-02	8.726900E-02	6.754087E-08	7.164421E-07	1.320438E-01	7.196194E-07
43	8.400000E-04	9.883234E-02	8.703662E-02	2.900486E-08	6.916986E-07	1.316936E-01	6.923324E-07
44	8.600000E-04	9.856060E-02	8.680929E-02	-3.793677E-09	6.654465E-07	1.313394E-01	6.658578E-07
45	8.800000E-04	9.827929E-02	8.658722E-02	-3.351567E-08	6.393780E-07	1.309816E-01	6.402559E-07
46	9.000000E-04	9.798856E-02	8.637066E-02	-5.964708E-08	6.126737E-07	1.306202E-01	6.155704E-07
47	9.200000E-04	9.768855E-02	8.615984E-02	-8.243356E-08	5.861722E-07	1.302558E-01	5.919402E-07
48	9.400000E-04	9.737943E-02	8.595502E-02	-1.042783E-07	5.665264E-07	1.298885E-01	5.760435E-07
49	9.600000E-04	9.706136E-02	8.575649E-02	-1.163049E-07	7.400919E-07	1.295197E-01	8.491834E-07
50	9.800000E-04	9.673449E-02	8.556452E-02	-1.888111E-05	-6.152151E-07	1.291466E-01	1.849112E-05
51	1.000000E-03	9.639900E-02	8.537941E-02	-7.507671E-04	-6.439300E-04	1.287727E-01	9.890291E-04

ITERATION NUMBER 1522

MAXIMUM ERROR IN H = 2.026499E-05
MAXIMUM ERROR IN P = 2.029912E-05

I	X	R(H)	I(H)	R(P)	I(P)	ABSH	ABSP
1	0.	1.000000E-01	1.000000E-01	7.537800E-05	7.297921E-05	1.414214E-01	1.049181E-04
2	2.000000E-05	1.003163E-01	9.951640E-02	8.969256E-08	-1.840356E-06	1.413042E-01	1.842540E-06
3	4.000000E-05	1.006137E-01	9.903726E-02	7.702596E-08	-4.468111E-07	1.411790E-01	4.534818E-07
4	6.000000E-05	1.009924E-01	9.856272E-02	1.204041E-07	-4.922369E-07	1.410457E-01	4.970408E-07
5	8.000000E-05	1.011524E-01	9.809287E-02	1.525020E-07	-5.042441E-07	1.409045E-01	5.260004E-07
6	1.000000E-04	1.013946E-01	9.762781E-02	1.091309E-07	-5.249195E-07	1.407553E-01	5.579526E-07
7	1.200000E-04	1.016198E-01	9.716764E 02	2.302320E-07	-5.436800E-07	1.405983E-01	5.984192E-07
8	1.400000E-04	1.018284E-01	9.671243E-02	2.759579E-07	-5.597799E-07	1.404335E-01	6.241044E-07
9	1.600000E-04	1.020134E-01	9.626226E-02	3.263505E-07	-5.723740E-07	1.402610E-01	6.508759E-07
10	1.800000E-04	1.021844E-01	9.581719E-02	3.813099E-07	-5.805272E-07	1.400807E-01	6.945567E-07
11	2.000000E-04	1.023385E-01	9.537729E-02	4.405577E-07	-5.832267E-07	1.398928E-01	7.389282E-07
12	2.200000E-04	1.024759E-01	9.494261E-02	5.036016E-07	-5.794216E-07	1.396973E-01	7.676079E-07
13	2.400000E-04	1.025957E-01	9.451314E-02	5.697035E-07	-5.690649E-07	1.394941E-01	8.045245E-07
14	2.600000E-04	1.026999E-01	9.408905E-02	6.378571E-07	-5.491722E-07	1.392835E-01	8.418437E-07
15	2.800000E-04	1.027969E-01	9.367124E-02	7.067808E-07	-5.190950E-07	1.390654E-01	8.768074E-07
16	3.000000E-04	1.028457E-01	9.325679E-02	7.749303E-07	-4.795994E-07	1.388398E-01	9.113356E-07
17	3.200000E-04	1.029125E-01	9.284470E-02	8.405368E-07	-4.299492E-07	1.386069E-01	9.441178E-07
18	3.400000E-04	1.029517E-01	9.244600E-02	9.016731E-07	-3.699017E-07	1.383666E-01	9.746205E-07
19	3.600000E-04	1.029753E-01	9.204971E-02	9.563467E-07	-3.001669E-07	1.381191E-01	1.002347E-06
20	3.800000E-04	1.029936E-01	9.165683E-02	1.002615E-06	-2.214397E-07	1.378644E-01	1.026778E-06
21	4.000000E-04	1.029767E-01	9.127137E-02	1.038716E-06	-1.351952E-07	1.376027E-01	1.047477E-06
22	4.200000E-04	1.029559E-01	9.088935E-02	1.063198E-06	-4.324353E-08	1.373339E-01	1.064069E-06
23	4.400000E-04	1.029199E-01	9.051379E-02	1.075002E-06	5.227673E-09	1.370583E-01	1.076272E-06
24	4.600000E-04	1.029678E-01	9.014370E-02	1.073614E-06	1.490186E-07	1.367758E-01	1.083908E-06
25	4.800000E-04	1.028025E-01	8.977910E-02	1.059034E-06	2.445692E-07	1.364868E-01	1.086907E-06
26	5.000000E-04	1.027235E-01	8.942003E-02	1.031809E-06	3.365901E-07	1.361913E-01	1.805324E-06
27	5.200000E-04	1.026304E-01	8.906652E-02	9.929742E-07	4.229947E-07	1.358894E-01	1.079316E-06
28	5.400000E-04	1.025247E-01	8.871062E-02	9.439656E-07	5.019888E-07	1.355814E-01	1.069138E-06
29	5.600000E-04	1.024054E-01	8.837630E-02	8.865072E-07	5.721872E-07	1.352674E-01	1.055127E-06
30	5.800000E-04	1.022733E-01	8.803988E-02	8.224868E-07	6.326986E-07	1.349476E-01	1.037681E-06
31	6.000000E-04	1.021288E-01	8.770918E-02	7.538346E-07	6.830124E-07	1.346223E-01	1.017238E-06
32	6.200000E-04	1.019716E-01	8.738439E-02	6.824166E-07	7.230843E-07	1.342916E-01	9.942552E-07
33	6.400000E-04	1.018028E-01	8.706560E-02	6.099580E-07	7.531915E-07	1.339559E-01	9.691937E-07
34	6.600000E-04	1.016219E-01	8.675293E-02	5.379432E-07	7.739010E-07	1.336154E-01	9.424997E-07
35	6.800000E-04	1.014297E-01	8.644651E-02	4.676623E-07	7.859861E-07	1.332703E-01	9.145948E-07
36	7.000000E-04	1.012264E-01	8.614649E-02	4.001191E-07	7.903530E-07	1.329210E-01	8.858630E-07
37	7.200000E-04	1.010123E-01	8.585301E-02	3.360778E-07	7.879762E-07	1.325679E-01	8.566529E-07
38	7.400000E-04	1.007879E-01	8.556625E-02	2.760705E-07	7.798441E-07	1.322114E-01	8.272676E-07
39	7.600000E-04	1.005538E-01	8.528640E-02	2.204321E-07	7.669174E-07	1.318516E-01	7.979678E-07
40	7.800000E-04	1.003076E-01	8.501365E-02	1.693240E-07	7.500985E-07	1.314874E-01	7.689722E-07
41	8.000000E-04	1.000529E-01	8.474821E-02	1.227694E-07	7.302123E-07	1.311215E-01	7.404604E-07
42	8.200000E-04	9.978881E-02	8.449031E-02	8.068340E-08	7.079952E-07	1.307533E-01	7.125778E-07
43	8.400000E-04	9.951569E-02	8.424117E-02	4.298094E-08	6.840912E-07	1.303832E-01	6.854350E-07
44	8.600000E-04	9.923362E-02	8.399105E-02	9.199581E-09	6.590527E-07	1.300115E-01	6.591169E-07
45	8.800000E-04	9.894303E-02	8.376421E-02	-2.067993E-08	6.333468E-07	1.296386E-01	6.336836E-07
46	9.000000E-04	9.864416E-02	8.353192E-02	-4.701500E-08	6.073587E-07	1.292649E-01	6.091757E-07
47	9.200000E-04	9.833724E-02	8.332246E-02	-7.004226E-08	5.815270E-07	1.288909E-01	5.857306E-07
48	9.400000E-04	9.802268E-02	8.311514E-02	-9.208841E-08	5.564765E-07	1.285169E-01	5.699529E-07
49	9.600000E-04	9.770057E-02	8.291725E-02	-3.972717E-07	7.402769E-07	1.291437E-01	9.401309E-07
50	9.800000E-04	9.737124E-02	8.272112E-02	-1.864786E-05	-2.761420E-07	1.277704E-01	1.868935E-05
51	1.000000E-03	9.703508E-02	8.253109E-02	-7.553047E-04	-6.220394E-04	1.273949E-01	9.744774E-04

This page intentionally left blank.

UNCLASSIFIED

Security Classification

DOCUMENT CONTROL DATA - R & D

(Security classification of title, body of abstract and indexing annotation must be entered when the overall report is classified)

1. ORIGINATING ACTIVITY (Corporate author) Air Force Weapons Laboratory (WLEA) Kirtland Air Force Base, New Mexico 87117	2a. REPORT SECURITY CLASSIFICATION UNCLASSIFIED 2b. GROUP

3. REPORT TITLE

COUPLED ELECTROMAGNETIC AND ELECTRON ACOUSTIC WAVE PROPAGATION IN AN INHOMOGENEOUS LOSSY PLASMA LAYER

4. DESCRIPTIVE NOTES (Type of report and inclusive dates)

November 1969-August 1970

5. AUTHOR(S) (First name, middle initial, last name)

Hugh L. Southall

6. REPORT DATE September 1970	7a. TOTAL NO. OF PAGES 170	7b. NO. OF REFS 32
8a. CONTRACT OR GRANT NO	9a. ORIGINATOR'S REPORT NUMBER(S) AFWL-TR-70-110	
b. PROJECT NO 5791		
c.	9b. OTHER REPORT NO(S) (Any other numbers that may be assigned this report)	
d.		

10. DISTRIBUTION STATEMENT

This document has been approved for public release and sale; its distribution is unlimited.

11. SUPPLEMENTARY NOTES	12. SPONSORING MILITARY ACTIVITY AFWL (WLEA) Kirtland AFB, NM 87117

13. ABSTRACT

(Distribution Limitation Statement No. 1)

A hydrodynamic treatment is used to derive the coupled wave equations for wave propagation in a compressible plasma. Electron acoustic waves in the plasma are assumed to be excited by a vertically polarized electromagnetic wave obliquely incident upon a plane dielectric-plasma interface. Finite difference numerical solutions for the electromagnetic field and the scalar pressure field are obtained in a reentry-type plasma layer surrounding high-performance hypersonic reentry vehicles. An inhomogeneous plasma layer (or sheath) is modelled with a linearly increasing electron density profile. The coupling of acoustic waves to electromagnetic waves in this inhomogeneous region is investigated. Numerical results are obtained for the conversion of electromagnetic energy to plasma wave energy and vice versa.

DD FORM 1 NOV 68 1473

UNCLASSIFIED

Security Classification

14. KEY WORDS	LINK A		LINK B		LINK C	
	ROLE	WT	ROLE	WT	ROLE	WT
Electron acoustic waves						
Inhomogeneous plasma sheath						
Coupled wave equations						
Collision dominated plasma						
Plasma diagnostics						
Conversion efficiencies						
Hydrodynamics						